Linking long-term patterns of landscape heterogeneity to changing ecosystem processes in the Kruger National Park, South Africa

MacFadyen, S.

2018

document version
Publisher's PDF, also known as Version of record

citation for published version (APA)
MacFadyen, S. (2018). *Linking long-term patterns of landscape heterogeneity to changing ecosystem processes in the Kruger National Park, South Africa*.

ECOSYSTEM INTERACTIONS

IN A HETEROGENOUS LANDSCAPE

Linking long-term patterns of landscape heterogeneity to changing ecosystem processes in the Kruger National Park, South Africa

Sandra MacFadyen

Thesis Commitee:

Promotoren:	prof. dr. ir. P.H. Verburg
	prof. C. Hui
Co-promotor:	dr. A.J.A. van Teeffelen
Reading Committee:	prof. dr. J. Ellers
	prof. dr. H. Olff
	prof. M.P. Robertson
	prof. dr. A.K. Skidmore
	prof. dr. G.R. van der Werf
	dr. ir. E.E. van Loon

VRIJE UNIVERSITEIT

Linking long-term patterns of landscape heterogeneity to changing ecosystem processes

in the Kruger National Park, South Africa

ACADEMISCH PROEFSCHRIFT

ter verkrijging van de graad Doctor of Philosophy
aan de Vrije Universiteit Amsterdam en Stellenbosch University,
op gezag van de rectores magnifici
prof.dr. V. Subramaniam en prof. W. de Villiers,
in het openbaar te verdedigen
ten overstaan van de promotiecommissie
van de Faculteit der Bètawetenschappen
op maandag 10 september 2018 om 15.45 uur
in de aula van de universiteit,
De Boelelaan 1105

door

Sandra MacFadyen

geboren te Pretoria, South Africa

promotoren: prof. dr. ir. P.H. Verburg

                prof. C. Hui

copromotor: dr. A.J.A. van Teeffelen

Linking long-term patterns of landscape heterogeneity to changing ecosystem processes

in the Kruger National Park, South Africa

by

Sandra MacFadyen

Dissertation presented for the degree of Doctor of Philosophy in the Faculty of Science at Stellenbosch University. This dissertation has also been presented to Vrije Universiteit Amsterdam, the Netherlands in terms of a joint-degree agreement

Supervisors:	Prof. C. Hui	Stellenbosch University, South Africa
	prof. dr. ir. P.H. Verburg	Vrije Universiteit Amsterdam, Netherlands
Co-supervisor:	dr. A.J.A. Van Teeffelen	Vrije Universiteit Amsterdam, Netherlands

September 2018

DECLARATION

By submitting this dissertation electronically, I declare that the entirety of the work contained therein is my own, original work, that I am the sole author thereof (save to the extent explicitly otherwise stated), that reproduction and publication thereof by Stellenbosch University will not infringe any third party rights and that I have not previously in its entirety or in part submitted it for obtaining any qualification. This dissertation has also been presented to the Vrije Universiteit Amsterdam, the Netherlands in terms of a joint-degree agreement.

This dissertation includes two original papers published in peer-reviewed journals and three as yet unpublished publications, two of which are currently in review with peer-reviewed journals. The development and writing of the papers (published and unpublished) were the principal responsibility of myself and, for each of the cases where this is not the case, a declaration is included in the dissertation indicating the nature and extent of the contributions of co-authors.

Date: September 2018

SUMMARY

Biodiversity loss is a global threat to ecosystem function and human well-being. Environmental heterogeneity is a recognised driver of biodiversity under a niche-based view of available species habitats. As such, an increase in environmental heterogeneity is expected to promote species coexistence, persistence and diversification. Loss of environmental heterogeneity is therefore considered proximal evidence of biodiversity loss. At a landscape scale, this heterogeneity is defined as the degree of difference between landscape elements and is often described as landscape heterogeneity. Patterns of landscape heterogeneity are generated and maintained by the physical landscape template or abiotic environment (e.g. topography, geology and climate), upon which complex adaptive interactions between landscape pattern (structure and composition) and ecological processes (function) occur. Landscape pattern can therefore be described as the self-organising expression of landscape function which varies not only across space but also through time. Accordingly, observable variations in landscape pattern are conjectured to signify divergence in landscape function. This thesis explores this relationship further within the Kruger National Park (Kruger): a large (~ 20,000 km^2), long-established (proclaimed 1898) protected area in South Africa's semi-arid savanna. Results therefore describe landscape heterogeneity, in terms of the abiotic and biotic components (environmental drivers) that generate and maintain landscape pattern in Kruger, to inform strategic biodiversity planning. Chapter 1 introduces the reader to landscape heterogeneity and its relevance to protected area management and biodiversity conservation. Chapter 2 begins by isolating the effects of 'stationary' landscape properties on environmental heterogeneity through their relationship with Landsat spectral variance. Results show this relationship is sensitive to season and rainfall with the effects of dynamic ecosystem processes dominating many areas. Thereafter, Chapters 3 and 4 examine in more detail the nature of selected dynamic

drivers in Kruger, namely rainfall and elephants. Results demonstrate the existence of long-term spatiotemporal changes in both rainfall and elephant density and distribution patterns in Kruger from 1985-2015. Together these results feed into chapter 5, where a Structural Equation Model (SEM) is used to investigate the causal structure of landscape heterogeneity with stable landscape properties, rainfall, herbivory and fire. Results are presented as path coefficients and long-term driver dominance maps showing the magnitude and direction of the different cause and effect relationships between heterogeneity, the physical landscape template, rainfall, herbivory and fire return interval. Finally the nature of the environmental-heterogeneity theory is operationalised in Chapter 6 using R, Shiny and Leaflet to provide an interactive web interface for protected area managers to explore heterogeneity differences in context with park specific research questions. Chapter 7 concludes the thesis with a brief synthesis of results in context with current literature and highlights future research opportunities and possible directions.

ACKNOWLEDGEMENTS

TABLE OF CONTENTS

INTRODUCTION

1

INTRODUCTION

Biodiversity conservation is a global priority for the maintenance of healthy ecosystems and the services they provide. Despite international efforts, global predictions warn of widespread biodiversity declines in the near future (Tittensor *et al.* 2014). Large protected areas can act as strongholds of biodiversity, making their long-term maintenance a primary concern for biodiversity protection. They are also unique in that they can sustain relatively intact species assemblages, insulate vast wilderness areas from human influence and support numerous ecological processes essential for ecosystem integrity (Cantú-Salazar and Gaston 2010). The numerous pressures that threaten their existence are however ubiquitous and can include for example i) the expanding reach of human influence linked to growing population numbers, ii) unsustainable resource use, iii) climate change and iv) poor management strategies due to inadequate resources or holistic ecosystem knowledge (Cantú-Salazar and Gaston 2010). To help secure these valuable biodiversity estates, regionally specific biodiversity protection plans with functional measures of biodiversity trends are an important addition to both global and local conservation strategies (MEA 2005; Egoh *et al.* 2009; Thomsen *et al.* 2017). Much research has consequently been focused on the development of cost-effective, systematic and repeatable methods of mapping and monitoring biodiversity over large areas (e.g. Reyers and McGeoch 2007; Duro *et al.* 2007; Lengyel *et al.* 2008; Pettorelli *et al.* 2014). As a result, various indicators have been established to track the state and trends of biodiversity, especially over vast wilderness expanses of large protected areas (Han *et al.* 2014; Paganini *et al.* 2016; Walpole *et al.* 2017).

One such indicator, environmental or landscape heterogeneity, is the expression of complex, adaptive interactions between compositional, structural and functional dimensions of biodiversity, which manifest as patterns in the landscape (González-Megías *et al.* 2011; Tuanmu and Jetz 2015).

LANDSCAPE HETEROGENEITY

The terms environmental and landscape heterogeneity are used interchangeably here and across diverse urban, agricultural and natural environments to describe the degree of difference (heterogeneity) in the landscape (Kolasa *et al.* 1995; Fahrig *et al.* 2011; Stein *et al.* 2014; Dronova 2017). It is considered the self-organising expression of landscape function, which can be used to infer ecosystem health and detect ecosystem change (Wiens 2002; Chapin *et al.* 2011). It has also been described as an important mechanism of biodiversity, species coexistence, population dynamics and diversification (MacArthur and Pianka 1966; Wiens 2002; Seiferling *et al.* 2014; Tuanmu and Jetz 2015). The nature of the heterogeneity–biodiversity relationship is however non-ubiquitous (Bar-Massada and Wood 2014), varying across scale (Stein *et al.* 2014), level of ecosystem modification (Seiferling *et al.* 2014), species geographic range (Katayama *et al.* 2014) and available habitat area (Fahrig 2013). Nonetheless, when such limitations are taken into account, landscape heterogeneity may be considered a universal driver of species richness (Stein *et al.* 2014 for a full summary). The theoretical basis for this philosophy is the Habitat-Heterogeneity Hypothesis, where species diversity is predicted to be positively correlated with habitat heterogeneity (MacArthur and Pianka 1966; González-Megías *et al.* 2011). From this perspective (i.e. an ecological niche), a wider range of landscape characteristics will result in different habitat types which will support a larger diversity of species (Chase 2011). As such, any loss in heterogeneity is thus expected to represent a proximal loss in biodiversity (Pickett 1998).

Landscape heterogeneity is, therefore, increasingly used an as indicator of biodiversity change (e.g. Hernández-Stefanonia *et al.* 2012; Duro *et al.* 2014).

MEASURING LANDSCAPE HETEROGENEITY

For ecologists, heterogeneity theory can be somewhat convoluted with terms like habitat, landscape, resource and environmental heterogeneity, diversity and variability being used interchangeably and in combination with expressions of spatial and/or temporal effects or differences (Stein *et al.* 2014). Consequently, there is a pronounced lag in the development of practical solutions for 'real-world' applications (Rocchini *et al.* 2015). The ability to monitor biodiversity over the vast wilderness landscapes in protected areas is sorely needed in the face of increased biodiversity pressures (SANParks 2006). How environmental heterogeneity is defined and measured remains a key question for today's conservation agencies (Stein *et al.* 2014; Jongman *et al.* 2017). For example, if a patch-mosaic approach is used, landscape complexity is reduced to discrete patches that may not physically or functionally occur in reality (Turner 1989; McGarigal *et al.* 2009). While this approach has proven successful in urban and agricultural landscapes (Fahrig *et al.* 2011), in natural ecosystems environmental gradients are arguably better able to reflect the continuous nature of environmental heterogeneity (Doebeli and Dieckmann 2003; Guisan and Thuiller 2005). Remote sensing offers a cost-effective, systematic and repeatable method of potentially mapping and monitoring this heterogeneity using spectral variation (e.g. González-Megías *et al.* 2011; Hernández-Stefanonia *et al.* 2012; Duro *et al.* 2014). Specifically, any object (or landscape element) on the earth's surface reflects or emits energy which satellites measure across different wavelengths to produce a particular spectral response pattern (Hutson 2006; Short 2010). Different response patterns are thus digital representations of different landscape elements that make up a unique landscape.

Each unique landscape may be formed and reformed over paleontological time scales. For instance, first the underlying geology is dynamically altered by tectonics and macro-climate conditions, forming a variety of topographic elements (elevation, slope, aspect), which in turn influences micro-climate conditions (Fig. 1.1a). Together these influence the movement of water through the landscape and as a result the formation of soils (Fig. 1.1a). With a soil substrate in place, flora and fauna can establish and interact (Fig. 1.1 b+c). The scope of our study is confined here (~ 50 year time frame), where established vegetation communities influence how animal assemblages distribute themselves across the landscape, and in turn influence their surrounding landscape (Fig. 1.1). At any point disturbance, whether natural or anthropogenic, may further influence these processes (Fig. 1.1 d). These in turn may also alter landscape pattern and how it functions, forming a pattern and process feedback loop (Fig. 1.1 e). In this way, ecosystems are characterised by compositional, structural and functional biotic and abiotic landscape elements that interact to form landscape pattern (Christensen 1997). Landscape heterogeneity is thus the term used to describe the variability of this pattern (Kolasa *et al.* 1995; Stein *et al.* 2014; Dronova 2017; Reynolds *et al.* 2017). Visible patterns of landscape heterogeneity are, therefore, both the cause and consequence of interacting physical landscape features (e.g. topography, geology, soils), abiotic (e.g. climate) and biotic (e.g. flora, fauna) components and different ecosystem processes (e.g. herbivory, fire) (Fig. 1.1) (Chapin *et al.* 2011).
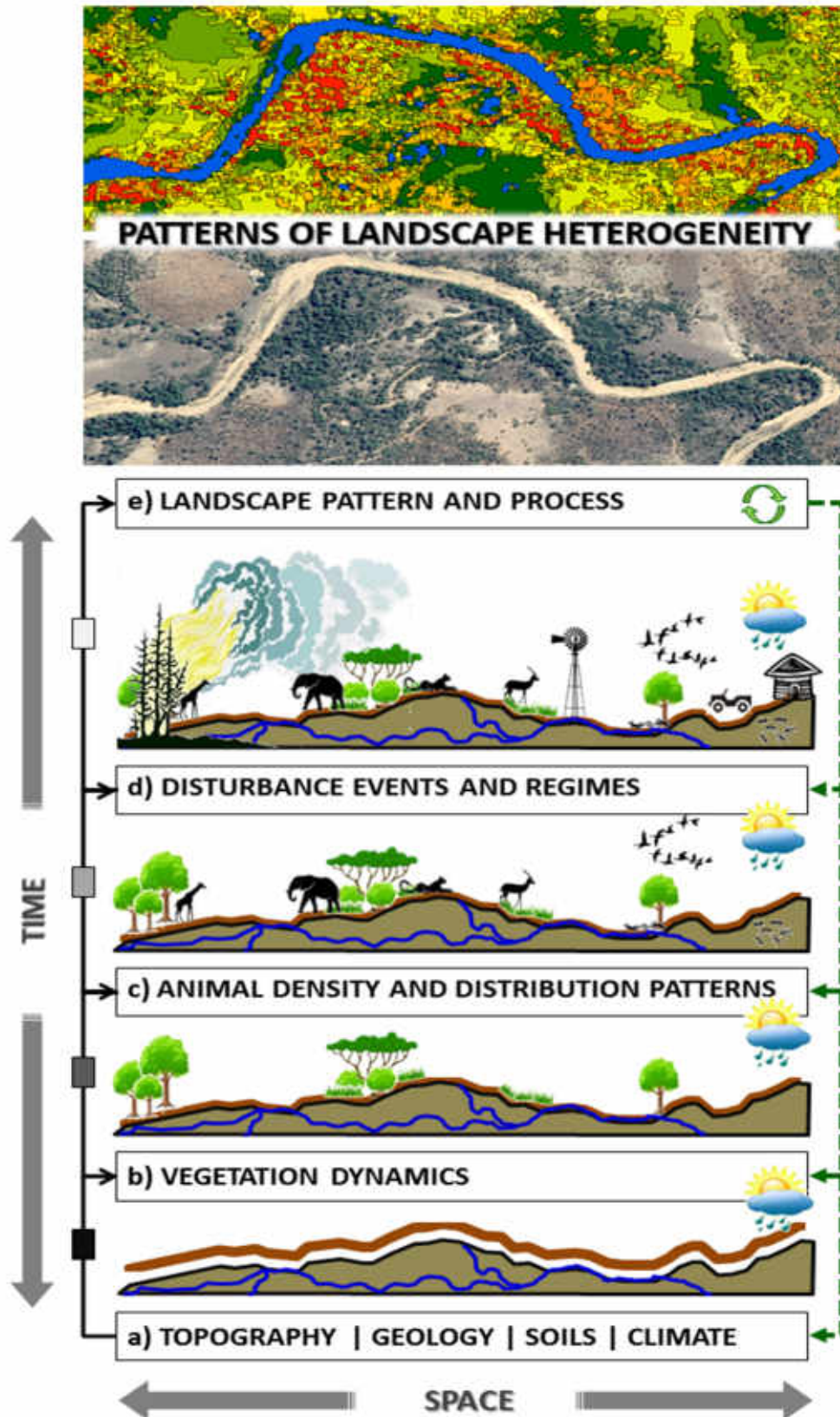
Fig. 1.1: Landscape heterogeneity as a physical construct of the effects of interactions between physical abiotic and dynamic biotic processes (a through to e). The two images above represent a 'real-world' view and the raster interpretation thereof for ecologically modelling.

RESEARCH CHALLENGES

While many of these abiotic and biotic elements (environmental drivers) have been studied in isolation, how they interact to generate and maintain landscape pattern remains an important research question (Levin 1992). A need exists for a more holistic understanding of the causes and consequences of spatiotemporal patterns of landscape heterogeneity to help disentangle complex ecological systems for protected area management. Commoner (1971) challenges this goal with his first law of ecology which states that in nature "everything is connected to everything else". That is, there exists an elaborate network of interactions between all living organisms, populations, species, individual organisms and their environment (Commoner 1971). Herein lies a universal challenge for protected area managers: How can the response of a specific component be explained without knowing how every other component, process and/or disturbance is connected? Without this knowledge one cannot know, for example, whether elephants respond to the legacy effects of fire in the landscape or if they actually cause fire regimes to be altered, or both (Dublin *et al.* 1990). The ability to separate the reciprocal cause and effects of key ecosystem drivers is recognised as a key missing element in the search for truly effective and holistic ecosystem management strategies (Levin 1992). This study is the first to disentangle the relative roles of key drivers in the growth or decay of heterogeneity over space and time in a large protected area, the Kruger National Park (Kruger) in South Africa (SA).

STUDY AREA

The Kruger National Park (Kruger) in South Africa (SA) is one of the few protected landscapes remaining where the true nature of heterogeneity and ecological response can be investigated (Pickett *et al.* 2003). Kruger is the largest of 19 parks managed by South African National Parks (SANParks).

It was officially proclaimed in 1926 under a strong protectionist philosophy that has evolved in response to political, socio-economic, intellectual and ethical changes in society (Carruthers 1995). Nested within South Africa's (SA) dominant savanna biome, Kruger covers an area of ~ 20,000 km^2 bordering Zimbabwe to the North and Mozambique to the East (Fig. 1.2). The area supports an impressive array of diversity with over 1980 plant, 856 animal and countless invertebrate species (SANParks 2017). Its underlying geology is dominated by granite, gneiss, schists, amphibolites, basalt and gabbro rock types (Schutte 1986; du Toit *et al.* 2003).
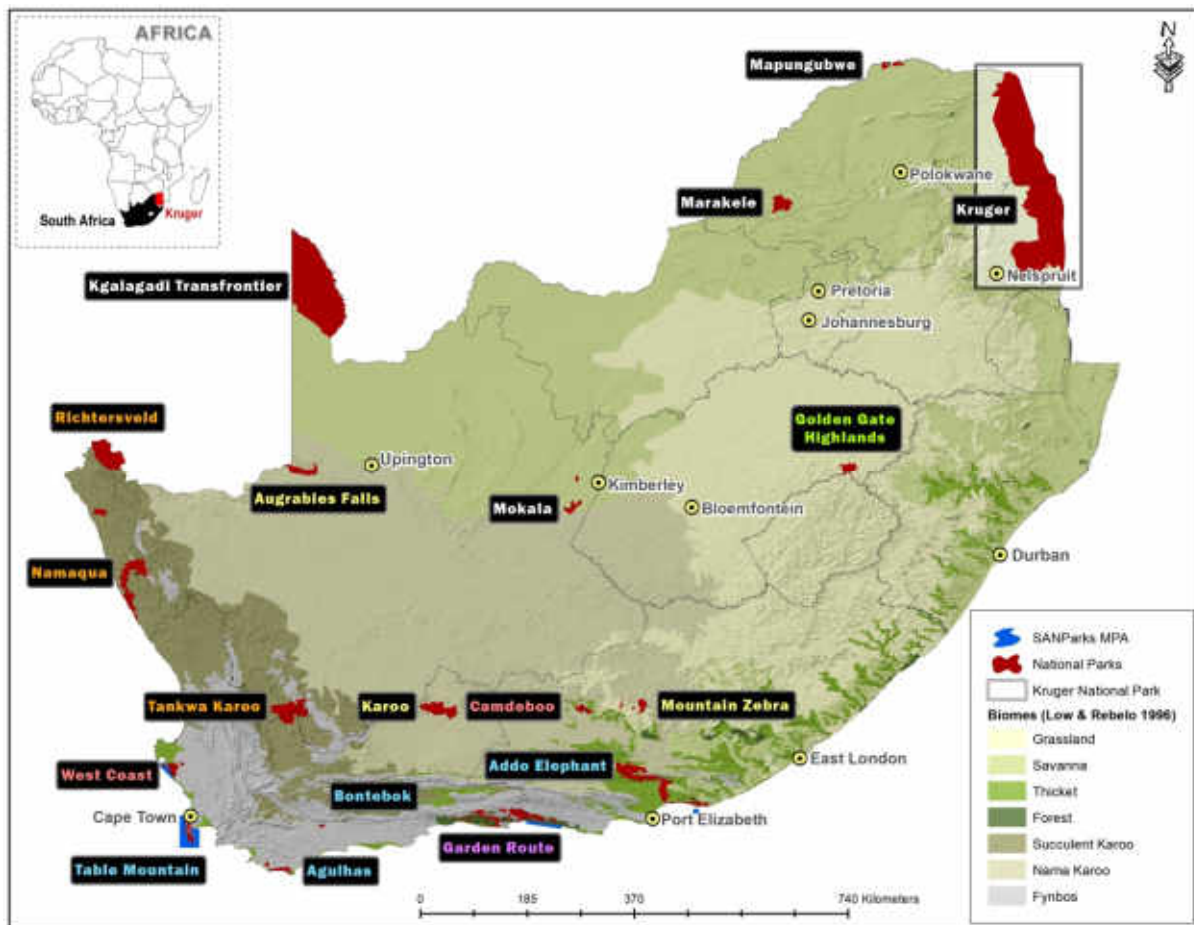
Fig. 1.2: Kruger National Park (Kruger) situated in the north-eastern corner of South Africa between latitudes 22°19'40" S - 25°31'44" S and longitudes 30°53'18" E - 32°01'59". The park is one of 19 National Parks run by South African National Parks (SANParks) and falling within the country's dominant Savanna Biome.

The terrain undulates moderately from 100 to 500 MASL, with three higher-lying areas, namely the Shitshova range near Punda Maria in the north-west (650 MASL), Lebombo mountain range bordering Mozambique in the east (480 MASL) and Khandizwe, near Malelane in the south-west (840 MASL; Fig. 2.1). This gently undulating topography and considerable biophysical diversity accommodates an extensive river network, which gives rise to a highly patchy landscape with both open grasslands and dense woodlands (Venter *et al.* 2003). The area is classified as semi-arid, falling within a climatic zone which extends over much of the central and north-eastern parts of SA (Rutherford and Westfall 1986; Trabucco and Zomer 2009). Climate is a major ecosystem driver in the park (Pickett *et al.* 2003; Venter *et al.* 2008). Decadal wet and dry rainfall cycles oscillate within a long-term annual mean of 350 mm in winter to 950 mm in summer (Gertenbach 1980). Rainfall also generally increases from north to south and from east to west as altitudes rise closer to the Drakensburg escarpment (Venter *et al.* 2003). Temperatures are sub-tropical, ranging from 26.4 °C in summer (December - March) to 17.8 °C in winter (June - August) making temperature less important as an ecosystem driver in Kruger (Zambatis 2006; Venter *et al.* 2008).

RESEARCH OBJECTIVES AND APPROACH

Savannas are inherently heterogeneous ecosystems driven by complex spatial interactions between rainfall, soil, disturbance and existing vegetation patterns (Groen *et al.* 2007). Due to its substantive size and long conservation history, Kruger is a model protected area ecosystem in which natural processes have generally been allowed to play themselves out (see du Toit *et al.* 2003 for a synthesis). It therefore presents a rare opportunity to investigate the mechanistic linkages between landscape heterogeneity, abiotic drivers, species biogeography and the effects of natural disturbances in the relative absence of unnatural anthropogenic impacts.

Using Kruger as a model ecosystem, this work strives to develop a more holistic understanding of the innate cause and effect relationships of large complex adaptive protected area ecosystems. To achieve this, each chapter is aimed at improving our understanding of key drivers of heterogeneity by establishing how landscape heterogeneity is driven by these key environmental components, both biotic and abiotic, using high resolution analyses, over a long time series and large spatial scale. The selection of key components is Kruger-specific but includes a variety of agents, substrates, controllers, and responders that can easily be applied to other areas (Pickett *et al.* 2003). The key environmental components selected and associated research objectives are targeted to identify links between long-term patterns of landscape heterogeneity and changing ecosystem processes in Kruger as follows:

1. How does the **UNDERLYING PHYSICAL LANDSCAPE TEMPLATE** affect environmental heterogeneity and the detection thereof?

2. As a dynamic ecosystem driver, what are the long-term (1981-2015) spatiotemporal patterns of **RAINFALL**?

3. As dynamic ecosystem drivers, how do **LARGE HERBIVORES** (specifically elephants) respond to the long-term (1985-2012) spatiotemporal distribution of rainfall, fire and the availability of surface water?

4. How do all of the above (herbivores, climate, landform) and fire interact to generate and maintain **LANDSCAPE HETEROGENEITY**?

5. How can the heterogeneity-biodiversity theory be operationalised into a **HETEROGENEITY TRACKER** to help globalise biodiversity protection strategies in future?

In answering the above questions, the first three chapters explore single or compound components, describing in detail their long-term spatiotemporal dynamics.

These outcomes are then collectively modelled in chapter 5 to derive a more holistic understanding of how these different ecosystem components fit together to form and maintain landscape heterogeneity.

THESIS LAYOUT

Overall the thesis is laid out to describe the cause and effect relationships between landscape heterogeneity, its underlying physical landscape template, rainfall, large herbivore distribution and density patterns, and fire return periods from 1985-2012. The methodological details of each are described in full under each chapter heading.

Chapter 2 begins by investigating how much of the variability in the landscape (heterogeneity), as observed from remotely sensed images (Winter: 1984, 1991, 1998 and Summer: 1987, 1993, 2000), can be explained by stable landscape features using Geographically Weighted Regression (GWR) (Fig. 1.3). The amount of variation not adequately explained by the landscape template is posited to reflect the effects of more dynamic system processes like rainfall, herbivory or fire.

Chapter 3 then describes the spatiotemporal patterns of Kruger's rainfall in more detail, using General Additive Mixed Effects Models (GAMM) to produce monthly rainfall grids from July 1981 to June 2015 (Fig. 1.3). To this end, local rainfall measurements are modelled as a function of global gridded rainfall data, elevation and distance to the Ocean to produce 408 fine scale (1 km^2) monthly rainfall surfaces (Fig. 1.3).

Thereafter Chapter 4 investigates the spatiotemporal patterns of elephant populations in Kruger in relation to rainfall, fire and distance to water using Multiple Point Process Models (MPPM; Baddeley *et al.* 2015) and Breakpoint Analyses (BFAST; Verbesselt *et al.* 2010) from 1985-2012 (Fig. 1.3).
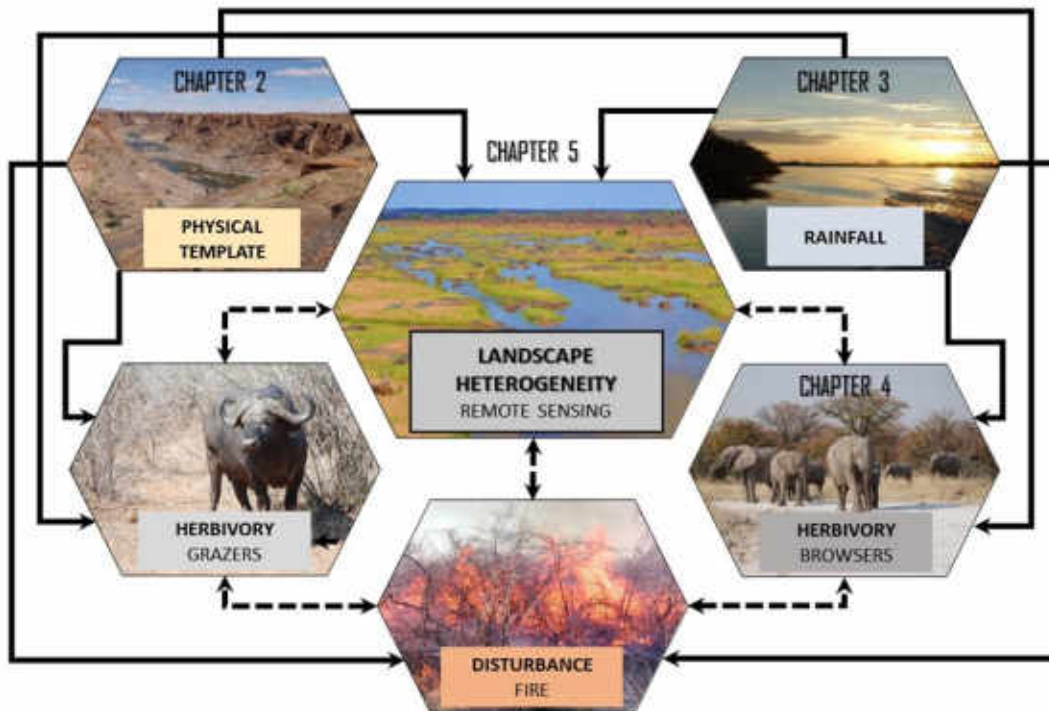
CHAPTER 7   **SYNTHESIS**
Providing insights into the causal structure of landscape heterogeneity through an understanding of the cause and/or respond of selected drivers thereof.

CHAPTER 6   **KNOWLEDGE SHARING USING SHINY R**
Heterogeneity Tracker: A Shiny R App. to monitor heterogeneity differences across protected areas [https://heterogeneity.shinyapps.io/globalheterogeneity/].

CHAPTER 5   **CAUSAL STRUCTURE OF AN ECOSYSTEM**
Piecewise Structural Equation Models to explore how the interactions of herbivores, fire, climate and landform determine landscape heterogeneity in an African Savanna.

CHAPTER 4   **HERBIVORY AS A DYNAMIC ECOSYSTEM DRIVER**
Spatiotemporal dynamics of elephant populations in response to rainfall, fire and surface water using Spatial Pont Pattern Process Models.

CHAPTER 3   **CLIMATE AS A DYNAMIC ECOSYSTEM DRIVER**
Using Generalised Additive Mixed-Effects Models (GAMMs) and derived regression surfaces to review spatiotemporal patterns of rainfall from 1981-2015.

CHAPTER 2   **UNDERLYING PHYSICAL LANDSCAPE TEMPLATE**
Quantifying spatiotemporal drivers of landscape heterogeneity using Geographically Weighted Regression.

CHAPTER 1   **INTRODUCTION**
Linking long-terms patterns of landscape heterogeneity to changing ecosystem processes in Kruger National Park, South Africa.

Fig. 1.3: Chapter details structured in the context of a hypothetical construct of cause and effect relationships between environmental heterogeneity, the physical landscape template, rainfall, herbivory and disturbance in Kruger National Park. Solid lines represent simple (one-way) interactions and dashed lines indicate complex (two-way) interactions.

Specifically, the spatiotemporal dynamics of increasing elephant numbers are described in context with these ecological drivers to elucidate population level resource selection functions underlying elephant distribution and abundance patterns.

Results and knowledge gained from chapters 2-4 are then integrated in Chapter 5 to describe the causal structure of landscape heterogeneity in Kruger using Structural Equation Models (SEM). Long-term (28 years) patterns of heterogeneity are thus assessed against the underlying physical landscape template, rainfall surfaces, herbivore densities and fire frequency to describe the magnitude and direction of effects and identify spatiotemporal patterns of driver dominance. Based on these findings, chapter 6 provides a globally interactive web interface, Heterogeneity Tracker Beta 1.0 (https://heterogeneity.shinyapps.io/globalheterogeneity), to enable protected area managers to explore heterogeneity in the context of their own park specific research questions.

Quantifying the underlying spatiotemporal drivers of environmental heterogeneity

Quantifying spatiotemporal drivers of environmental heterogeneity in Kruger National Park, South Africa

ABSTRACT

Environmental heterogeneity is considered an important mechanism of biodiversity, promoting species coexistence, persistence and diversification. How environmental heterogeneity is characterised by the compositional, structural and functional variation of biotic and abiotic components is a central conservation research theme. We explore how environmental heterogeneity relates to the underlying physical landscape template and how that relationship changes over space and time. We thereby examine how, in some areas, heterogeneity may be driven by dynamic ecological processes. We assess the ability of local Geographically Weighted Regression (GWR) models to map environmental heterogeneity through the relationship between Landsat spectral variance and stable physical landscape properties. We explore how the proportion of variability accounted for by this relationship varies spatially and temporally as a function of rainfall and season in Kruger National Park. The significance and direction of relationships varied over space and time and as a function of rainfall and season. Local adjusted coefficients of determination (R^2) generally decreased in higher rainfall summer months. Maps of R^2 reveal patterns of landscape complexity and the importance of dynamic factors relative to stable factors in explaining these patterns. Rainfall and seasonality are important drivers of environmental heterogeneity. GWR provides a spatial perspective to regression analysis, allowing us to map the relative influence of a physical landscape template on environmental heterogeneity. The spatial arrangement and magnitude of model agreement provide insight into the underlying processes driving heterogeneity. Resulting measures of Landscape complexity offer a novel approach to biodiversity research and monitoring prioritization.

2.1. INTRODUCTION

Ecologists have debated for long the relationship between environmental heterogeneity and biodiversity (e.g. MacArthur and Pianka 1966; Wiens 2002; Seiferling *et al.* 2014), with the consensus being that environmental heterogeneity is an important driver of biodiversity maintenance and ecosystem health. For rapid assessment in biodiversity monitoring, many studies have, therefore, focussed on modelling relationships between landscape heterogeneity and species diversity (e.g. MacArthur and MacArthur 1961; Tews *et al.* 2004; Tamme *et al.* 2010; Zhao *et al.* 2015). To this end, environmental heterogeneity is often considered equivalent to landscape heterogeneity in practice (Tscharntke *et al.* 2012). However, such practice inevitably reduces the realism of environmental complexity into discrete patches that may not physically or functionally occur in reality (Turner 1989; Cushman *et al.* 2010; Fahrig *et al.* 2011). Although such a mosaic approach of discretizing environmental/landscape heterogeneity has been successful, especially in urban and agricultural landscapes, it falls short in natural ecosystems where the classification of these patches discounts important within-patch heterogeneity (McGarigal *et al.* 2009).

Environmental gradients are considered as an alternative to this mosaic approach, one which arguably better reflects the continuous nature of environmental heterogeneity (Doebeli and Dieckmann 2003; Guisan and Thuiller 2005). Remote sensing offers a cost-effective, systematic and repeatable method of mapping and monitoring environmental heterogeneity as a continuous surface (e.g. González-Megías *et al.* 2011; Hernández-Stefanonia *et al.* 2012; Duro *et al.* 2014). The spectral response of satellite imagery is therefore often used to analyse ecosystem patterns and processes (Gould 2000; Wulder *et al.* 2004). Variations in this spectral response can originate from corresponding variations in the underlying properties of the physical landscape as well as from other biological features (Rocchini *et al.* 2013). Separating

out the different drivers of environmental heterogeneity from this spectral response however remains a challenge (Somers *et al.* 2011; Shi and Wang 2014).

There is to date no definitive method to quantify environmental heterogeneity, as such, a robust environmental heterogeneity–biodiversity relationship remains elusive (Allouche *et al.* 2012; Redon *et al.* 2014). Recent studies further suggest that the relationship itself is non-ubiquitous (Bar-Massada and Wood 2014), varying across scale (Stein *et al.* 2014; Oldeland *et al.* 2010), level of ecosystem disturbance (Seiferling *et al.* 2014), species geographic range (Katayama *et al.* 2014) and available habitat area (Fahrig 2013). We expect this is due to environmental complexity and the contingency of identifying key drivers of environmental heterogeneity using conventional methods (Johnson 2007). Nevertheless, in the face of increasing concerns of global biodiversity loss (MEA 2005; Hooper *et al.* 2012) how environmental heterogeneity is defined and measured is a key question for today's conservation agencies.

While many studies have sought to develop cost-effective, systematic and repeatable methods of mapping and monitoring biodiversity (e.g. Reyers and McGeoch 2007; Duro *et al.* 2007; Lengyel *et al.* 2008; Pettorelli *et al.* 2014b), few have explored the spatial and temporal variability of environmental heterogeneity itself. Using traditional global models, inherent spatial structures are often ignored and important information about how relationships between observed heterogeneity and physical landscape properties might change over space discounted (Guo *et al.* 2008; Matthews and Yang 2012). For instance, in the Kruger National Park (Kruger) in South Africa, we would expect to find highly variable relations between environmental heterogeneity and other spatially explicit drivers. Geographically Weighted Regression (GWR) is reportedly able to incorporate these local spatial relationships into a traditional regression framework (Fotheringham *et al.* 2002; Brunsdon *et al.* 2002).

We therefore anticipate GWRs application in Kruger to enable us to visualise the geographical variation of environmental heterogeneity and identify its key drivers across the park (Oliveira *et al.* 2014).

In this paper, we assess the ability of local GWR models to map the relationship between Landsat spectral variance and stable physical landscape properties. We explore how this relationship changes over space and time and examine how in some areas heterogeneity patterns may be driven more noticeably by dynamic ecological processes. We used spectral variation as a proxy for environmental heterogeneity which depicts the variability of a spectral response across different wavelengths or bands of a Landsat satellite image (Short 2005). For stable physical landscape properties we used landscape features that do not change over ~50 years, such as elevation and geology. Based on our findings, we identify the proportion of spectral variability in the landscape, as seen from the multispectral Landsat satellite, explained by stable landscape properties. Thereafter, we examine the sensitivity of this relationship to changes in season and rainfall and explore how mapped model results change as a result. We test the degree to which these mapped results can explain local plant species richness patterns and provide insight into its application for protected area managers.

2.2. METHODS

2.2.1 Study Area

KNP has considerable biophysical diversity and a long conservation history (du Toit *et al.* 2003). It is one of the largest protected areas (PAs) in the world (~ two million ha), situated in the north-eastern corner of South Africa (Fig. 2.1). The park is dominated by gently undulating topography (150-840 $_{MASL}$) underlying granite gneiss, schists, amphibolites, basalt and gabbros (Schutte 1986).
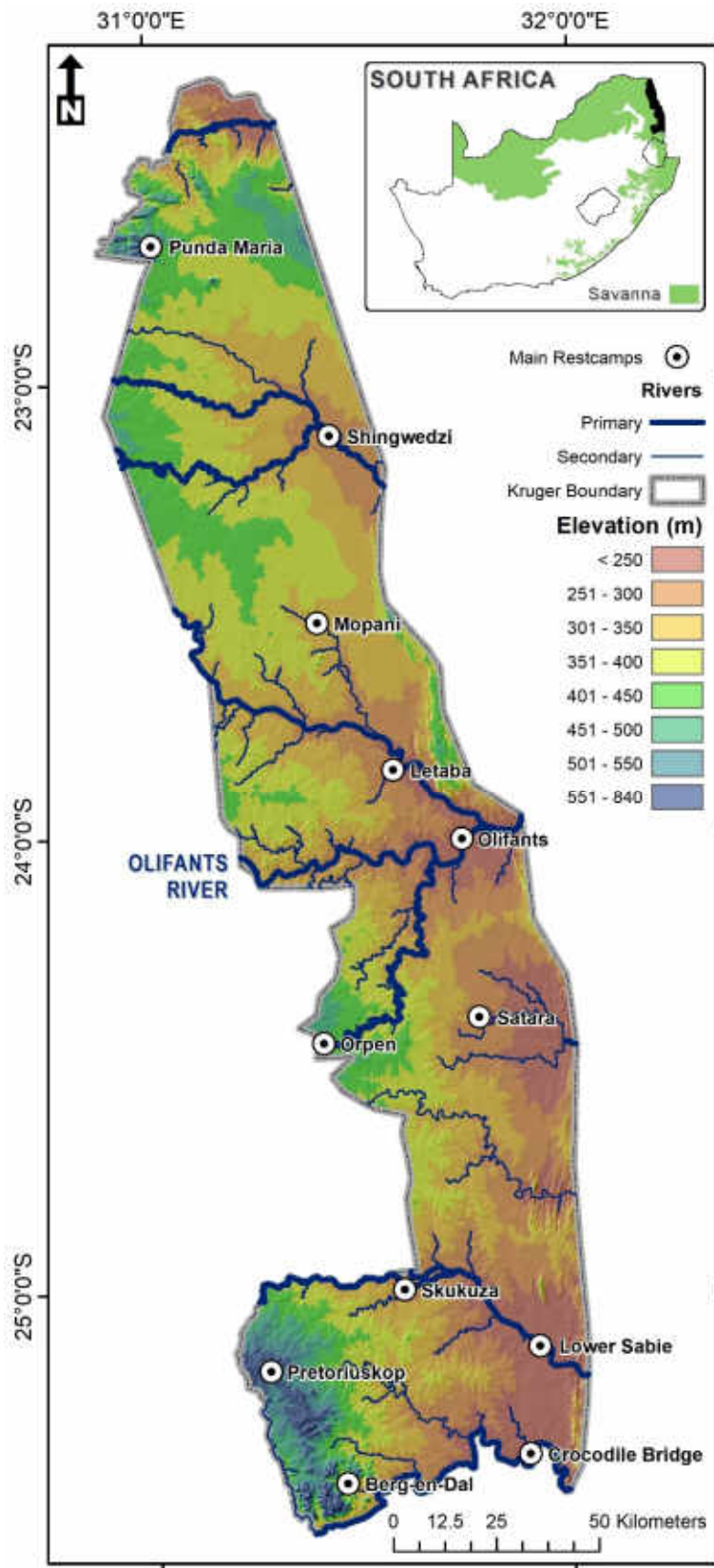
Fig. 2.1: Kruger National Park, situated in the north-eastern corner of South Africa between latitudes 22°19'40" S - 25°31'44" S and longitudes 30°53'18" E - 32°01'59" within the country's dominant Savanna Biome.

Mountainous areas occur in the east, along the border of Mozambique (Lebombo Mountains), in the south-west (Malelane Mountains) and in the north-west (Soutspansberg Mountains) (Schutte 1986). Climate is a major ecosystem driver (Pickett *et al.* 2003; Venter *et al.* 2008) with decadal wet and dry rainfall cycles occurring within a long-term annual mean of 350 mm in winter to 950 mm in summer from north to south-west (Gertenbach 1980). Average temperatures range from 26.4 °C in summer (December - March) to 17.8 °C in winter (June - August) (Zambatis 2006). KNP falls within South Africa's dominant savanna biome (Low and Rebelo 1996), an inherently heterogeneous ecosystem driven by complex spatial interactions between rainfall, soil, disturbance and existing vegetation patterns (Groen 2007).

2.2.2. Data analyses

All analyses were carried out in R version 3.0.2 (R Core Team 2013), RStudio version 0.98.978 (RStudio 2013) and GRASS GIS version 7.1.svn (GRASS 2014) in a step-wise manner: 1) Landsat spectral variation, 2) physical landscape variation, 3) GWR models, 4) interpretation of GWR model fit in terms of landscape complexity and how it relates to plant species richness.

2.2.2.1. Landsat spectral variation

Landsat imagery were available for the Skukuza region (path 168 - row 077, WRS2) from different sensors (MSS, TM, ETM$^+$, OLI) since 1972. Six images, representing late season winter conditions (July or August months) and summer conditions (March or April months), were selected for years signifying long-term mean, below and above average rainfall periods. Representative years were selected using a three-year rolling mean of daily rainfall records from the Skukuza weather station and associated availability of cloud-free images (*Fig. S2.1, in Appendix S2*).

Final image dates represent winter and summer 'windows' into low (1991-07-30; 1993-04-14), average (1984-08-27; 1987-03-13) and high (1998-08-18; 2000-04-09) rainfall conditions. Inherent sources of error were dealt with as follows: digital numbers were converted into surface reflectance units using the US Geological Survey's (USGS) on demand interface for the Earth Resources Observation and Science's (EROS) Centre Science Processing Architecture (ESPA Ordering Interface 2013); each band (excluding band 6) was geometrically and radiometrically calibrated to the Standard Terrain Correction (1T) level (Irish 2000) with a UTM WSG84 36S projection using GRASS (2014).

Before calculating spectral variation, a correlogram (Wright 2016) and local Moran's I measure of spatial autocorrelation (Hijmans 2015) were calculated for bands 1-5 and 7, revealing a non-stationary covariance structure, typical of remote sensing data (Wulder and Boots 2000; Propastin 2009). That is, bands were found to be significantly collinear (*Fig. S2.2 in Appendix S2*) and spatially autocorrelated (*Table S2.1 in Appendix S2*). We removed the first source of error (inter-band collinearity) by transforming individual bands into principle components (PC) using the *i.pca* function in GRASS (2014) interfaced through R (R Core Team 2013). Spatial autocorrelation (i.e. intra-band collinearity) was addressed through the use of GWR (discussed later).

Once individual bands were transformed into PCs, the resulting eigenvalues (or loadings; summarised in *Table S2.2 in Appendix S2*) explained the proportion of variance accounted for by each PC across the different years. For example, a high PC1 loading suggests a large percentage of the variation in the landscape can be measured using only the first principle axis (Ringnér 2008). Conversely, a low PC1 loading suggests one axis rotation is not enough to account for all the variability in the landscape. The structure of the data, and in our case the landscape, is therefore more complex.

Exploratory results indicate the proportion of variance accounted for by PC1, for example, is generally higher in winter and lower rainfall periods compared to summer and higher rainfall periods (*Fig. S2.3 in Appendix S2*). This suggests season and rainfall are potentially important drivers of environmental complexity. To better understand environmental/landscape heterogeneity (Rocchini and Neteler 2012), we further calculated the textural variance, entropy and uniformity (ASM, Angular Second Moment) for each PC (1-6) using *r.texture* within a three by three pixel moving-window neighbourhood, as well as Shannon's, Simpson's and Rényi's Entropy diversity indices and Pielou's Evenness index using *r.diversity* (See Rocchini *et al.* 2013 and the GRASS 2014 reference manual for details about index formulas).

2.2.2.2. *Physical landscape variation*

Environmental heterogeneity depicted by spectral variation is then regressed by the variability of stable physical landscape properties. These are underlying properties of the landscape template which do not change over ~ 50 years, namely elevation, slope, aspect, flow direction, watershed area, potential surface wetness index and soil form, depth and clay content (Fig. 2.2). Kruger's slope and aspect were calculated from a 5 m Digital Elevation Model (DEM) (Van Niekerk 2012) using *r.slope.aspect* in GRASS (2014); flow direction, watershed area (sink) and a surface wetness index (TCI, Topographic Convergence Index) using *r.terraflow* (GRASS 2014). Soil form, depth and clay content were extracted from the Mpumalanga Province Natural Resources dataset (Wessels *et al.* 2001). We selected an uncorrelated subset of explanatory variables using the Variance Inflation Factor (VIF), which excludes highly correlated variables through a stepwise procedure (Naimi 2015). Flow direction, which was negatively correlated with aspect (-0.63) and soil clay content, which was positively correlated with soil form (0.67), both had higher VIF values and were therefore removed along with watershed area (VIF = 3.1).
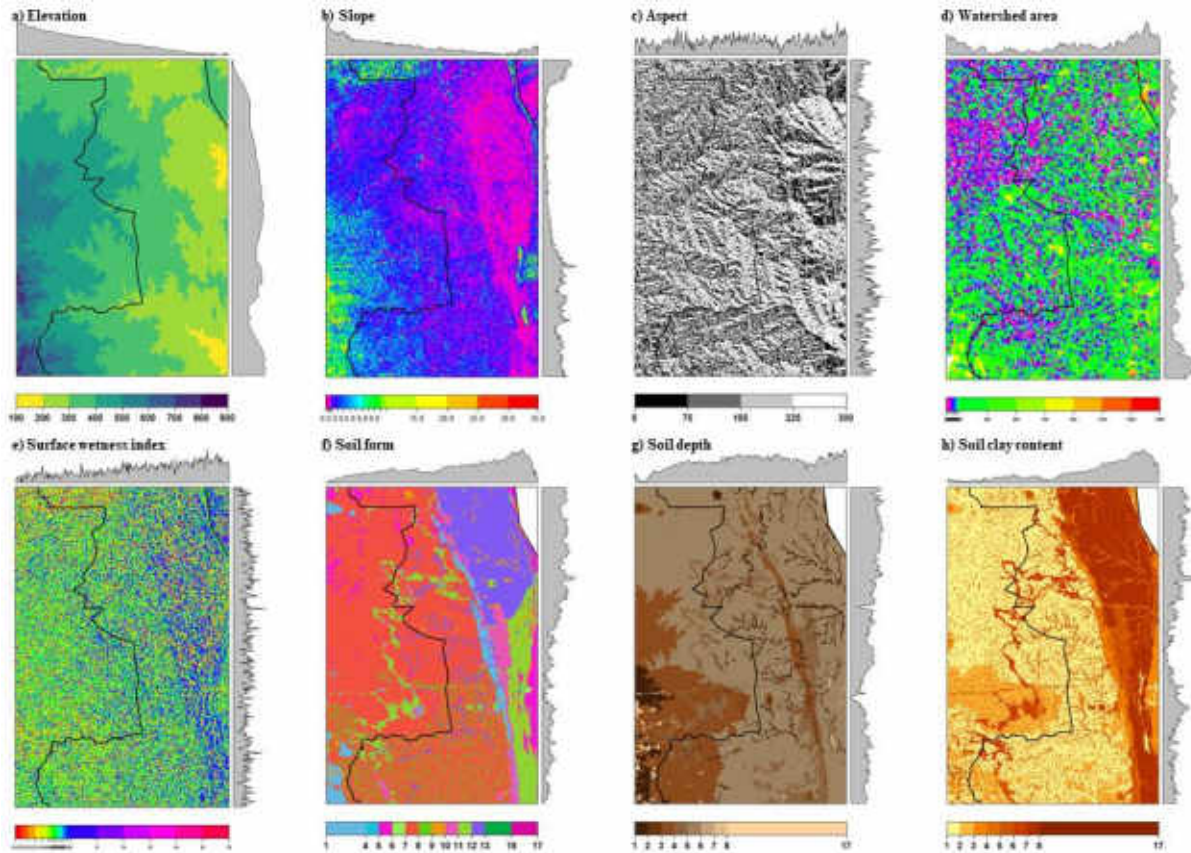
Fig. 2.2: Stable physical landscape elements that do not change over a 50 year period, forming Kruger National Park's physical landscape template: a) elevation, b) slope, c) aspect, d) watershed area, e) potential surface wetness index and f) soil form, g) soil depth and h) soil clay content).

After these variables were removed, final VIF scores were all below 1.5 (*Fig. S2.4 in Appendix S2*). We continue with our analysis using elevation, aspect, slope, TCI, soil form and soil depth as our explanatory variables. As with spectral variation, we express their variability in the landscape in terms of both textural features measured as variance, entropy and uniformity (*r.texture)* as well as the same diversity indices (*r.diversity*) of properties (Rocchini *et al.* 2013), within a three by three moving window area (GRASS 2014).

2.2.2.3. Geographically Weighted Regression (GWR)

The relationships between the resulting measures of variance for spectral and physical landscape properties were estimated using GWR (Gollini *et al.* 2015) for different seasons and rainfall conditions. We included season and rainfall because they could potentially affect vegetation structure, the intensity of disturbance (e.g. fires) and the distribution of large fauna (Chirima *et al.* 2012; Smith *et al.* 2013). The *optimal bandwidth* for each model was determined using the Akaike Information Criterion (AIC) with an adaptive bisquare bandwidth setting (Gollini *et al.* 2015). We compared model fit of the different variance measures using AIC and selected the 'best' measure to explore relationships further. Thereafter, we examined how GWR model results vary across winter and summer months of representative low (1991-1993), average (1984-1987) and high (1998-2000) rainfall periods using a multiple comparison test after Kruskal-Wallis (Giraudoux 2015) as well as an Analysis of Variance model (ANOVA). We then calculated contrasts for factor interactions to explore how seasonal contrasts of GWR coefficients differ between rainfall groups (de Rosario-Martinez 2015). Resulting local adjusted coefficients of determination (R^2) were mapped to highlight the spatial variability of model performance against season and rainfall, and spatial non-stationarity was tested using Leung's F3 statistic (Leung *et al.* 2000).

2.2.2.4. Interpretation of GWR results in terms of landscape complexity and plant species richness

The proportion of total variation in spectral response explained by physical landscape properties is captured by the R^2 from GWR and is a measure of model agreement. The remaining, unexplained proportion ($1-R^2$) therefore represents spectral variation that cannot be explained by physical landscape properties alone.

There are many dynamic landscape properties that could help explain this remaining variation in the landscape, for example fire, vegetation dynamics, herbivore distribution and human footprint. However, detailed records of these properties are rarely available. As an alternative, we interpret $1-R^2$ as a measure of *landscape complexity*, distinguishing the level of influence of dynamic landscape processes and stochastic disturbance events, from the underlying physical landscape template.

We tested this theory by examining the degree to which *landscape complexity* explained local plant species richness. Woody plant species data were obtained from the historical surveys of Venter (1990), recently described by Kiker *et al.* (2014). These data contain detailed surveys of woody vegetation cover and composition subset to our study area (n = 692 sites, totalling 115 species). A species accumulation curve (SAC) was computed (Oksanen *et al.* 2015) using the random method to find mean SAC and the number of species for all sample sites in our study area. Relationships between resulting species richness per site and *landscape complexity* were assessed using, again, GWR. We summarised GWR results and examined how parameter estimates vary with season (winter and summer) and rainfall (low, average and high conditions). Moreover, we qualify the level of influence exerted by dynamic drivers compared to stable physical landscape properties by mapping the cumulated difference of *landscape complexity*. We do this by summing the difference of $1-R^2$ values from 1984 until 2000 across the surface of Kruger. Results are summarised as surface trend maps indicating areas in the Kruger where the degree of complexity fluctuates, and thus possibly biodiversity, with changing seasonal and rainfall conditions. All regressions were run on a sample (n = 2586) of the original raster data.
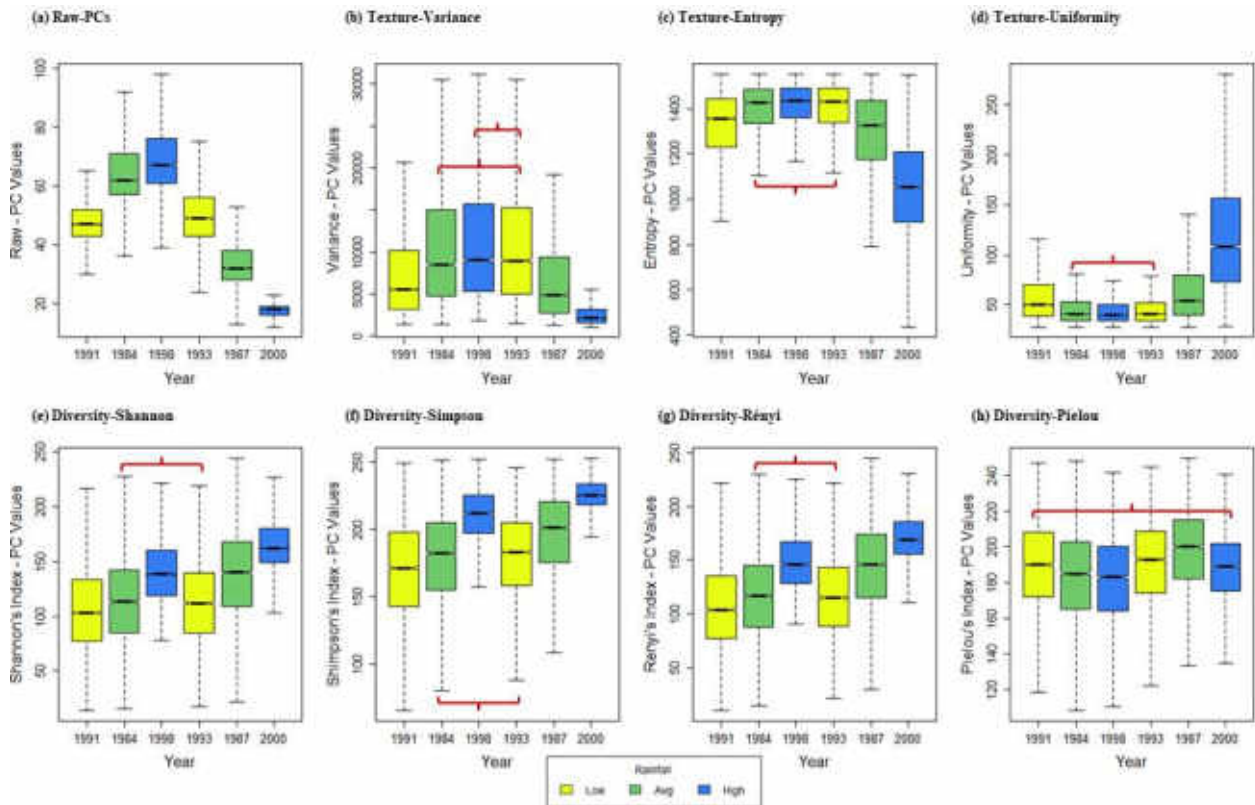
Fig. 2.3: Boxplots assessing the location, dispersion, and symmetry or skewness of spectral variation, as measured by different indices, across different seasons and rainfall conditions: a) Raw Principle Components (PC) of Landsat bands 1-5 and 7 (Kruskal-Wallis x^2 (K-W x^2) = 30081.27, df = 5, P-value < 0.0001); b) PC Textural variance (K-W x^2 = 11420.06, df = 5, P -value < 0.0001; c) PC Textural entropy (K-W x^2 = 12332.45, df = 5, P -value < 0.0001; d) PC Textural uniformity (K-W x^2 = 12189.02, df = 5, P -value < 0.0001; e) PC Shannon's diversity (K-W x^2 = 10276.83, df = 5, P -value < 0.0001); f) PC Simpson's diversity (K-W x^2 = 13792.39, df = 5, P -value < 0.0001); g) PC Rényi's diversity (K-W x^2 = 11715.88, df = 5, P -value < 0.0001; h) PC Pielou's evenness (K-W x^2 = 1637.187, df = 5, P -value < 0.0001). Red brackets indicate differences which are not significant according to the Kruskal-Wallis rank sum test (Giraudoux 2015). All other differences are significant.

2.3. RESULTS

2.3.1. Spectral and physical landscape variation

Box-and-whisker diagrams illustrate the shape of variation in spectral response of Landsat PCs across seasons and a rainfall gradient (Fig. 2.3). In general, dispersion of PC values tends to increase with increasing rainfall in winter months but decreases as rainfall increases in summer months (Fig. 2.3a). Textural measures of randomness (entropy, Fig. 2.3c) and its converse, uniformity (ASM, Fig. 2.3d), showed similar seasonal patterns i.e. winter entropy increased while summer entropy decreased and winter uniformity decreased while summer uniformity increased as rainfall increased. Diversity clearly increased as rainfall increased across both winter and summer months (Kruskal-Wallis x^2= 13792.39, df = 5, P < 0.0001; Fig. 2.3e-f-g). Variability of physical landscape properties (elevation, slope, aspect, flow direction, watershed area, potential surface wetness index and soil form, depth and clay content) are unchanged by year or season.

2.3.2. Geographically Weighted Regression (GWR)

Models with raw PC values representing spectral variation (response variables) and raw physical landscape properties (explanatory variables) were consistently better able to balance model fit and complexity than other indices, as indicated by the notably lower AIC scores (*Fig. S2.5 in Appendix S2*). Therefore, we only examined the local relationships between the linear combination of spectral PC values and uncorrelated stable physical landscape properties further.

GWR results show that relationships between spectral variation and Kruger's physical landscape template changed with season and rainfall and were spatially diverse (*Table S2.3 in Appendix S2*). Leung *et al.*'s (2000) F3 test for spatial non-stationarity shows elevation, surface wetness and soil form estimates vary significantly over the region for all years (Table 2.1).

While aspect, slope and soil depth appear constant in some years but significantly variable in others (Table 2.1). The proportion of spectral variance captured by physical landscape properties, as described by R^2, also varied within and between years (Fig. 2.4). A multiple comparison test after Kruskal-Wallis (Giraudoux 2015) indicated season and rainfall class both had a significant effect on R^2 values (Kruskal-Wallis $x^2 = 11951.46$, df = 5, P-value < 0.0001). On the surface, GWR results show model fit (R^2) generally increased from low to high rainfall ($\beta = 0.06$, $t(36420) = 34.184$, P < 0.001) and from winter to summer ($\beta = 0.05$, $t(36420) = 28.573$, P < 0.001). However, when adding an interaction effect between season and rainfall, this result was reversed for summer months. That is, R^2 values were significantly lower in higher rainfall summer months compared to lower rainfall winter months ($\beta = -0.17$, $t(36420) = -73.479$, P < 0.001). A contrast interaction test (de Rosario-Martinez 2015) confirmed R^2 seasonal contrasts differed significantly between rainfall groups: i.e. summer R^2 low to high rainfall contrasts were 0.17 less than those in winter months ($\beta = -0.174373$, df = 1, SS = 46.149, F = 5399.2, P < 0.0001). Similarly low rainfall R^2 winter to summer contrasts were 0.26 less than those for high rainfall periods ($\beta = -0.259394$, df = 2, SS = 106.16, F = 6210.2, P < 0.0001).

Table 2.1: Non-stationarity of coefficient estimates of physical landscape variables in GWR after Leung *et al.* (2000) (See *Table S2.3 in Appendix S2* for full results).

	1991	1984	1998	1993	1987	2000
Aspect	< 0.0001	0.5250	< 0.0001	< 0.0001	< 0.0001	< 0.0001
Elevation	0.0013	< 0.0001	< 0.0001	< 0.0001	< 0.0001	< 0.0001
Slope	< 0.0001	0.0843	0.0319	< 0.0001	< 0.0001	0.0105
Surface wetness (TCI)	0.0007	< 0.0001	< 0.0001	< 0.0001	< 0.0001	< 0.0001
Soil form	0.0730	< 0.0001	< 0.0001	< 0.0001	< 0.0001	0.0032
Soil depth	0.6962	0.0004	0.0479	0.1467	0.0008	< 0.0001
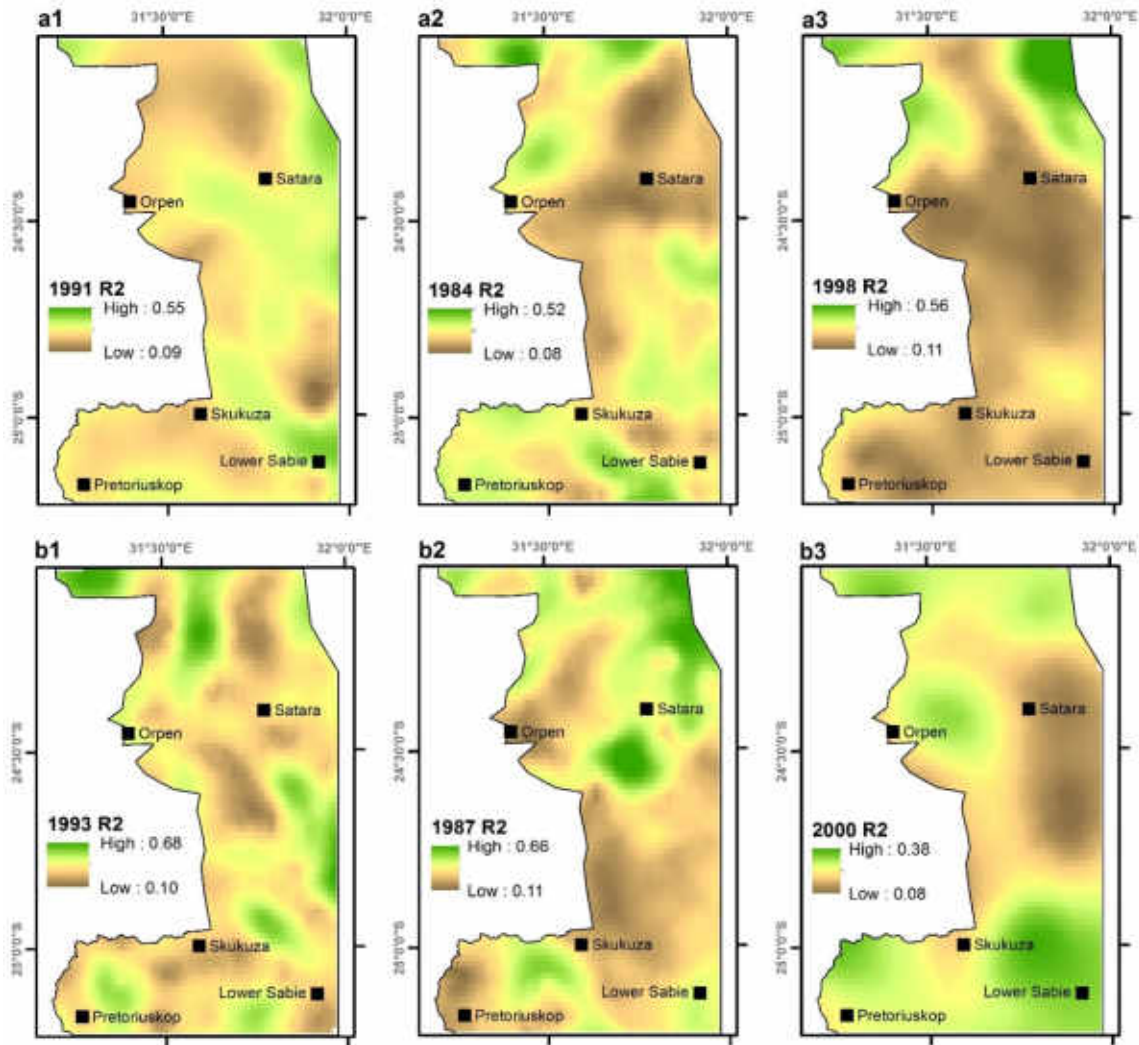
Fig. 2.4: GWR R^2 values for winter and summer months of representative low (1991-1993), average (1984-1987) and high (1998-2000) rainfall periods. Maps show the spatial heterogeneity in the proportion of spectral variance accounted for by physical landscape properties with season and rainfall (Kruskal-Wallis x^2 = 11951.46, df = 5, P -value < 2.2e-16). ANOVA results show model fit (R^2) generally increased from low to high rainfall (1 to 3; β = 0.06, t(36420) = 34.184, P < 0.001) and from winter to summer (a to b; β = 0.05, t(36420) = 28.573, P < 0.001). R^2 values were significantly lower in higher rainfall summer months (b3) compared to lower rainfall winter months (a1) (β = -0.17, t(36420) = -73.479, P < 0.001). A contrast interaction test (de Rosario-Martinez 2015) showed R^2 seasonal contrasts differed significantly between rainfall groups: i.e. summer R^2 low (b1) to high rainfall (b3) contrasts were 0.17 less than those in winter months (a1 and a3) (β = -0.174373, df = 1, SS= 46.149, F=5399.2, P < 0.0001). Similarly, low rainfall R^2 winter (a1) to summer (b1) contrasts were 0.26 less than those for high rainfall periods (a3 and b3) (β = -0.259394, df = 2, SS = 106.16, F = 6210.2, P < 0.0001

2.3.3. Interpretation of GWR results in terms of landscape complexity and plant species richness

GWR R^2 results mapped over the spatial extent of our study area (Fig. 2.4) illustrates the degree to which model agreement differed spatially across winter and summer months of representative low (1991-1993), average (1984-1987) and high (1998-2000) rainfall periods. We interpret its inverse, $1-R^2$ (model disagreement), as the level of complexity in the landscape. GWR results show a significant proportion of the variance in plant species richness can be explained by our measure of *landscape complexity* (R^2 values ranged from 0.70 to 0.78) (Table 2.2).

Table 2.2: GWR results of plant species richness modelled as a function of model fit (R^2). The first (Q1), second (Med) and third (Q3) order quartiles show the local variability of *landscape complexity* coefficient estimates. The inter-quartile range (IQR) summarise the range where 50% of all coefficient estimate values fall. Significance values (P) show 1987 (P < 0.0001), 1991(P = 0.0319) and 1993 (P < 0.0001) are significant. Leung *et al.*'s (2000) F statistic (F3) tests the significance (Fp) of the effect of spatial non-stationarity for each year's coefficients using the numerator (nDF) and denominator degrees of freedom (dDF).

	Q1	Med	Q3	IQR	p	adjR2	AICc	nNN	F3	nDF	dDF	Fp
1991	-39.66	-2.68	32.20	-7.46	0.0319	0.76	5413	18	5.29	246	561	< 0.0001
1984	-37.30	-1.34	27.40	-9.90	0.1340	0.71	5517	21	6.40	224	579	< 0.0001
1998	-34.11	-3.85	25.78	-8.33	0.8725	0.70	5558	18	2.18	210	558	< 0.0001
1993	-9.42	2.45	36.28	26.86	< 0.0001	0.78	5433	14	3.70	118	519	< 0.0001
1987	-11.45	0.35	15.97	4.52	< 0.0001	0.74	5475	18	3.38	251	549	< 0.0001
2000	-29.54	6.43	76.91	47.37	0.1805	0.75	5433	18	4.73	172	564	< 0.0001

Model settings: gwr.basic (Kernel function = bisquare; adaptive bandwidth = number of nearest neighbours (nNN); regression points = same locations as observations; distance metric = Euclidean distance metric) (Gollini et al. 2015).

These results showed significant improvement over GWRs of raw physical landscape properties and raw surface reflectance PC values, which only accounted for 62% and 57% of the variance in plant species richness respectively (*Table S2.4 in Appendix S2*). There was a significant increase in landscape complexity associated with species richness in the years closest to sample collection dates ~ 1989 (1987: $R^2 = 0.74$, median $\beta = -2.68$, $F(1,691) = 21.36$, $P < 0.0001$; 1993: $R^2 = 0.78$, median $\beta = 2.45$, $F(1,691) = 18.07$, $P < 0.0001$). In contrast, a less significant decrease in *landscape complexity* was associated with species richness in 1991($R^2 = 0.76$, median $\beta = 0.35$, $F(1,691) = 4.623$, $P = 0.0319$). Although, 1989 and 1993 both showed positive relationships, 1991 showed a slightly negative one. We propose this result may be confounded by the severe drought Kruger experienced in 1991/1992 (Zambatis and Biggs 1995). A map of the residuals for 1993 illustrates the spatial variability of this relationship (Fig. 2.5a).

Surface trend maps indicate areas in the Kruger that change in terms of this complexity with changing seasonal and rainfall conditions. Green areas on the map show regions in Kruger in which our measure of *landscape complexity* increased from 1984 to 2000 (Fig. 2.5b). While in red areas our measure of *landscape complexity* decreased and in yellow areas it remained relatively unchanged (Fig. 2.5b).
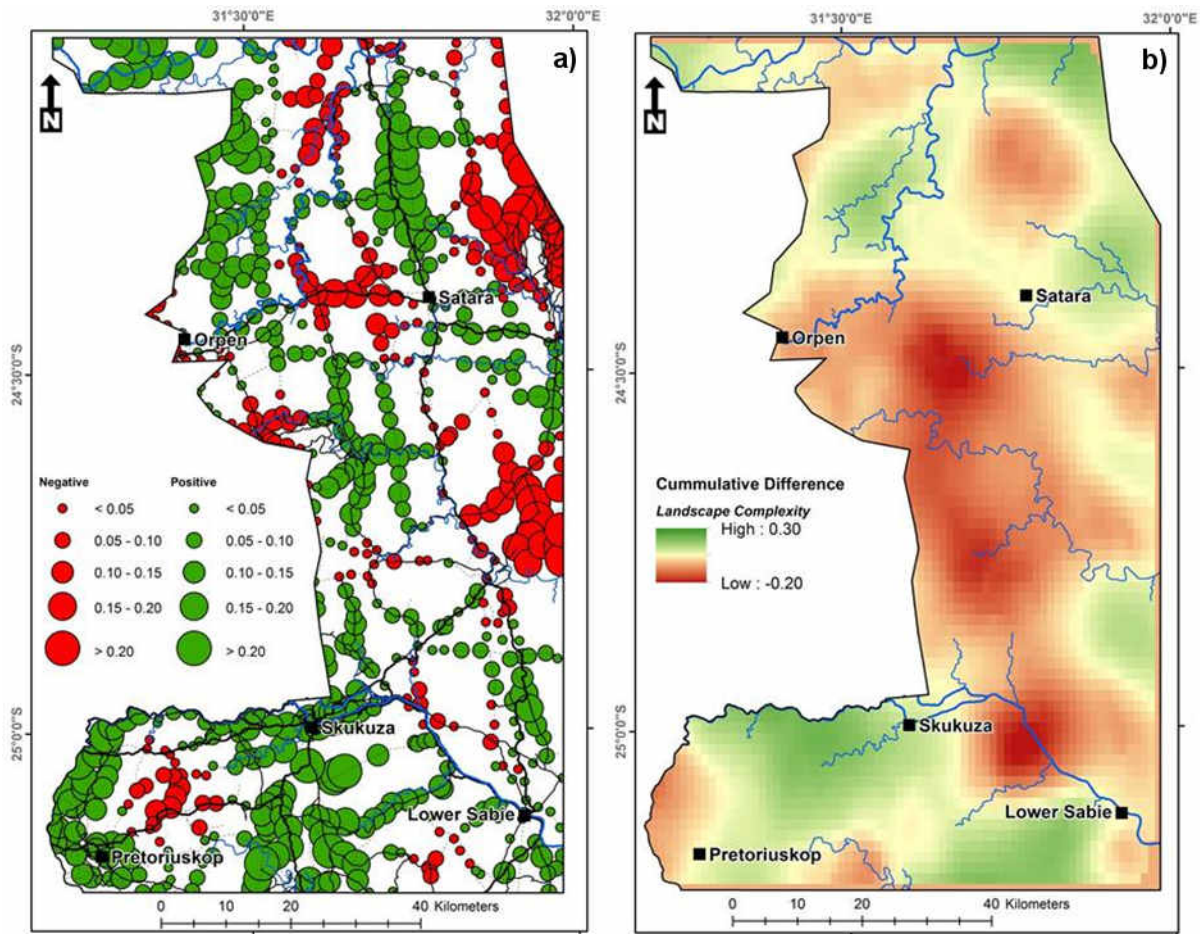
Fig. 2.5: a) A map of the 'raw' residuals (observed - fitted) for 1993 illustrating the spatial variability of the relationship of species richness with landscape complexity. Regionally there is a significant increase in landscape complexity is associated with species richness in 1993 (R^2 = 0.78, median β = 2.45, $F(1,691)$ = 18.07, $P < 0.0001$). b) Total accumulated difference of landscape complexity (GWR 1-R^2) across low (1991-1993), average (1984-1987) and high (1998-2000) rainfall periods. Shades of green indicate areas that increase in landscape complexity, shades of red decrease in landscape complexity and shades of yellow remain unchanged from 1984-2000.

2.4. DISCUSSION

In their meta-analysis, Field *et al.* (2009) found environmental heterogeneity to be an important driver of species richness. Remotely sensed spectral heterogeneity is recommended by several authors (Duro *et al.* 2007; Rocchini *et al.* 2010; Nagendra *et al.* 2013; Pettorelli *et al.* 2014b) as a proxy for environmental heterogeneity and the consequent rapid assessment of biodiversity properties. It stands to reason that, a more diverse spectral response will represent a more diverse landscape in that spectral heterogeneity will reflect the associated variation of environmental properties in the landscape (Stein *et al.* 2014). However, we expect this relationship will be dynamic, changing across different and interactive space-time scales. We demonstrated this using Fotheringham *et al.*'s (2002) GWR technique with Landsat surface reflectance and stable physical landscape properties. By allowing relationships to vary over space, we were able to account for spatial non-stationarity and visualise the resulting patterns (Brunsdon *et al.* 1996).

Results showed that the relationship between spectral heterogeneity and stable physical landscape properties is sensitive to season and rainfall condition. We therefore stress the importance that remote sensing studies be accompanied by locally concurrent field sampling data. Moreover, we showed that textural measures of entropy increased with rainfall in winter but decreased with rainfall in summer. While, textural measures of uniformity (ASM) also showed an inverse pattern of decreasing ASM with increasing rainfall in winter and increasing ASM with increasing rainfall in summer. We suggest these results are representative of both 1) true structural diversity in the landscape and 2) the limitations of remotely sensed Landsat data: 1) we expected structural diversity to increase with rainfall up to a threshold where vegetation cover, for example, would reach an asymptote thereby decreasing structural entropy and increasing structural uniformity. However, 2) we also recognise that this outcome may affect what is 'visible' to the Landsat's passive sensor. Under dense and extensive cover conditions,

this satellite is less able to detect under-canopy variability in the landscape. Prospective studies may wish to explore the use of active sensors like Lidar in future.

Regionally, spectral diversity increased with increasing rainfall across both winter and summer months. Intuitively these results represent the increase in environmental diversity as water availability becomes less limiting. This is corroborated by our findings that the proportion of satellite surface reflectance variance captured by a single PC axis rotation, for example, was generally higher in winter and during lower rainfall periods as compared to summer and during higher rainfall periods. Locally, raw PC values representing spectral variation and raw physical landscape properties were consistently better able to balance model fit and complexity than other textural or diversity measures. This is consistent with the findings of Warren *et al.* (2014), who found spectral diversity yielded reasonable estimates of plant species richness using a simple Pearson correlation to measure linear relationship strength. Our results add a spatial component which proved spatial non-stationarity was statistically significant and highlights the importance of using a geographical approach when analysing environmental data (Leung *et al.* 2000; Brunsdon *et al.* 2002).

This was made further evident by the clear differences in the proportion of spectral variation captured by relatively stable physical landscape properties over space and time. We found that increasing summer rainfall reduces the explanatory power of stable physical landscape properties on environmental heterogeneity (as measured by Landsat spectral variation). We postulate that this general reduction in the explanatory power of models fitted to data from summer periods, and periods of high rainfall versus winter and lower rainfall periods, is indicative of dynamic environmental processes not captured by physical landscape properties. These dynamic processes are driven by season and rainfall and include, for example fire, vegetation dynamics, herbivore distribution, and human development. Under higher rainfall

conditions vegetation activity, for instance, is increased and herbivore density and distribution patterns will change in response.

We hypothesised that the proportion of spectral variation unexplained by the underlying physical landscape template is representative of the level of *landscape complexity*. We tested this theory against plant species richness data and found a strong, significant relationship between *landscape complexity* and species richness. These findings show that indeed other processes than physical landscape properties shape environmental heterogeneity and biodiversity over space and time. However, empirical knowledge of dynamic processes is often not available for protected area managers, and even if accessible, is rarely spatially explicit or temporally continuous. Nevertheless, such knowledge remains central to understanding the functioning of natural systems and their effectual management as protected areas. Our approach provides a starting point by mapping the relative importance of stable physical landscape properties compared to other dynamic processes for environmental heterogeneity. We showed how dynamic processes move across the landscape over time and suggest that biodiversity monitoring programmes be designed to capture this variability. For example, Kruger's annual dry-season herbivore counts may be missing important changes in distribution patterns driven by seasonal changes in *landscape complexity* (Martin *et al.* 2015).

The cumulative difference of these changes highlight areas where relatively little change in *landscape complexity* has taken place between seasons (winter-summer) and rainfall (low-average-high) conditions and represent comparatively stable landscapes. While those where change in *landscape complexity* has been consistent, represent more dynamic landscapes. Visually it appears basalt dominated areas in the east are generally becoming more complex than their granitic counterparts in the west. This is consistent with the findings of Colgan *et al.* (2012) who showed above-ground biomass production on basalts was driven largely by herbivore-fire interactions rather than soil properties themselves. In other words, basaltic areas

appear to be driven by more dynamic processes. This may also be partially due to the subtle east-west rainfall gradient in the park. Nevertheless, armed with these *landscape complexity* maps, protected area managers will have a blueprint to start disentangling the role of major ecosystem drivers. For example, are highly complex and diversifying landscapes largely driven by herbivore dynamics, disturbance events or management action? Park monitoring and research planning can be stratified using these 'blueprints' to begin answering these and other questions related to landscape complexity.

Cressie *et al.* (2009) and Lechner *et al.* (2012) stress the importance of accounting for uncertainty in the analysis of complex ecological data. We highlighted here the importance of accounting for spatial structure in ecological data analysis but did not assess the influence of resolution scale on analysis results. In future studies we hope to examine these results against different pixel and moving-window sizes. How these results relate to intra-annual dynamics of land surface phenology in Kruger, is another interesting question for the future (Garonna *et al.* 2014).

2.5. CONCLUSION

Despite the fact that ecological components and processes in the environment have an underlying spatial structure that is locally heterogeneous, ecological regression models often employ 'global' techniques which assume relationships are constant over space. Using GWR models that account for spatial variation and dependencies, we were able to provide local detail on where and when physical landscape properties drive environmental heterogeneity and how this relationship changes spatially with rainfall and season. We conclude that GWR is particularly valuable for ecological studies as emergent patterns are often influenced by processes interacting at different spatial as well as temporal scales (Hewitt *et al.* 2007).

The spatial arrangement and magnitude of model disagreement is proposed here as a measure of *landscape complexity*. Areas where environmental heterogeneity is not explained by stable physical landscape properties are, instead, driven by unknown complex dynamic processes. Unfortunately, empirical data for these dynamic processes is not always available under limited park management resources. However, even if resources were not limiting, drivers are often unknown in the face of environmental complexity. Maps of *landscape complexity* can therefore be an effective tool for targeting monitoring and prioritization of research to further our understanding of the drivers of environmental heterogeneity and biodiversity.

Long-term spatiotemporal patterns of rainfall from 1981-2015

3

Long-term rainfall regression surfaces for the Kruger National Park, South Africa: A spatiotemporal review of patterns from 1981-2015

ABSTRACT

As an important bottom-up driver of ecosystem processes, rainfall is intrinsically linked to the dynamics of vegetation and species distributions through its effects on soil moisture content and surface water availability. Rainfall effects are thus spatially and temporally specific to different environmental role-players. Knowledge of its spatiotemporal pattern is therefore essential to understanding natural ecosystem flux and potential climate change effects. Climate change poses a serious threat to protected areas in particular, as they are often isolated in fragmented landscapes and confined within hard park boundaries. In consequence, a species' natural movement response to resulting climate induced niche shifts is often obstructed. Long-term, accurate and consistent climate monitoring data are therefore important resources for managers in large protected areas like the Kruger National Park (Kruger). In this paper we model local rainfall measurements as a function of global rainfall surfaces, elevation and distance to the Ocean using a Generalised Additive Mixed Effects Model to produce fine scale (1 km^2) monthly rainfall surfaces from July 1981 to June 2015. Results show a clear seasonal cycle nested within an oscillating multi-decadal trend. Most noticeably, seasonality is shifting both temporally and spatially as rainfall moves outside of the typical dry/wet periods and areas. In addition, high rainfall seasons are generally receiving more rainfall while low rainfall seasons are receiving less. North-western regions of the park are experiencing more extreme annual rainfall differences, while far northern and southern regions show greater seasonality changes. The well described north-south and east-west rainfall gradient is still visible but the spatial complexity of this pattern is more pronounced than expected. Taken together, we show that Kruger's spatiotemporal rainfall patterns are changing significantly in the short to medium term. The resulting raster dataset is made freely available to promote holistic ecosystem studies and support longer-term climate change research (http://dataknp.sanparks.org/sanparks/ metacat/judithk.111609.2/sanparks).

3.1. INTRODUCTION

Rainfall plays a central role in a myriad of natural processes, including river health, the transportation of nutrients (Strauch 2013), soil moisture (Berry and Kulmatiski 2017), vegetation dynamics (Ekblom *et al.* 2012), fire regimes (Archibald *et al.* 2009), animal movement and distribution patterns (Seydack *et al.* 2012), and landscape heterogeneity (MacFadyen *et al.* 2016). Within protected areas these processes function together to safeguard ecosystem integrity, helping to ensure the survival of places like the Kruger National Park (Kruger) as strongholds of biological diversity, socio-economic wealth and protectorates of natural resources and other ecosystem services (SCBD 2008). The spatiotemporal patterns of rainfall are thus an important variable to include in any ecological study, especially in the face of current climate change predictions (Hitz and Smith 2004; Chapin *et al.* 2011). The Intergovernmental Panel on Climate Change's (IPCC's) recent projections warn of severe declines in renewable surface and ground water resources for the sub-tropics (IPCC 2014). South Africa (SA) in particular is projected to become progressively hotter and drier (DEA, 2013), raising serious concerns for local protected area management agencies to respond (van Wilgen *et al.* 2016). These concerns stem from protected areas being especially vulnerable to the effects of climate change because they are often isolated in fragmented or bounded landscapes where species movement response is restricted (Hannah *et al.* 2007). Subtle changes to species (floral and/or faunal) composition and distribution dynamics in these natural systems can therefore act as early warning indicators of climate change effects (Garcia *et al.* 2014).

Ecosystem level research, practiced at the scale of a protected area, can then be an important addition to global climate monitoring efforts if channelled through Long Term Ecological Research networks (Knapp *et al.* 2012). This type of research is often focussed around elucidating cause-and-effect relationships amongst various components of the ecosystem to anticipate potential state changes that may compromise system integrity (Pienaar 1977).

To do this effectively, reliable data on bottom-up substrates (e.g. topography, climate, geology, soils and vegetation) and top-down agents (e.g. fire and herbivory) are needed to discern undesirable change from natural ecosystem dynamics (Pickett *et al.* 2003; Venter *et al.* 2003). The need for robust, well documented and continuous long-term climate data is therefore crucial (Kemp *et al.* 2012). Long-term datasets make it possible, for example, to quantify the effects of past extreme climatic events on ecosystem dynamics (e.g. vegetation patterns) to provide insights into the potential effects of varying climatic conditions in the future.

A large number of global climatological datasets have become available in recent years and are increasingly easy to access and use (see examples in *Table S3.1 in Appendix S3*). They are however modelled predictions of real-world climate, inherent with statistical bias and uncertainty (Muñoz *et al.* 2011; Kearney *et al.* 2014; Stoklosa *et al.* 2015). Moreover, the coarse resolutions at which these data are generated (e.g. 5 km CHIRPS; *Table S3.1 in Appendix S3*) are often not suitable for finer scale ecological research (Kearney *et al.* 2014). To overcome these limitations a number of bias correction (Haerter *et al.* 2015) and spatial interpolation methods have been developed (Wagner *et al.* 2012). Most common amongst these, especially for data sparse regions like Africa, is the use of ground-based measurements and environmental covariates to augment globally modelled climate surfaces (Plouffe *et al.* 2015; Verdin *et al.* 2016). The importance of local long-term climate networks therefore needs to be more firmly recognised (van Wilgen *et al.* 2016). Since the effects of rainfall on ecosystem dynamics play out at different spatiotemporal scales local finer scale data will remain irreplaceable sources of information for both regional and global scale ecosystems research (Williams *et al.* 2007; Odiyo *et al.* 2015, MacFadyen *et al.* 2016). We illustrate this by providing a comprehensive analysis of regional (~ 20,000 km^2), short to medium-term patterns and trends of local rainfall in Kruger from 1981 to 2015.

Although countless studies conducted in Kruger cite the importance of climate, specifically rainfall, many are restricted to using park-wide averages or nearest station estimates (Owen-Smith and Ogutu 2003; Smit *et al.* 2013a; Trollope *et al.* 2014). We expect the dynamics of Kruger's rainfall are more complex, varying at different spatiotemporal scales that are undetectable when using simple regional averages. As a consequence, the spatiotemporal range of potential rainfall effects could also be more dynamic and further reaching than previously studied. We try to answer some of these questions by i) assessing the temporal trends and spatial patterns of rainfall in Kruger over the last 34 years, ii) identify significant changes to the spatial rainfall patterns, and ultimately iii) make the resulting spatiotemporal regression surface products freely available for future research.

3.2. METHODOLOGY

3.2.1. Study Area

Some of the world's largest protected areas are found in African savannas (IUCN, UNEP-WCMC, 2016). Large protected areas in these savannas, like Kruger, are important for the preservation of large scale intact environments and the conservation of diverse wildlife assemblages and extensive wilderness qualities (Cantú-Salazar and Gaston 2010). South Africa (SA) has a highly variable climate and pronounced rainfall seasonality, driven predominantly by sea surface temperatures, the effects of the El Niño Southern Oscillation (ENSO) - both its warm (El Niño) and cool (La Niña) phases and the Inter Tropical Convergence Zone (ITCZ) (Philippon *et al.* 2014; Dedekind *et al.* 2016; Favre *et al.* 2016). The displacement of ITCZ to the south of the equator during the austral summer produces the South Indian Convergence Zone which restricts most of SA to a summer rainfall region (Dedekind *et al.* 2016). Kruger falls within a semi-arid zone which spans much of the central and north-eastern parts of SA (Rutherford and Westfall 1986; Trabucco and Zomer 2009).

On average, 84% of Kruger's total annual rainfall is concentrated between the summer months of November and April (Zambatis 2003). Regionally, the area is split into two distinct climatic zones: Northern Arid Bushveld with 300-500 mm annual rainfall and Lowveld Bushveld with 500-700 mm annual rainfall, roughly north and south of the Olifants River respectively (Fig. 3.1; SAWS 1986). Locally the terrain is moderately undulating (100 to 500 $_{MASL}$) with three higher-lying areas, namely the Shitshova range near Punda Maria in the north-west (650 $_{MASL}$), Lebombo mountain range bordering Mozambique in the east (480 $_{MASL}$) and Khandizwe, near Malelane in the south-west (840 $_{MASL}$; Fig. 3.1). Here updrafts associated with higher elevation increase rainfall and with it soil leaching, thereby producing sandier more nutrient poor soils. For the rest of Kruger, rainfall is generally accepted to increase from north to south and from east to west as altitudes increase closer to the Drakensburg escarpment (See Venter *et al.* 2003 for a full account of local climate).

3.2.2. Data

3.2.2.1. Local climate station records

Kruger has a long history of weather and rainfall monitoring, started by early naturalists in 1903 (Zambatis, 2003). Park rangers were later responsible for recording *in situ* rainfall measurements from 1920, which were augmented with six formal weather stations erected in partnership with the South African Weather Services (SAWS) in 1961 (Joubert, 2007). These stations included Skukuza, Pretoriuskop, Satara, Letaba, Shingwedzi and Punda Maria (Fig. 3.1).
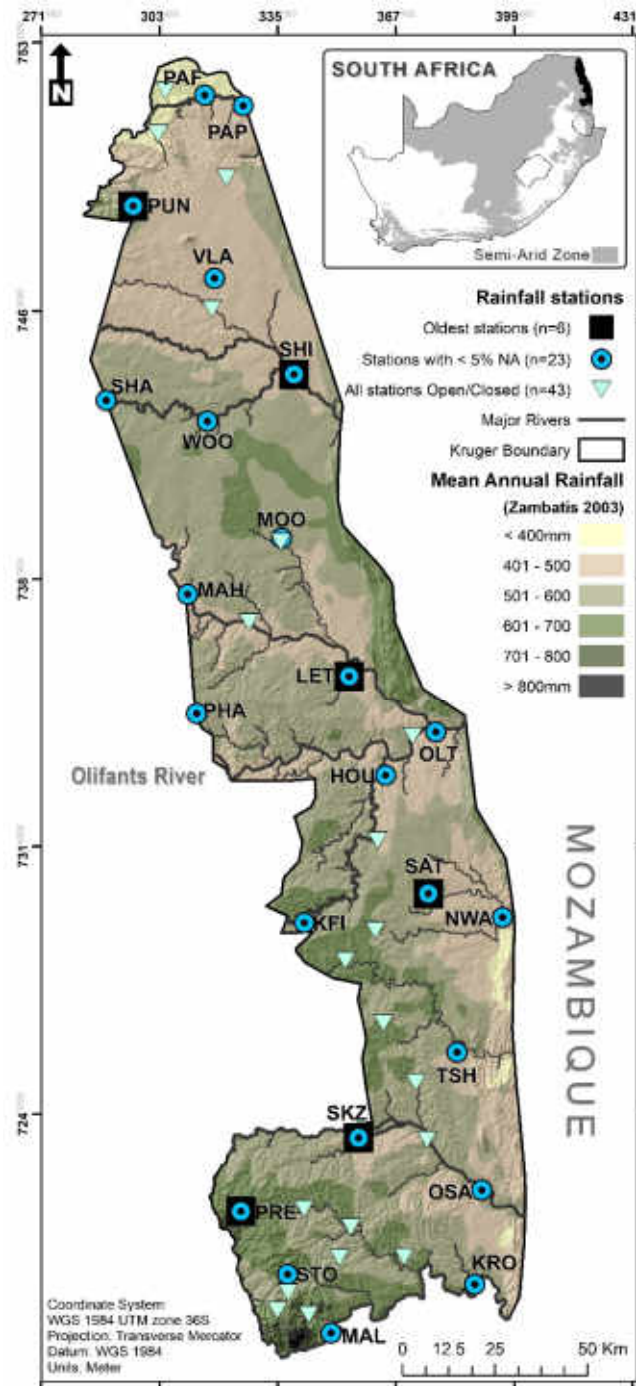
Fig. 3.1: General climatic zones of the Kruger National Park. Inset: Kruger National Park is situated in the north-east corner of South Africa between latitudes *-25.5289°S* to *-22.3279°S* and longitudes *30.8884°E* to *32.0332°E*. Long-term rainfall monitoring stations include: PAF-Pafuri Section; PAP- Pafuri Police; PUN- Punda Maria; VLA- Vlakeplaas; SHI- Shingwedzi; SHA- Shangoni; WOO- Woodlands; MOO- Mooiplaas; MAH- Mahangeni; PHA-Phalaborawa; LET- Letaba; OLT- Olifants; HOU- Houtboschrand; KFI- Kingfisherspruit; NWA- Nwanetsi; TSH- Thokwane; SKZ- Skukuza; PRE- Pretoiuskop; OSA- Lower Sabie; STO- Stolznek; MAL- Malelane; KRO- Crocodile Bridge.

More stations were gradually added, culminating in 43 recording stations located across the park and providing a good representative sample of Kruger's different climatic zones, habitats and geographic range (Fig. 3.1). Apart from a number of sanctioned station closures over the years, missing data records threaten to compromise the quality and reliability of Kruger's climate station data. From the original 43 stations in Kruger we filtered for those stations with <10% missing daily rainfall records, resulting in 23 stations with a reliable data collection history from 1981-2015 (Fig. 3.1). We obtained additional rainfall records for 39 stations outside of Kruger, within 100 km of the boundary, with a similar rate of <10% missing daily records (SAWS 2012). Another 12 stations from Kruger and 47 from SAWS, containing >10% but <20% missing values, were combined for cross-validation. In total we collated daily rainfall records from July 1981 to June 2015 for 62 rain gauges for model training and 59 rain gauges for model validation (total n=121). Rainfall records were reclassified into rainfall years (01 July to 30 June) rather than calendar years to capture a full dry and wet season per rain year i.e. in Kruger rainfall is generally restricted to December, January and February months, with little falling in June or July (*Fig. S3.1 in Appendix S3*).

3.2.2.2. Covariates: CHIRPS, DEM and DIOC

Daily and monthly CHIRPS GeoTIFF data were downloaded for the period July 1981 to June 2015 from the Climate Hazards Group (GHCN) data portal (Funk *et al.* 2015). CHIRPS is a gridded global rainfall surface product, which combines local station data with satellite rainfall estimates to produce a moderate resolution (~ 5 km), long-term precipitation dataset (Funk *et al.* 2015). Being a global product, Kruger's rain gauges are poorly represented in the GHCN's network of climate stations i.e. only three stations inside Kruger's boundary and another two SAWS stations within 2 km of the park boundary are represented in GHCN (Menne *et al.* 2012). Resulting daily (n=12418) and monthly (n=408) CHIRPS GeoTIFFs were then stacked and the

CHIRPS rainfall values extracted for each climate station locality (Hijmans, 2015). Ground elevation values were also extracted from a 5m Digital Elevation Model (DEM) (Van Niekerk, 2012) for the same 62 sites and the straight-line distance to the Indian Ocean coastline (DIOC) calculated. DEM and DIOC were included here because the combined effects of elevation and distance to the warm Agulhas current are expected to increase rainfall. More specifically, as the warm inland air meets the cooler sea air and the orographic effect of topography forces this air upwards, moisture condenses forming rain (Aalto *et al.* 2013).

3.2.3. Statistical analyses

3.2.3.1. General rainfall trends

Mean annual rainfall (MAR) summaries from 1910 to 2015 were extracted from Kruger's rainfall records, from which the long-term annual mean (541 mm) was calculated, along with a three-year moving average. These summaries were derived from a variable number of stations across Kruger for different years, for example MAR in 1910 was calculated using 1 station while 2015 comprised 22 stations. A continuous Morlet Wavelet Transform of mean monthly rainfall from July 1981 to June 2015 was then preformed to identify temporal frequency and variance patterns in Kruger's rainfall (Chan 2000). Wavelet analysis is an established tool for climate research because of its ability to decompose non-stationary signals, like rainfall, into time-frequency representations using the wavelet power spectrum (de Jongh *et al.* 2006; Unal *et al.* 2012). The spectrum depicts the relative strengths (variance on z-axis) of rainfall frequencies (months on y-axis) smoothed across time steps (years on x-axis) to deliver a contour image illustrating rainfall periodicities (Chan 2000).

3.2.3.2. Spatiotemporal regression surfaces

Missing daily rainfall records were first filled using a nonparametric imputation procedure with random forests (Stekhoven, 2013). In this way missing values from our 62 stations were filled using a random forest model with the observed daily rainfall measurements and related CHIRPS records (see Stekhoven and Buehlmann 2012 for full methodological detail). This process yields an 'out-of-bag' error estimate, for which our data had a 0.001% error rate expressed as a normalized root mean squared error (NRMSE) of rainfall in millimetres. The filled data series was subsequently summed by year and month (year-month) to produce monthly summaries (n=12) for each station (n=62) and year (n=34). A full 1 km^2 spatiotemporal grid (raster) was then generated over Kruger for 12 months by 34 years (n=408) and the associated monthly CHIRPS, DEM and DIOC values extracted. Our response variable (rainfall) was therefore known at some dispersed localities (n=62) across the study area for the study period (n=408) while our explanatory variables (CHIRPS, DEM and DIOC) were known over the full spatiotemporal domain (Kilibarda *et al.* 2014). A correlation matrix confirmed no serious problems of collinearity between covariates that could cause overinflated standard errors (*Fig. S3.2 in Appendix S3*). Importantly however, CHIRPS, DEM and DIOC are all spatial covariates and therefore may be collinear because of their geographic position, thus making them inherently spatially autocorrelated (see latitude and longitude entries in *Fig. S3.2 in Appendix S3*). We accounted for both spatial and temporal autocorrelation by including a nested rational quadratic correlation structure (corRatio) which captured the dependence between observations close in space (*u*) and nested in time (*t*) (Hefley *et al.* 2017). Rainfall and thus its relationship with our covariates are also expected to be non-stationary.
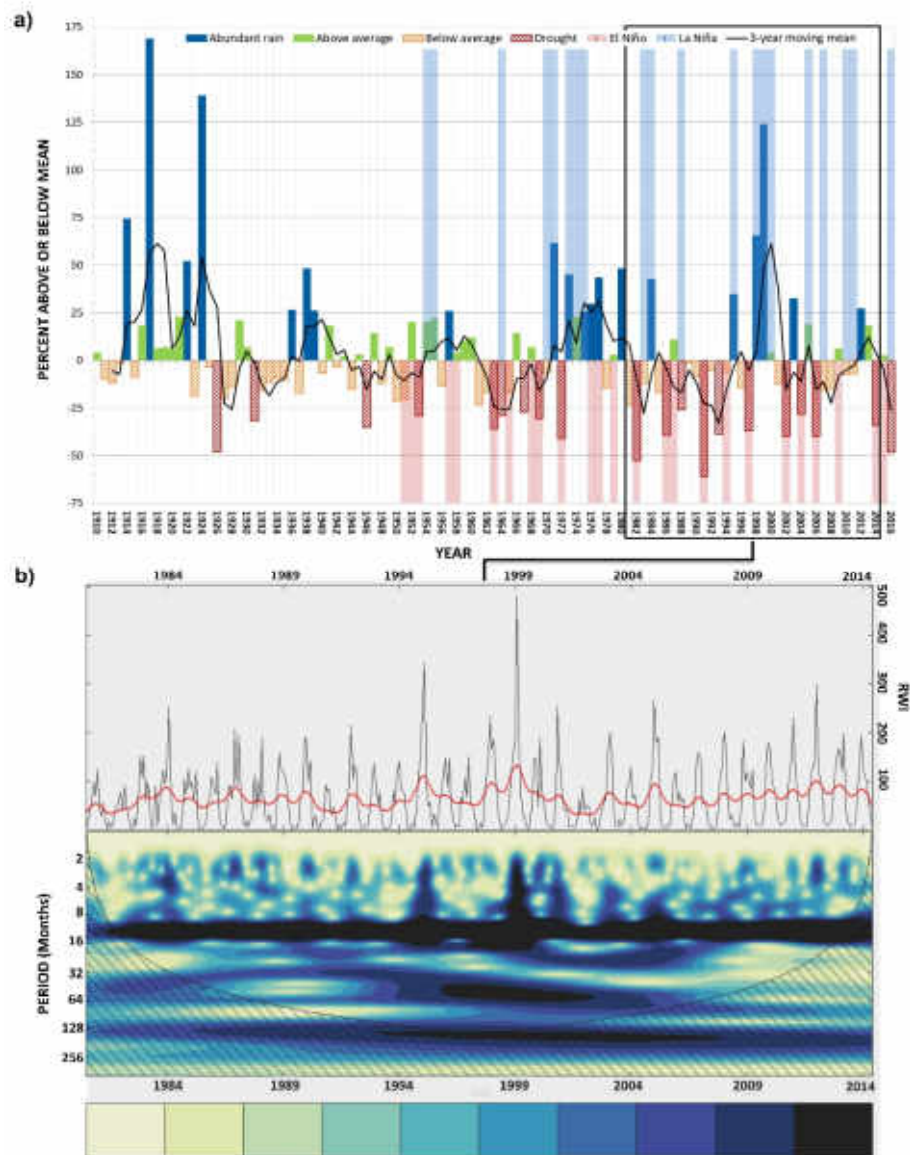
Fig. 3.2: Long-term patterns of a) annual and b) monthly rainfall (mm) of Kruger climate records: a) Deviation of rainfall from long-term annual mean for the past 105 years. X-axis labels represent climatic years (e.g. 1910 = July 1910 to June 1911). Weak to very strong El Niño years are marked with vertical bars below the zero line while weak to strong La Niña years are marked with vertical blue bars extending above the zero line according to Huang *et al.* (2017). b) Continuous Morlet Wavelet Transform of monthly mean rainfall from July 1981 to June 2015. The top panel shows rainfall (mm) over time with a smoothed spline (trend) over 20 years (f = 0.5; nyrs = 20). The bottom panel shows a filled contour plot of the continuous wavelet transform. Colours represent the power (Power^2) of the signal in regions of interest. Dark colours depict more dominant cycles or concentrated powers compared to lighter colours. Any information falling inside the hatched region is outside the "cone of influence" and should be ignored (Bunn *et al.* 2016).

We accounted for this non-stationarity using a General Additive Mixed Effects Model (GAMM) which allows the relationship of our measured rainfall and CHIRPS to change smoothly across continuous levels of DEM and DIOC (spatially) and time (seasonally and annually). In this way our measured rainfall response is explained by its non-linear relationship with CHIRPS, DEM and DIOC over space, seasonal cycle (within year) and longer term trend (between years), including both fixed and random effects (Zuur *et al.* 2009).

$$\sqrt{rain_{ut}} = \alpha + f_1(chirps_{ut}) + f_1(dem_u) + f_1(dioc_u) + f_2(mnth_t) + f_3(year_t)$$
$$+ f_4(year_t, mnth_t) + f_5(chirps_{ut}, dem_u) + f_5(chirps_{ut}, coast_u)$$
$$+ f_6(chirps_{ut}, year_t) + f_6(chirps_{ut}, mnth_t) + \varepsilon_{ut}$$

[1]

Specifically, we used different Cubic Regression Spline (CRS) smoothing bases to estimate *rain* (rainfall in mm) at location u (u = 1 to 62) and time t (t = 1 to 408). Firstly, a standard CRS [f_1] was used for *chirps* (CHIRPS), *dem* (DEM) and *dioc* (DIOC). A cyclic CRS [f_2] was then used for *mnth* (month) with 12 pre-assigned knots, and again a standard CRS [f_3] for *year* (rainfall year) with 34 pre-assigned knots. The random effects caused by interactions between variables were estimated using tensor product interaction terms, namely [f_4] for *year* and *mnth* with CRS and cyclic CRS smoothers respectively; [f_5] for *chirps, dem* and *dioc* with Gaussian process (kriging model) smoothers which account for the non-linear effect DEM and DIOC have on the contribution of CHIRPS to the fitted rainfall response; and finally [f_6] for *chirps, year* and *mnth* with a thin plate regression spline, cyclic CRS and CRS smoothers to account for seasonal cycles and longer term trends. ε represents i.i.d random variables expressed as N(0, $\sigma^2\Lambda$) with Λ describing the residual autocorrelation nested within time t and location u using corRatio (Wood 2006).

A variety of model structures were tested until ultimately the model with the lowest Akaike Information Criterion (AIC) was selected as the best predictor of Kruger's spatiotemporal rainfall patterns (Zuur *et al.* 2009). Described above **[1]**, predictions generated from this model were based on the full 1 km^2 spatiotemporal grid of covariates for Kruger. Cross-validation of results was performed using a Pearson's product-moment correlation of predicted monthly rainfall surface values with ground measurements from 59 stations held back for model validation. The Root Mean Squared Error (RMSE) is also reported, providing a good overall measure of model performance (Aalto *et al.* 2013). Final outputs were saved as 408 interpolated 1 km^2 surface grids describing Kruger's monthly rainfall patterns from 1981-2015. All analyses were conducted using statistical software R (version 3.1.3; R Core Team 2016), and associated R packages referenced in the text.

3.2.3.3. Spatiotemporal variations in rainfall

We described the seasonal (within-year) and longer term (between years) trends in the resulting rainfall surface layers using another GAMM with spline interactions. Specifically, the within year seasonal effect (t_1= 1 to 12 months) of our predicted monthly rainfall was allowed to vary smoothly with a between year trend effect (t_2= 1 to 34 years) over space (u) (Wood 2006, Zuur *et al.* 2009; Van Rij *et al.* 2015) as follows:

$$\sqrt{\widehat{rain}_{ut}} = \alpha + f_1(mnth_t) + f_2(year_t) + f_3(mnth_t, year_t) + f_4(x_u, y_u) \\ + f_5(x_u, y_u, mnth_t) + f_5(x_u, y_u, year_t) + \varepsilon_{ut}$$

[2]

Where $\widehat{rain}$ is the GAMM **[1]** estimated measurement of rainfall at location u (latitude y and longitude x) and time t. The seasonal cycle *mnth* and overall trend *year* were modelled as f_1, a cyclic CRS and f_2, a standard CRS with 12 and 34 knots. f_3, the tensor interaction thereof was

included to reflect how rainfall responds to different combinations of month and year in comparison to the overall trend and seasonal cycle in f_1 and f_2 (Wood, 2006). A thin plate CRS f_4, of the x, y coordinates at location u, was also included to examine the distribution of monthly rainfall across Kruger's landscape. The amount by which this pattern differs over time was analysed using f_5, a tensor interaction of x, y coordinates at location u with *mnth* and *year* at time t.

3.3. RESULTS

3.3.1. General rainfall trends

As expected, Kruger's rainfall patterns are cyclical in nature, varying seasonally from winter to summer and oscillating between wet and dry cycles (Fig. 3.2). Upon inspection of annual rainfall deviations from long-term means for the past 105 years, wet and dry cycles appear to occur about every 5 years (Fig. 3.2a). From Fig. 3.2a it appears these high and low rainfall periods generally match La Niña and El Niño years (see *Fig. S3.3 in Appendix S3* for Kruger's MAR in relation to ENSO events). Patterns become clearer with a continuous Morlet Wavelet Transform of mean monthly rainfall from July 1981 to June 2015 (Fig. 3.2b). Results show the most significant pattern persists at an inter-annual scale of 10-16 months (Fig. 3.2b). Short term noise dominates monthly scale patterns with high rainfall years blurring wet and dry season extents. For example, the extreme rainfall year 1999/2000, during which Kruger experienced severe flooding, shows significantly concentrated power (darker shades) regions already from the third month through to the twentieth (Fig. 3.2b). With the occurrence of less extreme rainfall events over the last 10 years, inter-annual rainfall patterns are clearer. However, the power band between 10-16 months does appear to be widening slightly, suggesting seasonality may be shifting.
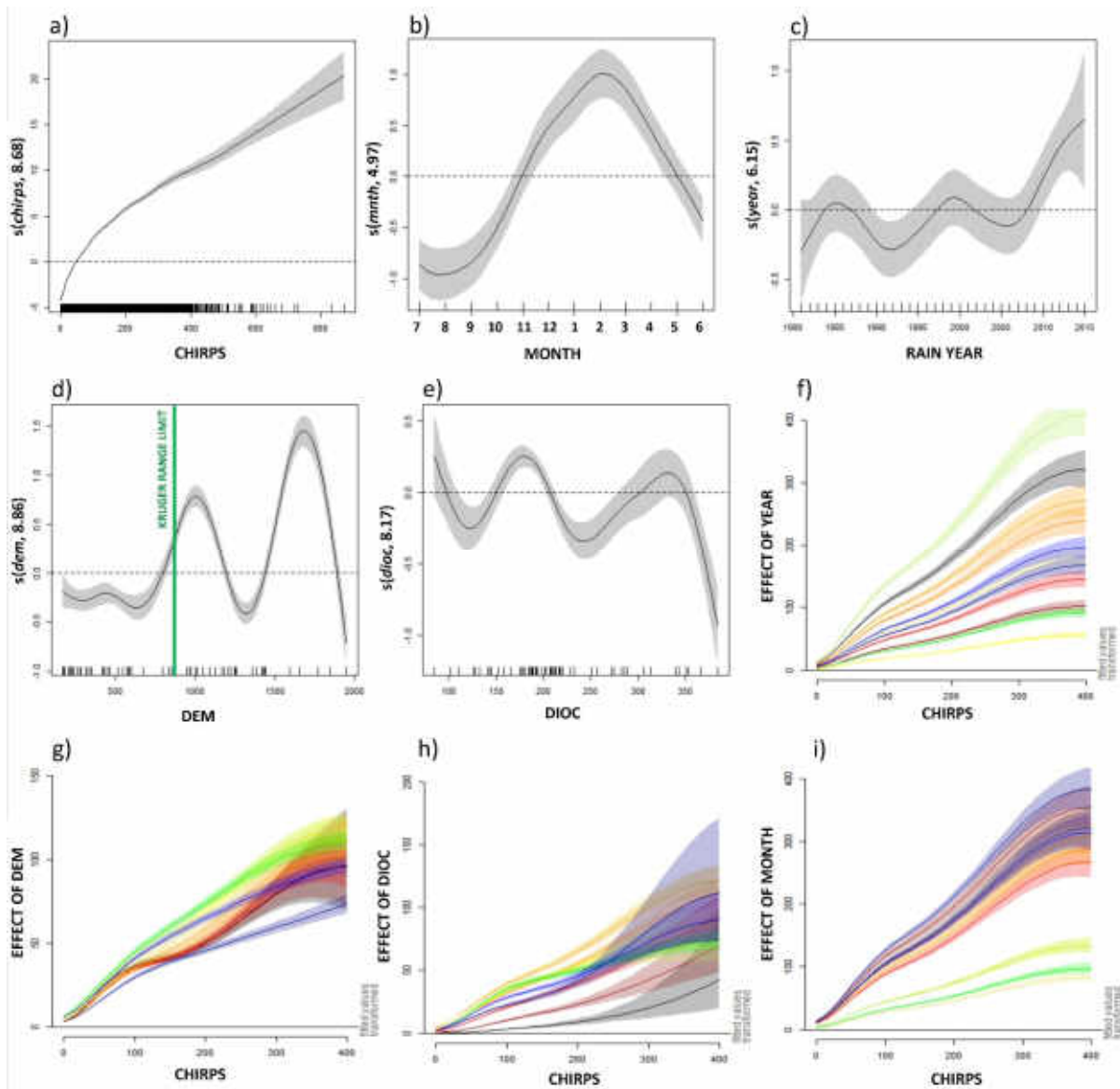
Fig. 3.3: Results of GAMM, illustrating the varying magnitudes of the contribution (effect) of different covariates to the fitted rainfall response, centred on zero where appropriate (dotted line). Solid lines represent the estimated smoothing for a) CHIRPS; b) rainfall month (season) and c) year (long-term trend); d) elevation; and e) distance to the Indian Ocean coastline. The influence of elevation; distance to the coastline; season and year, on the contribution of CHIRPS to the fitted rainfall response are displayed in panels g); h); i); and f) respectively. Shaded areas depict the 95% point-wise confidence bands. The different shades depict these confidence bands for selected f) years 86/87/88/91/92/95/96/99/00/05; g) DEM values 200/300/400/500/600/700/800/1000/1200/1500 $_{MASL}$; h) months 1989-8/9/10/11/12 and 1990-1/2/3/4/5/6 and; i) distances to the coast 100/120/140/160/180/ 250/300/350/380/400 km.

A significant 4-5 year cycle (48-60 months) persists from 1997/1998 until 2001/2002 along with a 12-15 year cycle (144-176 months) from about 1998/1999 until 2005/2006. The 12-15 year cycle is however outside of the wavelet plot's "cone of influence" and therefore requires more data to interpret correctly (Fig. 3.2b ; Bunn *et al.* 2016). The spline smoothed trend line suggests no clear long term trend is visible from 1981 to 2015 (Fig. 3.2b).

3.3.2. Spatiotemporal regression surfaces

Model selection was based on AIC ranks, where the model with the lowest AIC was considered the best model of Kruger's rainfall (See **[1]** for selected GAMM equation and *Fig. S3.4 in Appendix S3* for model diagnostics). The non-linear trend of time and space with CHIRPS, DEM and DIOC and a temporally nested spatial autocorrelation structure explained 73% of the deviance (R^2) in Kruger's monthly rainfall (*Table S3.2 in Appendix S3*). The contribution of CHIRPS, DEM and DIOC were significantly non-linear ($P < 0.001$) with all estimated degrees of freedom (edf) > 8.0, thus precluding the use of standard linear regression techniques (Zuur *et al.* 2009; *Table S3.2 in Appendix S3*). The smoothed seasonal and longer term trend effects were also significant ($P < 0.001$; *Table S3.2 in Appendix S3*). CHIRPS was strongly positively related to measured rainfall (Fig. 3.3a), while the effects of DEM were more significant at higher altitudes falling outside of Kruger's altitudinal range of $200 - 840_{MASL}$ (Fig. 3.3d). DIOC elicited an unclear effect on rainfall (Fig. 3.3e) but its interaction effect on CHIRPS' contribution to rainfall response was significant ($P = 0.005$; Fig. 3.3h), as was that of DEM ($P < 0.001$; Fig. 3.3g). In other words, the relationship of CHIRPS with station measured rainfall varied significantly as a function of elevation and distance to the coastline.
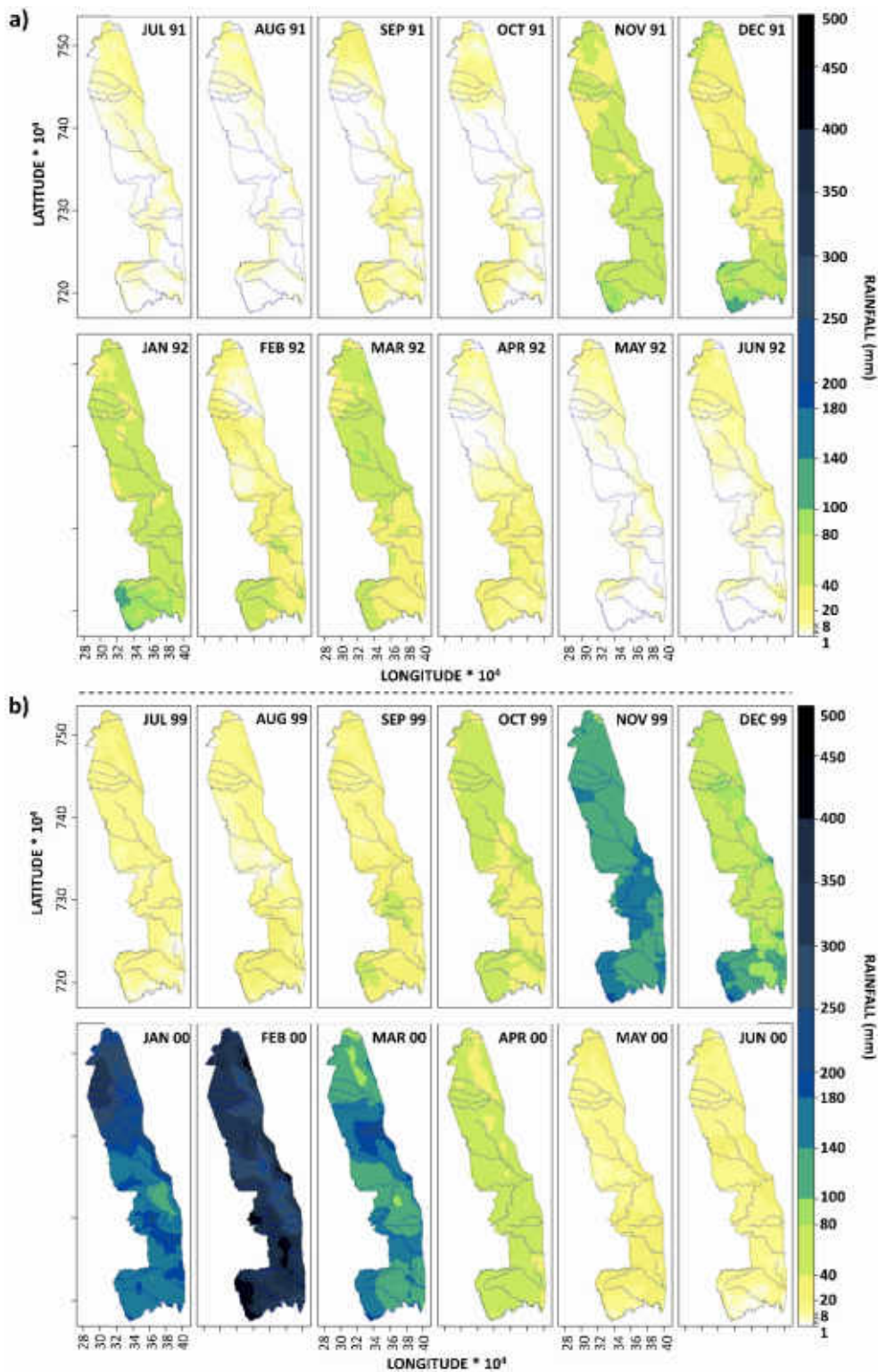
Fig. 3.4: Examples of monthly rainfall surfaces predicted from GAMM results on a full 1 km2 spatiotemporal grid of covariates. Panel a) shows rainfall patterns of drought conditions during rain-year 1991 (i.e. July 1991 to June 1992); b) shows rainfall patterns of abundant rain conditions during rain-year 1999 (i.e. July 1999 to June 2000; See *Animation S3.1 in Appendix S3* for full animation of results).

A strong seasonal cycle was clearly visible (Fig. 3.3b) with a more variable longer term trend showing decadal fluctuations in rainfall response (Fig. 3.3c). The non-linear effects of CHIRPS also varied significantly with season ($P = 0.025$; Fig. 3.3f) and year ($P < 0.001$; Fig. 3.3i).

Predicted rainfall surfaces, using GAMM [1] and the full 1 km^2 spatiotemporal grid of associated covariates, showed visible spatiotemporal changes to seasonal and annual rainfall (Fig. 3.4; see *Animation S3.1 in Appendix S3* for full animated results). Cross-validation of these regression surfaces against 59 model training stations (n=7645) confirmed predictions were accurate overall ($R^2 = 0.78$, $t = 107.5$, $df = 7643$, $P < 0.001$) with an RMSE error of 19.99 mm per year. The R^2 and RMSE did however vary over time, with higher rainfall years generally exhibiting smaller R^2 variations and greater RMSE variations (*Fig. S3.5 in Appendix S3*).

3.3.3. Spatiotemporal variations in rainfall

There exists a clear seasonal cycle ($P < 0.001$, edf: 10; Fig. 3.5a) with strong evidence of longer term patterns that vary significantly over 10 and 20 year cycles, making it difficult to interpret a general overall trend ($P < 0.001$, edf = 9; Fig. 3.5b). The interaction of rainfall year and month was significant ($P < 0.001$; edf = 90) and showed patterns of extreme rainfall conditions (Fig. 3.5c). In fact taking a ruler to Fig. 3.5c, beginning between August (8) and September (9), one could almost draw a perfect diagonal of high rainfall period moving later in the season until about April (4) 2007. Periods with earlier rainfall appear in sync with documented La Niña events while the El Niño link to lower rainfall periods is less clear (Fig. 3.5c and *Fig. S3.3 in Appendix S3*).
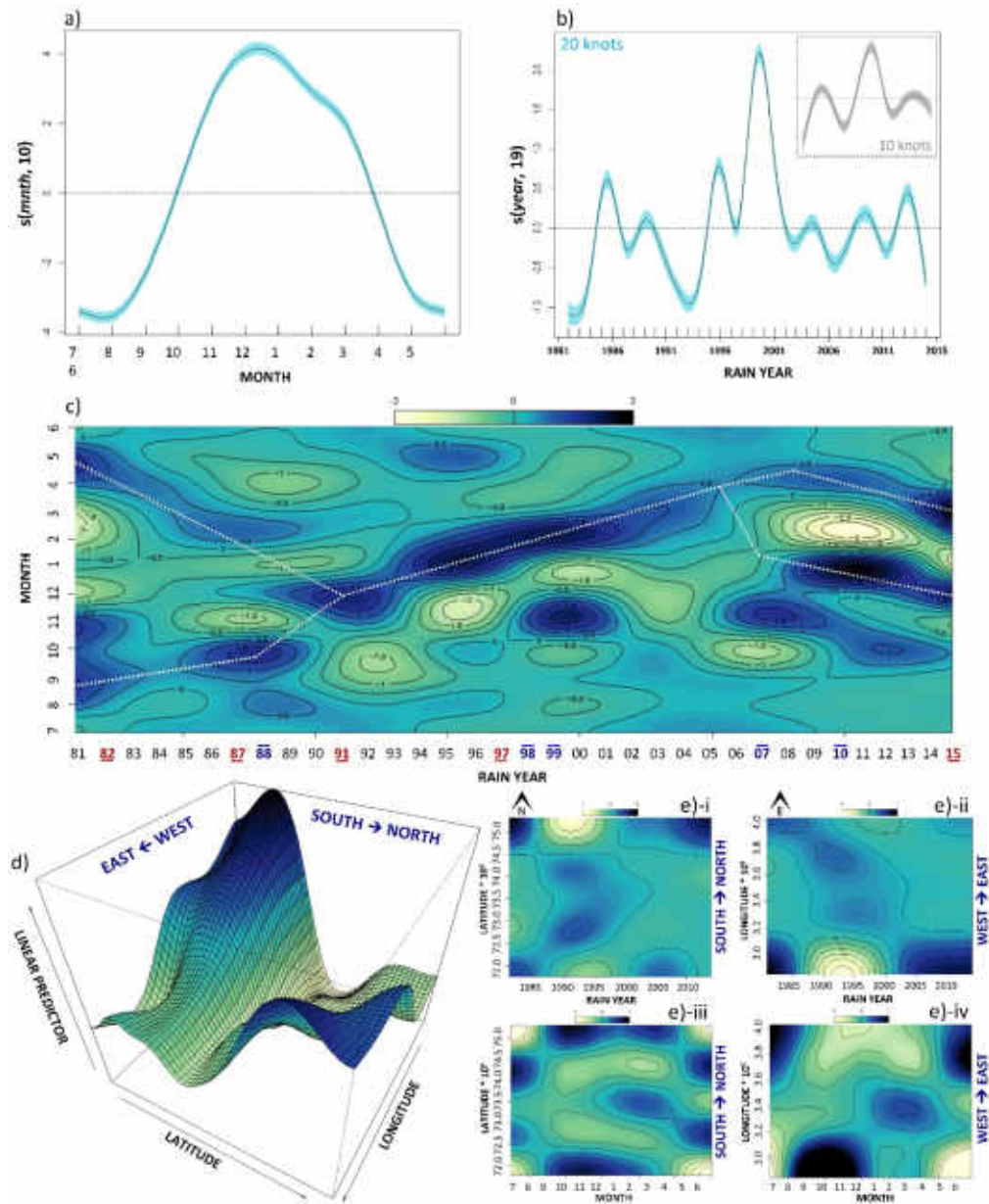
Fig. 3.5: Visualisation of GAMM results indicating the a) seasonal cycle of low (below dotted line) and high (above dotted line) rainfall months; b) Long-term trend in rainfall with oscillating high and low rainfall periods; c) contour plot of the partial nonlinear interactions of rainfall year and month showing the amount by which the fitted monthly rainfall is adjusted from the overall trend and seasonal cycle for any combination of month and year. Strong El Niño years are marked with _ below the year label and strong La Niña years with ‾ above year on the x-axis; d) perspective plot of the interaction effect of longitude (x) and latitude (y) on rainfall response; e) partial contour plots of latitude (south to north) and longitude (west to east) tensor product interaction terms showing the amount by which the fitted monthly rainfall is adjusted from the overall trend and seasonal cycle from south to north (i, iii) and west to east (ii, iv).

Rainfall response also differed significantly ($P < 0.001$, edf = 29) across space, with the effect of location (x, y) being significantly non-linear (*Table S3.3 in Appendix S3*) as rainfall varied from North to South and West to East (Fig. 3.5d). Rainfall was highest in the far South-West and lowest in the mid North-Western parts of Kruger (Fig. 3.5d). These patterns however changed annually and seasonally (Fig. 3.5e). Distinct periods of high rainfall were visibly more pronounced in the South compared to the North (Fig. 3.5e-i and iii). Similarly, higher rainfall periods were more pronounced in the West compared to those experienced in the East (Fig. 3.5e-ii and iv) (see *Table S3.3 in Appendix S3* for a full description of model results). These results suggest more localised or regional changes may dominate Kruger's rainfall dynamics than previously studied.

3.4. DISCUSSION

A recent assessment by the IPCC rated Africa as having a "high and significant" risk of climate-change, and thus should expect severe water resource constraints in the near future (IPCC, 2014). This desiccation is further supported by Chen and Chen (2013) and Rubel *et al.* (2017) in their reassessments of Köppen's (1930) global climate classification for the period 1901 to 2010, which shows much of Kruger becoming drier. Adding to these results we found a more noticeable spatiotemporal change in the short to medium-term seasonal cycles of low-high rainfall, rather than a clear increasing or decreasing trend. Our findings are supported by a recent larger scale assessment of climate change across all South African National Parks (SANParks) by van Wilgen *et al.* (2016), who found increased rainfall variability in parks to the East. Similarly, they found no significant annual trend in Kruger's rainfall but suggest an increase in seasonality with longer dry periods (van Wilgen *et al.* 2016). At a finer scale we found this shift to be spatiotemporally dynamic.

Fig. 3.5c illustrates the seasonal shifts in rainfall patterns as they are affected by strong La Niña events. Philippon *et al.* (2014) found similar patterns for Southern Africa as vegetation greenness (NDVI) was dampened during El Niño and increased during La Niña events. Fig. 3.5d shows the distribution of rainfall across the Park from West (e.g. Pretoriouskop) to East (Mozambique border) and from South (e.g. Malelane) to North (e.g. Pafuri). As described by Gertenbach (1980) and Zambatis (2003), the more southern latitudes generally receive higher rainfall, as do the more western longitudes. However, Fig. 3.5d suggests this spatial pattern is clearly more complex than can be adequately accounted for by regional averaging of the past. Moreover, these spatial patterns are also continually changing with both high and low rainfall periods lengthening or shortening, and/or shifting outside of recognised wet/dry season windows over the short to medium term (Fig. 3.5e). For example, the Northern latitudes have gone through extreme wet, dry, wet cycles in comparison to the South from 1981 to 2015 (Fig. 3.5e-i). This pattern is mirrored in the Western longitudes (Fig. 3.5e-ii), suggesting the far North-West of Kruger is undergoing significant spatiotemporal rainfall changes over the short to medium term.

A strong seasonal shift is also apparent in the west, where October (early season) rainfall is generally increasing while June (mid-dry season) is decreasing (Fig. 3.5e-iv). Similarly, in the far north and south of Kruger, summer rainfall is generally increasing while winter rainfall is decreasing (Fig. 3.5e-iii). In contrast, Kruger and Nxumalo (2017) analysed the historical rainfall trends in SA from 1921-2015 and found no significant trends in seasonal rainfall totals for our area. They did however find a significant downward trend in total annual rainfall for the Northern and Southern regions of Kruger, although this signal was not significant for individual stations in the area (Kruger and Nxumalo 2017). Our results suggest that these linear averages conceal seasonal and spatial rainfall trends at the local level in Kruger. If wetter seasons and areas are becoming wetter while drier seasons and areas are becoming drier, as seen in Figs.

3.5c; 3.5e-i; 3.5e-ii; 3.5e-ii and 3.5e-iv, park-wide averages would indeed obscure these changes. Taken together these shifts in extremes could lead to an increased risk of droughts or floods (Pohl *et al.* 2017), like the floods experienced in Kruger in 2000 and 2012 (Knight and Evans 2017).

Though these spatiotemporal changes may obscure broad scale trends (e.g. Kruger and Nxumalo 2017; van Wilgen *et al.* 2016), they will continue to have significant effects on ecosystem processes like species population dynamics and fire. As a result, they should form an important component for management planning. For example, in understanding these spatiotemporal dynamics, park management can better explore the effects of different climate change forecast scenarios, by examining the environmental response to past extreme climatic events. The severe drought of 1991/1992 for example had significant effects on woody and herbaceous plant species composition and consequently predator-prey dynamics, as well as a negative effect on river geomorphic diversity (Heritage and van Niekerk 1995; Viljoen 1995; Zambatis and Biggs 1995). Similarly, the large Sabie River flood in February 2000 changed river geomorphology and associated riparian vegetation and species distribution patterns (Parsons *et al.* 2006). Future studies might consider including the new high-resolution (1 km^2) global cloud cover product described by Wilson and Jetz (2016). This new dataset combines Moderate Resolution Imaging Spectroradiometer (MODIS) imagery from 2000-2014 to derive long-term cloud-cover dynamics aimed at improving spatial autocorrelation errors, typical of interpolated climate data, towards a better spatiotemporal understanding of global biodiversity and ecosystem properties (Wilson and Jetz 2016).

Rainfall is indisputably a significant driver of numerous bottom-up and top-down drivers of biodiversity in protected areas (Garcia *et al.* 2014). It is strongly associated with vegetation dynamics and thus ungulate population dynamics (Owen-Smith and Ogutu 2003; Dunham *et al.* 2004), predator densities and demography (Celesia *et al.* 2010) and disease outbreaks (e.g.

malaria, Colón-González *et al.* 2016). Reductions in rainfall can have severe implications for the provision and management of artificial water, which in itself may prove to have far-reaching impacts (Smit 2013). In light of the landscape scale changes we found, research and monitoring in Kruger will need to become more spatiotemporally dynamic with climate considered more as a multiscale driver than a general stratification template.

3.5. CONCLUSION

In Kruger, the importance of rainfall monitoring was stressed as far back as 1901, which is reflected in the current research objectives describing rainfall as a major factor effecting biodiversity (SANParks 2008). Despite its obvious importance, funds for inventorying and long-term monitoring are increasingly restricted as focus shifts to other conservation priorities (e.g. anti-poaching). Amplified by the 'publish-or-perish' mentality and the need for rapid data collection and analysis, the time-cost-benefit of maintaining long-term *in situ* monitoring programs continues to wax and wane (Sarewitz 2016). However as we have shown, local rain gauge observations in combination with satellite derived rainfall estimates, can both supplement global products for local finer scales studies as well as potentially improve the accuracies of global assessments. To support these initiatives, we provide our data as an open source gridded rainfall surface dataset for Kruger from 1981-2015 to encourage the development of a better understanding of rainfall-driven system response patterns (http://dataknp.sanparks.org/sanparks/metacat/judithk.111609.2/sanparks).

In light of projected climate change impacts, protected areas in particular may become increasingly susceptible as hard park boundaries act as physical barriers to animals seeking to move in response to bioclimatic range shifts. Without adaptive conservation strategies and climate-change conscious spatial planning, these systems may ultimately transform into undesirable states as a consequence of altered species dynamics. Since the effects of altered

climatic conditions will be landscape and species specific, studies of local climate change patterns need to be spatiotemporally explicit. Rainfall for example, will act as a driver of change at multiple scales and should be assessed as such when used to make management decisions.

Space is not 'irrelephant': Spatiotemporal distribution of elephants in response to density, rainfall, rivers and fire

4

Space is not 'irrelephant': Spatiotemporal distribution dynamics of elephants in response to density, rainfall, rivers and fire in Kruger National Park, South Africa

This chapter is currently in review as:

MacFadyen S, Hui C, Verburg PH and Van Teeffelen, AJA (*in Review*) Space is not 'irrelephant': Spatiotemporal distribution dynamics of elephants in response to density, rainfall, rivers and fire in Kruger National Park, South Africa. *Diversity and Distributions* [manuscript ID: DDI-2018-0047]

Author contributions: I conceived the research idea, collated the data, designed the methodology, analysed the data and wrote the manuscript with the scientific leadership of CH, PV, AVT. All authors contributed critically to manuscript drafts and gave final approval for publication.

ABSTRACT

Aim: African elephants are ecosystem engineers. As such their long-term patterns of distribution and abundance (i.e. space-use intensity) will influence ecosystem structure and function. We elucidate these patterns by analysing the spatiotemporal dynamics of an increasing elephant population in relation to key ecological drivers: rainfall, distance to major rivers and time since last fire. In doing so, we unveil population level resource selection functions underlying elephant space-use intensity, and identify significant changes to long-term patterns of density and group-type (bull vs. herd) probabilities.

Location: Kruger National Park, South Africa

Methods: Using almost three decades of census records (1985-2012), we applied Multiple Point Process Models to assess the influence of rainfall, rivers and fire in shaping elephant space-use. In addition, significant changes in long-term patterns of elephant density and group-type were identified using kernel density estimates and the spatially-varying probabilities of encountering bull vs. herd groups.

Results: Bull and herd groups are no longer clearly segregated and available empty-space has become limited. Bull and herd elephants have dichotomous resource selection functions, in that bulls concentrate in areas receiving lower rainfall but more frequent fires while herds concentrate in higher rainfall areas experiencing less frequent fires. Both bull and herd groups concentrate closer to major rivers, emphasizing rivers as important spatial drivers. Overall, densities increased most significantly closer to rivers and in areas experiencing fewer fires. Fire was also a strong agent of group-type change, as the probability of finding bulls, contrary to herds, significantly increased as fire return periods shortened.

Main conclusions: Elephant distribution and abundance patterns have homogenised in response to increased space limitations, with group-specific, fire-driven patterns emerging in the distribution of bull and herd groups. These results can be used to manage elephant space-use through establishing possible refuge areas and developing empirical elephant-impact research in future.

4.1. INTRODUCTION

African elephants (*Loxodonta africana*) are ecosystem engineers that alter and create habitats as they select for preferred resources in the landscape (Pringle 2008; Ripple *et al.* 2015). Their role in shaping the structure and function of habitats is therefore a central research theme for Southern African states where elephant populations are thriving (Kerley *et al.* 2008; IUCN 2015). The disparity between states in terms of elephant conservation management is however very broad, even in the face of heightened concerns over increased elephant poaching and illegal trade (Wittemyer *et al.* 2014; IUCN 2015; IUCN 2016; MIKE 2016). For example, as Central Africa fights to protect elephants from extinction, protected areas in Southern Africa struggle to balance the conservation of this iconic species against their potentially damaging effects to the environment and other species (Kerley *et al.* 2008). The Kruger National Park (Kruger) in South Africa is one such protected area, with elephant numbers rising from ~10 animals in 1905 to over 17 000 in 2015 (Ferreira *et al.* 2017). As these numbers continue to grow, questions persist about the effects of high elephant densities on integrated biodiversity outcomes (Ferreira *et al.* 2012; Ferreira *et al.* 2017). Key concerns include changes to vegetation structure, associated species diversity and distribution patterns, system processes such as fire regimes, and the exacerbation of potential human-animal conflicts (Kerley *et al.* 2008; Scholes and Mennel 2008; SANParks 2008; Ferreira *et al.* 2012; Rutina and Moe 2014). Understanding the long-term distribution dynamics of elephants is a fundamental component for elephant conservation management strategies that aim to address these concerns.

Over the years studies conducted on Kruger's elephants have helped develop much of today's general understanding of elephant distribution dynamics and their role in the ecosystem (e.g. van Aarde *et al.* 1999; Grainger *et al.* 2005; Codron *et al.* 2006; de Knegt *et al.* 2011; Asner and Levick 2012). Despite this cache of knowledge, Kruger's new elephant management plan (Ferreira *et al.* 2012) distinguishes gaps in our understanding of the population level

drivers of elephant distribution and abundance patterns. Ferreira *et al.* (2012) strongly recognise the complexity of elephant conservation and call for biogeographical research into possible mechanisms and drivers of elephant distribution and abundance in Kruger. Dubbed space-use intensity, the patterns of elephant distribution and abundance are described as an expression of an elephant's response to key resources, as well as anthropogenic and natural disturbance events (de Knegt *et al.* 2011). Moreover, elephant foraging behaviour and associated distribution patterns are known to be sexually dimorphic (Stokke and du Toit 2002; Smit *et al.* 2007; de Knegt *et al.* 2011). This simply means bull and mixed herd groups will use space differently as a result of different social or habitat cues (Ruckstuhl 2007). Elephant bull and herd groups are therefore expected to have varied responses to the spatial arrangement of key resources, disturbances in the landscape and the relative positions of other elephant groups.

Establishing key landscape drivers of the dimorphism (bull vs. herd) in elephant space-use intensity is important for developing resource selection functions that may guide future management actions (Ferreira *et al.* 2012; MacFadyen *et al.* 2013). In Kruger, key drivers may include rainfall variability (Birkett *et al.* 2012), surface water availability (Chamaillé-Jammes *et al.* 2007; Loarie *et al.* 2009), vegetation phenology (Young *et al.* 2009), topography and landscape heterogeneity (Grainger *et al.* 2005; Murwira and Skidmore 2005). Significant disturbance events may include elephant culling operations between 1966 and 1994 (Whyte 2001), the erection of more than 400 artificial water points from 1946 until 1995 (Smit 2013) and fire (Smit *et al.* 2013b, van Wilgen *et al.* 2014). Using a biogeographical approach, we study broad scale distribution and abundance patterns of elephants in Kruger from 1985-2012, in relation to the patterns of possible drivers. We posit that in distinguishing significant changes to these long-term patterns, we may determine where elephant impacts to shared habitats and associated species may potentially be most significant (Grainger *et al.* 2005; Valeix *et al.* 2011). Ultimately this should help focus research into the more empirical effects of high elephant

densities in confined areas. Our overall aim is therefore to examine the long-term changes to sexually dimorphic gradients of elephant space-use and identify underlying resource selection functions. Using almost three decades of elephant population data we investigate how the densities of bull versus mixed herd groups relate to changes in various environmental conditions, namely rainfall, distance to major rivers and fire frequency or return intervals. The influence of rainfall, rivers and fire in shaping elephant space-use is assessed using a Multiple Point Process Model (MPPM; Baddeley *et al.* 2015). Together with MPPM, we also diagnosed significant changes in long-term elephant distribution and abundance and group-type dominance patterns using kernel density estimates and the spatially-varying probabilities of encountering bull vs. herd groups. Specifically, we investigated i) what spatial processes govern the assembly of elephant bull versus elephant herd animals (elephant resource selection function), while controlling for density increase over time; ii) significant changes to long-term elephant distribution and abundance patterns (regardless of group-type) and; iii) significant changes to long-term elephant group-type distribution patterns (spatial probabilities of encountering bull versus herd elephants in the landscape).

4.2. MATERIAL AND METHODS

4.2.1. Study area

Kruger is South Africa's largest protected area (~ 20,000 km^2), located in the North-East of the country, bordering Zimbabwe and Mozambique. Falling within the savanna biome, Kruger is bounded by the Limpopo River in the North and the Crocodile River in the South. The area receives summer rainfall (long-term mean of 542 mm) which generally decreases from south to north and slightly increases from east to west (Gertenbach 1980). Temperatures are sub-tropical, ranging from 26.4 °C in summer (December - March) to 17.8 °C in winter (June - August) (Zambatis 2006). Historical elephant records begin with approximately 10 animals

recorded in 1905 (Pienaar *et al.* 1966), followed by an exponential increase in numbers from 1977 to 2015 (Fig. 4.1a) culminating in over 17 000 animals (Ferreira *et al.* 2017).

4.2.2. Data collation

4.2.2.1. Elephant records

Elephant population data have been collected annually in Kruger since 1962 (Pienaar *et al.* 1966), using aerial census techniques described in full by Whyte (2001) and later by Ferreira *et al.* (2017). In summary, helicopter counts were conducted annually between July and August for the whole park. Importantly, all results reported here are therefore representative of the winter distribution and abundance patterns of elephants in Kruger. We recognize that these patterns will vary seasonally (Codron *et al.* 2006; van Aarde *et al.* 2008), but since elephants utilise woody plants more heavily in these drier winter months (Codron *et al.* 2006; Thomas *et al.* 2008) data from this time period may be more relevant to understanding elephant impacts in future. We collated these census records from 1985 to 2012 (SANParks 2016) as point localities (*x, y*) georeferenced to Universal Transverse Mercator (UTM) zone 36 South, World Geodetic System 1984 (WGS84). Each point is characterized by the census year, elephant group type (bulls or mixed herd) and total number of elephants in each group (Fig. 4.1b and *Animation S4.1 in Appendix S4*). The resulting dataset represents mark-weighted localities of bull and mixed herd groups from 1985-2012 (group points n = 35117, individual animals n = 276306, years n = 28). From these we created a hierarchical data frame (hyperframe) containing 28 separate point pattern data frames for each year marked by group type and weighted by the total number of animals in each group (functions 1 – 3 in *Table S4.1 in Appendix S4*; Baddeley *et al.* 2015).
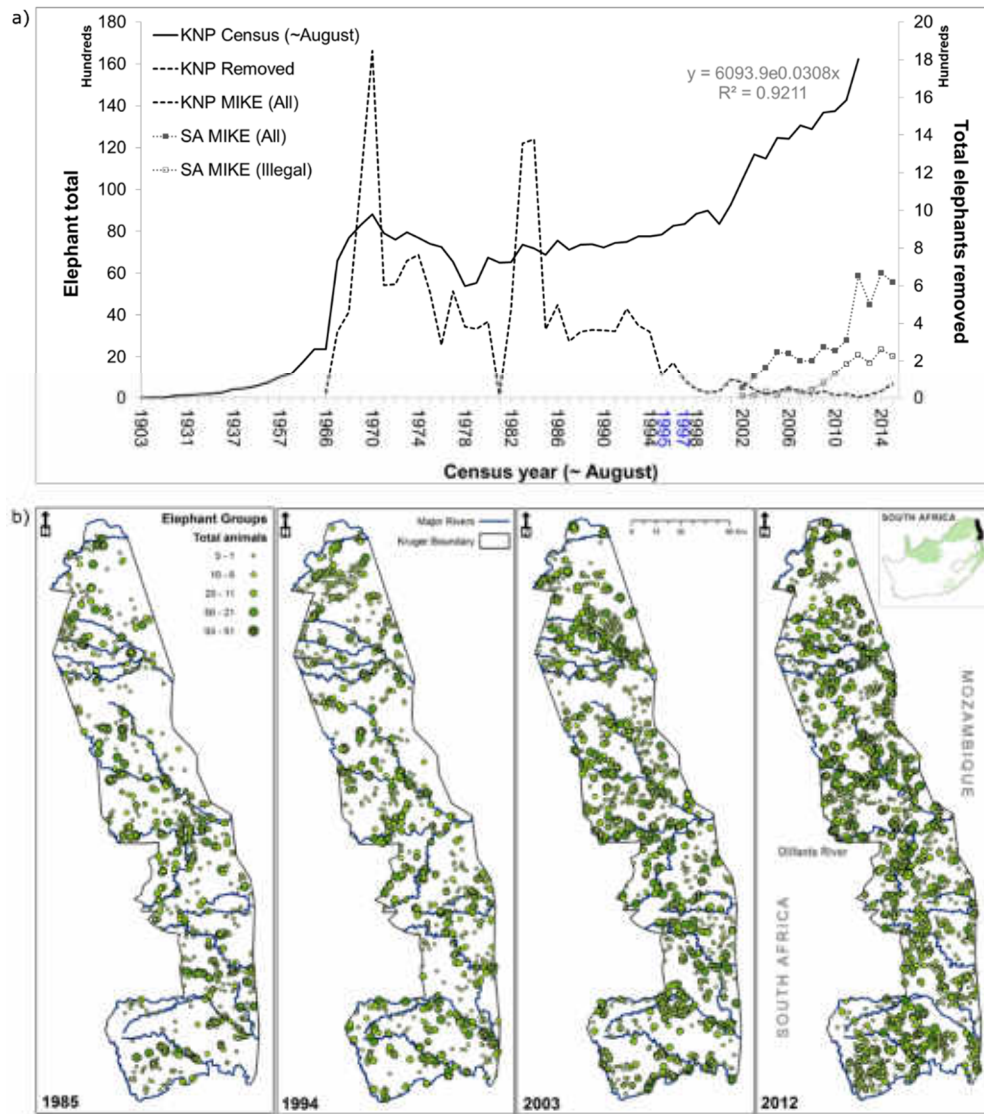
Fig. 4.1: Elephant populations in the Kruger National Park (KNP) from 1985-2012. Panel (a): Elephant population growth from 1905 to 2012 (solid line), with numbers of animals culled or translocated from 1966-2003, and carcasses recorded by the Convention on International Trade in Endangered Species of Wild Fauna and Flora (CITES) programme for Monitoring the Illegal Killing of Elephants (MIKE) from 2002-2015 (dashed lines; CITES 2016). Grey dotted lines with [■] markers represent MIKE records of all elephant carcasses for Southern Africa, while those marked with [□] represent MIKE records of illegally killed elephants in Southern Africa (MIKE 2016). The equation in grey-text on the top-right shows the exponential trend for increasing elephant numbers from 1977-2015 (y = 6093.9e$^{0.0308x}$; R^2 = 0.9211). Years marked in blue on the y-axis, represent the moratorium on large-scale culling operations (1995), and the start of KNP's artificial water-point closure program (1997; Whyte 2001; SANParks 2016). Panel (b): Elephant population maps for selected years in KNP: 1985, 1994, 2003 and 2012 (see Animation S1 for all years).

All point patterns and subsequent covariates were rescaled from UTM meters to kilometres to avoid singularity errors and simplify the interpretation of graphs (function 4 in *Table S4.1 in Appendix S4*). While our aim was to explain the natural variability in winter distribution and abundance patterns of elephants, we accept that some variability may in part be due to measurement error or sampling variation (Baddeley *et al.* 2015). However, we assume these effects to be negligible since the census methodology has remained unchanged since 1985 and considering elephants are highly mobile animals any small locational errors will be of little consequence.

4.2.2.2. Rainfall and distance to rivers

Rivers and rainfall are known to influence elephant movement and distribution response at different scales (Grainger *et al.* 2005; Chamaillé-Jammes *et al.* 2007; de Knegt *et al.* 2009).We therefore selected distance to all major rivers and annual rainfall as key spatial covariates of Kruger's elephant distribution and abundance patterns (Fig. 4.2a). Annual precipitation data (CHIRPS) were collated from the Climate Hazards Group data portal for the period 1983-2012 (Funk *et al.* 2015), these data were processed and stored as array entries in the hyperframe already containing the individual marked point patterns (functions 17, 19, 18 and 23 in *Table S4.1 in Appendix S4*). A three-year moving mean was then calculated for each year to capture the influence of not only the current but the preceding three years rainfall on vegetation resources and ultimately elephant distribution patterns (Birkett *et al.* 2012; Garstang *et al.* 2014). We used a three-year moving average to represent potentially longer term rainfall effects since we did not expect the winter distribution and abundance patterns of elephants to respond strongly to rainfall received in only a single preceding summer season.
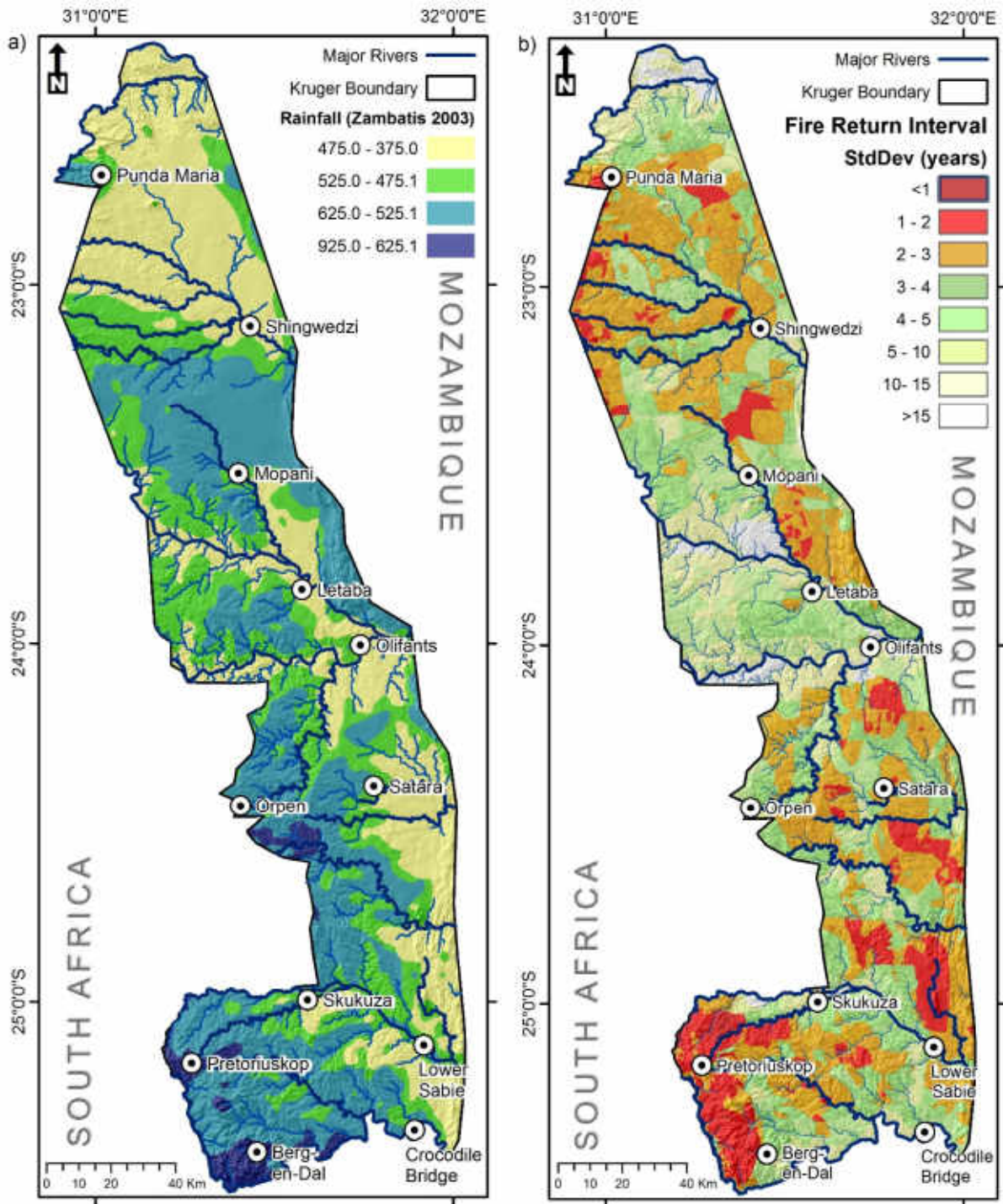
Fig. 4.2: Long-term mean annual rainfall and fire return intervals with major rivers in the Kruger National Park. Panel (a) Mean annual rainfall after Zambatis (2003) and Panel (b) Fire return intervals after Smit *et al.* (2013b) displayed in increments of standard deviation in the number of years since the last fire.

Our distance to rivers covariate was created using all major rivers (i.e. third order and higher), which are more likely to hold permanent water and support riparian vegetation favoured by elephants (Cullum and Rogers 2011). These rivers were imported as a data frame of spatial lines and converted into line segment patterns ultimately forming a distance to major rivers surface which was added as a function class to our hyperframe (functions 24, 10 and 11 in *Table S4.1 in Appendix S4*).

4.2.2.3. Fire return interval

The synergistic relationship between elephants and fire is well documented, i.e. fire stimulates elephant foraging activities while intensive browsing by elephants followed by fires can increase tree mortality rates (Dublin *et al.* McGlade, 1990; Shannon *et al.* 2011). In African savannas, the separate and compound effects of elephants and fire can therefore alter habitat composition and structure to the point where an ecosystem state may change, for example from a woodland to a grassland state (Dublin 1990; Asner *et al.* 2015; Levick *et al.* 2015). Fire return interval was therefore added to test whether longer or shorter fire return intervals had any effect on the point patterns of elephants in Kruger. Return intervals were calculated from Kruger's burn-scar geodatabase, which has polygon records of known fires from 1941 until the present (see Smit *et al.* 2013b and Govender *et al.* 2012). We overlaid all burn scar polygons from 1941-2012 and converted the resulting polygon attributes to a binary rasterstack (0 = no burn; 1= burn) (functions 20 and 17 in *Table S4.1 in Appendix S4*). A moving fire return table was computed by iteratively counting the intervals between fires for each pixel from 1941-2012 (Fig. 4.2b; Smit *et al.* 2013b). The fire return intervals were then added to the hyperframe of elephant point patterns as annual pixel image objects (functions 3 and 23 in *Table S4.1 in Appendix S4*).

4.2.3. Analysis

4.2.3.1. Elephant point patterns

Prior to running any regression analyses we tested whether the data violated standard statistical assumptions of homogeneity and stationarity. Furthermore, a Monte Carlo test of spatial segregation, an inhomogeneous empty-space function and a standardised form of the inhomogeneous cross-type L function, with border correction and a random labelling simulation expression was used to determine whether bulls and herd groups be treated differently in proceeding models (functions 8 and 9 in *Table S4.1 in Appendix S4*).

4.2.3.2. Elephant resource selection

We first investigated the spatial processes that may govern the assembly of elephant bull versus mixed herds in winter using the aforementioned spatial covariates: rainfall, distances to major rivers and fire return interval (i.e. higher/longer return intervals = fewer fires). To evaluate the influence of key resources, while still accounting for unknown random variability, we used a mixed-effects point process model for multiple point patterns (MPPM). MPPMs are similar in structure and output to generalized linear models. The key difference however is that the response variable is a series of point patterns of which the intensity is a function of different covariates (Baddeley *et al.* 2015). This means our response variable is essentially the spatial distribution of elephant densities from 1985-2012. Time since 1985 was included to control for the confounding effects increased densities would have on detecting general elephant resource selection functions. Distance to rivers, rainfall and fire return interval were included as fixed effects representing observable spatial covariates that may account for known variability in our point patterns (Baddeley *et al.* 2015). However, we also acknowledge the existence of random effects that are unobserved and will likely produce random or unknown variability in our point pattern processes (Baddeley *et al.* 2015). We therefore included census year as a random

variable to represent those unknown annual effects not accounted for by our covariates. Our mixed-effects point process model (function 12 in *Table S4.1 in Appendix S4*) was then fitted simultaneously to all point patterns using the following formula:

$$\lambda(u)_n = \exp(\beta_0 + m_{bh}\beta_1 S(u)_n + m_{bh}\beta_2 R(u)_n + m_{bh}\beta_3 F(u)_n + m_{bh}\beta_4 Y(u)_n + \alpha_n) \qquad \text{[1]}$$

where $\lambda(u)_n$ is the elephant point pattern (or space-use) intensity function for each year n (1985-2012), β_0 is the intercept, β_1; β_2; β_3 and β_4 are coefficients to be estimated, and $S(u)$; $R(u)$; $F(u)$ and $Y(u)$ are the effects of surface rainfall as a three-year moving average, distance to rivers, fire return interval and number of years from the start of the data record (1985) at location u and year n respectively. These fixed effects were conditioned upon elephant group type, i.e. points classified as bull m_b or mixed herd m_h elephant groups. Random effects α_n were included to account for unknown variability amongst years within each group type. With the above model specifications, the intensity of elephant space-use [$\lambda(u)_n$] was thus allowed to vary as a function of the average amount of rainfall received in the preceding 3 years (i.e. the three-year moving average), distance to major rivers, fire return interval and number of years since 1985, for each year. The response was also allowed to vary annually by group type (bull versus herd).

Due to the large sample size (n = 35117 group points, df = 276306 total animals and denDf = 1596369 residual degrees of freedom i.e. the denominator estimated during MPPM using standard kernel density estimation techniques) it is important to consider the potential for the "*p*-value problem" to affect our MPPM results (Lin *et al.* 2013). Results are therefore interpreted in the context of the magnitude of the effect size rather than significance alone (Lin *et al.* 2013). Consequently, effect size was calculated using the above formula **[1]**, where the intercept value β_0 represents the estimated logarithmic intensity of elephants per km^2 [$\lambda(u)_n$] excluding all covariate effects (i.e. if covariate values were zero). The standard deviation is the

deviation of $\lambda(u)_n$ caused by annual random effects $[\alpha_n]$. The coefficient values β_{1-4} are thus the logarithmic factor by which $\lambda(u)_n$ would increase or decrease should the covariate value increase or decrease by one unit. Model validation was performed using an analysis of deviance (ANOVA) for MPPM and a residual K-function (i.e. goodness-of-fit test) to access model accuracy according to Baddeley *et al.* (2015) (functions 13 and 14 in *Table S4.1 in Appendix S4*).

4.2.3.3. Elephant space-use intensity change

Changes to long-term elephant distribution and abundance patterns in Kruger from 1985-2012 were estimated as follows: (a) Elephant density was first calculated using a kernel smoothed intensity function for each point pattern (n=28) with a 5 km bandwidth (σ) and Diggle's edge correction (function 16 in *Table S4.1 in Appendix S4*). We chose 5 km as a bandwidth as this represents half the distance an elephant would be expected to travel in a day (de Knegt *et al.* 2011). Diggle's edge correction was used to minimise the bias of the park boundary edge effect in our analysis (Baddeley *et al.* 2015). (b) Significant changes to these long-term density patterns were then identified using the kernel density estimates, which were stacked and indexed by time to detect significant Breaks in the Seasonality and Trend (BFAST) of elephant density (functions 17, 21, 22 and 24 in *Table S4.1 in Appendix S4*; Verbesselt *et al.* 2010; DeVries *et al.* 2015). BFAST is a time-series change detection method originally developed for remotely sensed time series products (Verbesselt *et al.* 2012). Changes to Kruger's elephant density patterns were thus assessed by comparing historical (1985-1997) and current patterns (1998-2012) using the function bfmSpatial (function 25 *Table S4.1 in Appendix S4*; Dutrieux *et al.* 2014). Historical and current subsets were simply chosen as the half-way mark in our data record history (i.e. 1997/1998). Changes detected were then mapped to illustrate areas experiencing significantly higher or lower densities of elephants in the past 14 years (1998-

2012) compared to the previous 14 years (1985-1997). (c) The areal proportions of grouped distance to rivers (11 discrete distance classes) and fire return period classes (9 discrete classes) were then calculated for different magnitude categories of density change from (b) and the relative proportions of these significant changes analysed (function 20 in *Table S4.1 in Appendix S4*). The effects of distance to major rivers and fire frequency on the magnitude of change in overall elephant density were then assessed using a Pearson's chi-squared test of independence (function 26 in *Table S4.1 in Appendix S4*).

4.2.3.4. Elephant group-type distribution change

Changes in distribution patterns of elephant bull groups vs elephant herd groups were estimated in a similar three-step process described above. However, instead of elephant density (2.3.2.a), group-type probabilities were calculated for each year as the (a) spatially-varying probabilities of encountering bull versus herd groups, which were mapped using a relative risk function (function 15 in Table S1; De Lucca *et al.* 2013; Baddeley *et al.* 2015). In this way the probability of encountering a specific group type (i.e. bull or herd) was computed using a smoothing bandwidth (σ^2) of 5 km and Diggle's edge correction function as described above (Baddeley *et al.* 2015).

All analyses were carried out in R version 3.3.1 (R Core Team, 2016) with all R packages and functions used, and references thereof, described in Table S1. Larger computations were performed using the Rhasatsha High Performance Computing system at Stellenbosch University (Rhasatsha HPC 2016).

4.3. RESULTS

4.3.1. Elephant point patterns

A Monte Carlo test confirmed our initial hypothesis of significant sexual segregation: point clustering (Ripley's Inhomogeneous K-function) differed each year by group-type (T= 0.3354, P < 0.05; Baddeley *et al.* 2015; function 5 and 6 in *Table S4.1 in Appendix S4*). Results of the border-corrected inhomogeneous empty-space function similarly showed highly variable clustering distances across years (function 7 in *Table S4.1* and *Fig. S4.1 in Appendix S4*). That is, elephants were significantly clustered (P < 0.05) in earlier years with observed empty-space distances below the theoretical curve of random distribution. More recent years (e.g. 2009-2012) however, showed no significant evidence of clustering (*Fig. S4.1 in Appendix S4*), which can possibly be attributed to the increased elephant density. The cross-type L function further illustrates how the level of this segregation has changed between years (*Fig. S4.2 in Appendix S4*), leading us to differentiate sexes in the proceeding model.

4.3.2. Elephant resource selection

Controlling for density increase over time, bull and mixed herd elephant groups differed in their response to rainfall and fire but responded similarly to the effects of increased distance to rivers (Table 4.1). Both bull and mixed herds concentrated closer to major rivers, although this effect was stronger in herd groups (33% less animals 1 km further from rivers) compared to bulls (11% less animals 1 km further from rivers). Bull densities were significantly lower in areas receiving higher rainfall (26% less bulls in areas with 100 mm more rain) while herd densities in such areas did not change from the mean (Table 4.1). Bull densities were also lower in areas experiencing longer fire return intervals (3% less bulls with a 5 year fire return interval) while herd densities were significantly higher in areas experiencing fewer fires (10% more herds with a 5 year fire return interval). As expected the densities of both groups have significantly

increased over time, with the difference of 10 years resulting in 7% more bulls and 39% more herd elephants (Table 4.1). Random annual effects accounted for 7.8% of the remaining variability in elephant herd and bull densities from 1985-2012. Although model fit did fluctuate from year to year, these differences were not significant indicating good model fit for bulls, χ^2 = 24830, df = 24775, P = 0.401 and herds, χ^2 = 23673, df = 23618, P = 0.399 overall.

Table 4.1: Results of the mixed-effects multiple point process model. Linking herd and bull group intensity of space-use to environmental variables. The intercept value represents the linear predictor or the estimated logarithmic intensity of elephants per km^2 excluding covariate effects (i.e. if covariate values were zero). The standard deviation (StdDev) represents the deviation of the linear predictor caused by annual random effects. The coefficient values represent the logarithmic factor by which this linear predictor would increase/decrease should the covariate value increase/decrease by 1.0.

Random effects [Formula: ~1	year]					
StdDev: 0.022					
Relative StdDev: 7.76					
Fixed effects					
	Value	Std.Error	t-value	p-value	Effect
(Intercept)	-1.264	0.050	-25.16	<0.001	
3yr moving rainfall - Bulls	-0.003	0.000	-25.81	<0.001	-26% [+100]
Distance to rivers - Bulls	-0.119	0.015	-7.73	<0.001	-11% [+1]
Moving fire intervals - Bulls	-0.006	0.002	-2.71	0.007	-3% [+5]
No. of years since 1985 - Bulls	0.007	0.003	2.58	0.016	+7% [+10]
3yr moving rainfall - Herd	0.003	0.000	39.40	<0.001	0% [+100]
Distance to rivers - Herd	-0.281	0.018	-15.76	<0.001	-33% [+1]
Moving fire intervals - Herd	0.025	0.002	10.59	<0.001	+10% [+5]
No. of years since 1985 - Herd	0.026	0.002	12.44	<0.001	+39% [+10]
ANOVA					

Effect: +100 mm rainfall | +1 km from major river | +5 years to fire return interval | +10 years from record start 1985

4.3.3. Elephant space-use intensity change

The increasing trend in elephant densities is spatially variable (*Animation S4.2 in Appendix S4*). The location and timing of significant changes (P < 0.05) to elephant density from 1998-2012 compared to 1985-1997 is likewise spatiotemporally dynamic (Fig. 4.3). The strongest increase in density occurred in 2003 (Fig. 4.3a), which was a below average rainfall year that consequently also experienced relatively few fires (i.e. 1000 km^2 burned vs long-term average of ~ 3000 km^2; *Fig. S4.3 in Appendix S4*). The overall magnitude and direction of these changes, shown in Fig. 4.3b, illustrate those areas experiencing significant decreases to long-term elephant density patterns in lighter shades of blue; and those experiencing significant increases in darker shades of red on the map. Areal proportions of the above density changes, classified within zones of different fire frequencies and distances to river classes, revealed varied relationships (Fig. 4.4; *Fig. S4.4 in Appendix S4*). Fire was identified as a significant agent of density change, χ^2 (16, 27) = 73.501, p < 0.0001 (Fig. 4.4a). More specifically, areas experiencing higher fire frequencies (intervals of ≤ 2 years between fires depicted by darker shades of red in Fig. 4.4a) were generally associated with decreased elephant densities, more so than would be expected by chance (Fig. 4.4a; *Fig. S4.4a in Appendix S4*). In contrast, areas experiencing intermediate to low fire frequencies (intervals of ≥ 5 years between fires depicted by lighter shades of red in Fig. 4.4a) were associated with increased densities (Fig. 4.4a; *Fig. S4.4a in Appendix S4*). Areas undergoing significant increases in elephant densities were found overwhelmingly closer to rivers, χ^2 (20, 33) = 29.834, p = 0.073 (Fig. 4.4b; darker shades of blue). Looking at this in more detail, the largest increases occurred closer to rivers (< 2 km), while the largest decreases happened further than > 5 km away from major rivers (*Fig. S4.4b in Appendix S4*).
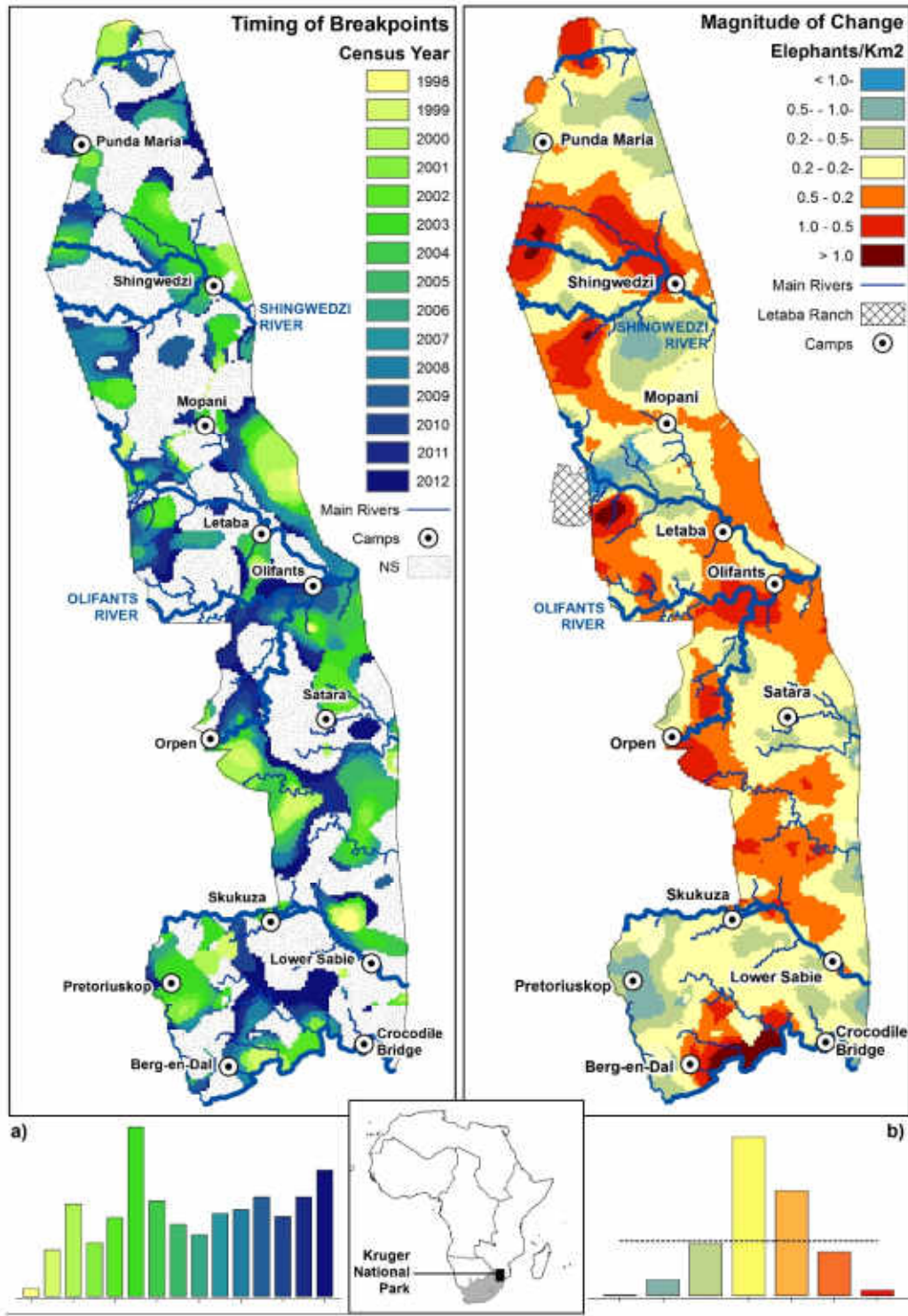
Fig. 4.3: Results of Breaks for Additive Seasonal and Trend (BFAST) (Verbesselt *et al.* 2010) analysis, showing the location and timing of significant change to elephant density patterns across Kruger from 1985-2012 (BFAST, P < 0.05). Panel a) shows the timing of the most significant changes (breakpoints) with NS representing no significant change. Panel b) shows the magnitude and direction of (positive-darker red or negative-lighter blue) change.
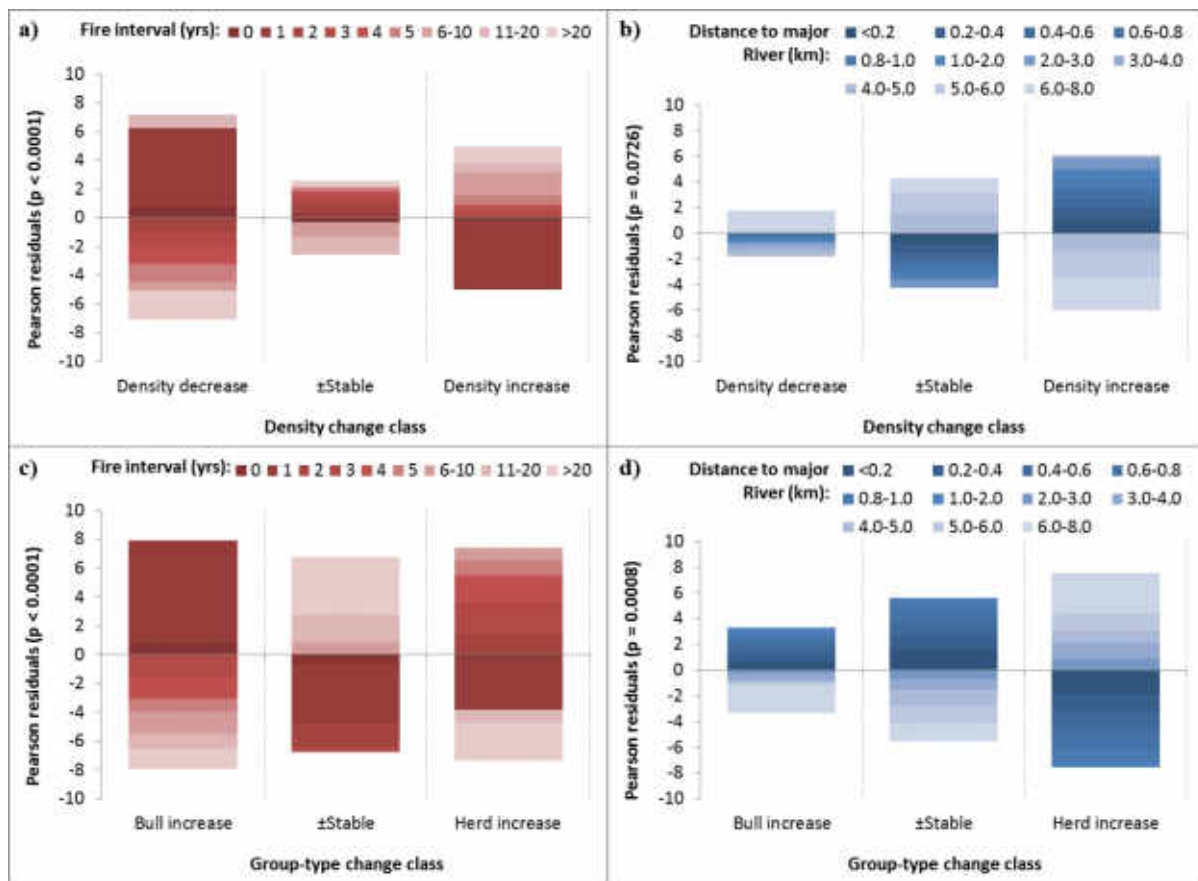
Fig. 4.4: Pearson residuals plots from chi-squared test of independence showing the relation between fire return periods, distance to major rivers and significant changes to elephant density and group-type probability during the period 1998-2012 compared to the period 1985-1997. The y-axis represents the standardised difference between the observed and expected values of elephant densities. Negative and positive values therefore depict greater decreases or increases than would be expected by chance. The different panels show a) the significant effect of fire as an agent of density change; b) the marginally significant effect distance to major rivers have on density change. Although, areas undergoing significant increases were overwhelmingly closer to rivers (darker blues); c) the significant effect of fire as an agent of group-type probability change, with shorter fire return intervals (darker reds) dominating those areas showing an increase in the probability of encountering bull elephants; d) the significant effect distance to major rivers has on group-type probability change with bull elephants increasing closer to rivers (darker blues), and herd elephants generally increasing further from major rivers (lighter blues).

4.3.4. Elephant group-type distribution change

Both bull and mixed herd elephant groups showed clear changes to their long-term patterns of distribution over time (*Animation S4.3 in Appendix S4*). Herd dominated areas have expanded in comparison to bull dominated areas (Fig. 4.5). The probability of encountering herd elephants has generally increased north of the Olifants River, except for small pockets south of the Shingwedzi River and into the Punda Maria sandveld where the probability of encountering a bull group has significantly ($P < 0.05$) increased instead (Fig. 4.5). Bull elephants also showed a significant ($P < 0.05$) increase in occurrence probability in the Pretoriuskop area. Similarly, the areal proportions of the above significant changes to long-term group-type probabilities showed fire was a significant agent of change, χ^2 (16, 27) = 134.52, $p < 0.0001$ (Fig. 4.4c). In general the probability of encountering bull elephants increased in areas with higher fire frequencies (darker shades of red in Fig. 4.4c; *Fig. S4.4c in Appendix S4*). Herd elephants appeared to do the same but at intermediate frequencies of fires (lighter shades of red in Fig. 4.4c; *Fig. S4.4c in Appendix S4*). Group-type probabilities also shifted significantly in relation to major river systems, χ^2 (20, 33) = 46.069, $p < 0.001$ (Fig. 4.4d). That is, areas experiencing a significant increase in the probability of encountering bull groups were clearly closer to rivers (darker shades of blue in Fig. 4.4d), whereas those experiencing a significant increase in herd groups were generally found further from major rivers (lighter shades of blue in Fig. 4.4d). There also appears to be a general increasing trend in the probability of finding herd elephants further away from rivers compared to bull elephants (Fig. 4.4d; *Fig. S4.4d in Appendix S4*). That is, the probability of encountering herds > 3 km from major rivers (lighter shades of blue in Fig. 4.4d) has increased more than can be explained by chance.
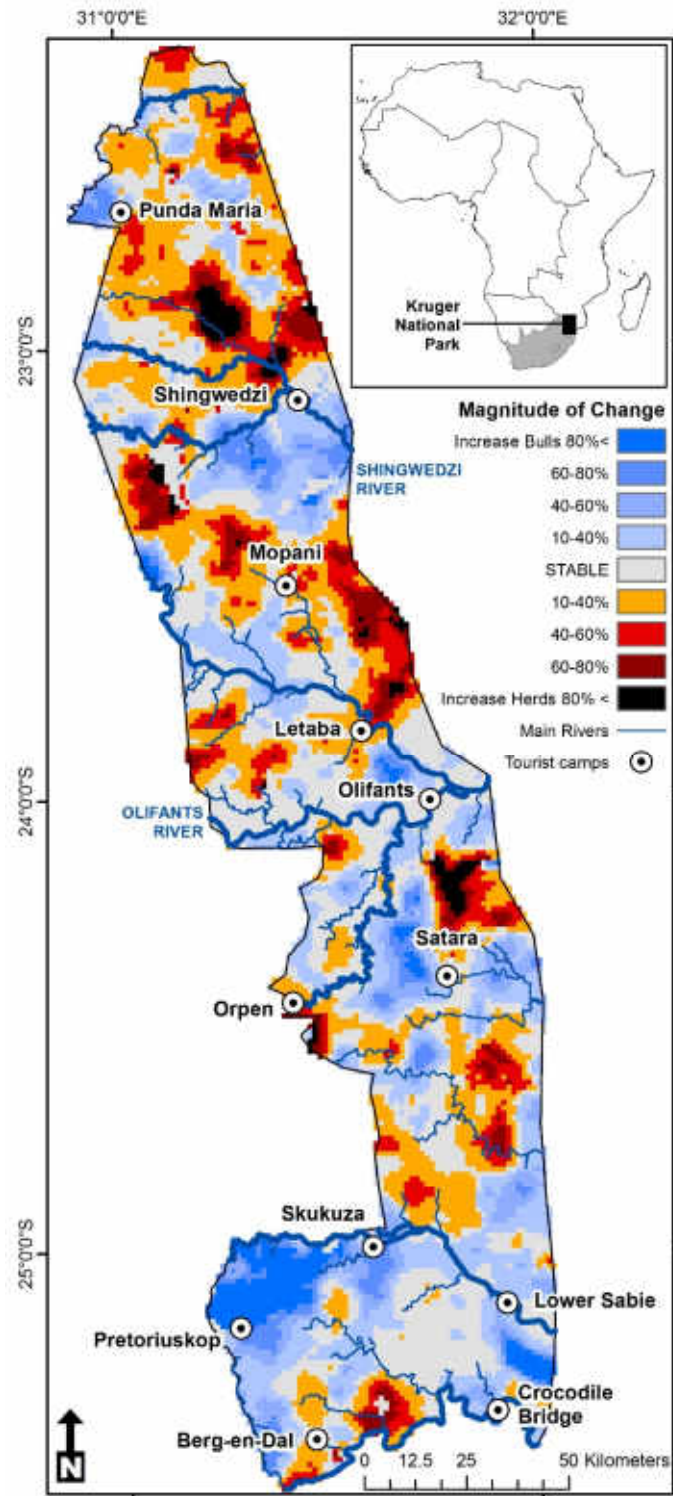
Fig. 4.5: Significant change in spatially-varying probabilities of bulls versus mixed herd elephant groups in the period 1985-2012 (BFAST, P < 0.05). Darker blue areas on the map represent those areas that are becoming increasing bull dominated. Darker red areas represent those areas that are becoming increasingly dominated by mixed herd groups.

4.4. DISCUSSION

4.4.1. Elephant point patterns

Ferreira *et al.* (2017) report an exponential increase in elephant numbers since 1995 while also suggesting that Kruger's elephant growth rate may be slowing in response to less intensive elephant management practises implemented after 1994. From a biogeographic perspective however, our results show Kruger's elephant distribution patterns have homogenised with a clear decrease in available empty-space from 2000 (*Fig. S4.1 in Appendix S4*). In addition, while bull and mixed herd groups were initially significantly segregated, this pattern changed from 2006 onwards (*Fig. S4.2 in Appendix S4*). As a result, groups are no longer showing significant levels of segregation and little clustering behaviour from distances > 4 km (*Fig. S4.2 in Appendix S4*). Since Shannon *et al.* (2008) describe this type of segregation as a natural behavioural response to social stimuli (e.g. breeding) and/or different habitat requirements of male vs. female body sizes, we suggest the implications of this change may be far-reaching. We argue that bull and mixed herd groups are being forced into closer proximity as empty-space constricts, and may no longer be able to select for preferred resources and maintain a more natural heterogeneous distribution pattern as prescribed by Ferreira *et al.* (2012). Anthropogenic factors like Kruger's perimeter fence may also have exacerbated this homogenization effect. Grant *et al.* (2008) for example, outline how fences can affect elephant ecology and population dynamics by restricting natural movement functions triggered by ecosystem cues. In this way, increasing populations may place more pressure on shared habitats and resources that may ultimately compromise other cohort species (Owen-Smith *et al.* 2006). This concept is supported by numerous cross-country (e.g. Loarie *et al.* 2009) and local scale studies (e.g. Vanak *et al.* 2010), and thus requires careful consideration by managers.

4.4.2. Elephant resource selection

Recognising the need for a holistic landscape management approach to elephant conservation in Kruger, Ferreira *et al.* (2017) call for a deeper understanding of the spatiotemporal response of elephants to resource heterogeneity. Using point pattern analysis our study reveals divergent resource selection functions for bull vs. mixed-herd groups. Both bull and herd elephants were found in higher concentrations closer to rivers (Table 4.1), a response driven by an elephant's preference for natural water sources and optimal foraging of riparian vegetation (Gaylard 2015). However, the stronger response of herds to river distance suggests they may be more dependent on riverine habitats (Stokke and du Toit 2002) for shelter (Smit *et al.* 2007) and potentially to fulfil browse requirements during the dry season (Shannon *et al.* 2013). This effect is less apparent in bulls as they roam over larger areas (Stokke and du Toit 2002) and will reportedly switch their diets to grass earlier in the season (Shannon *et al.* 2013).

Coupled to this, we expected rainfall driven vegetation dynamics or ancillary increases to surface water availability to emerge as important drivers of elephant distribution and abundance, as has been suggested by Chamaillé-Jammes *et al.* (2007) and Loarie *et al.* (2009). However we found this relationship only held for bulls and not herds. We speculate this may be an artefact of the winter view of elephant distribution and abundance patterns derived from July/August census data. Elephants may therefore not be responding strongly to rainfall while in their dry-season winter home ranges. Unfortunately, data is not available for the summer distribution patterns of elephants in Kruger. Interestingly though, bulls had a strong negative response to rainfall, which could be explained by bull elephant's dependence on artificial water sources described by Smit *et al.* (2007) and later by Gaylard (2015).

Fire return period also influenced elephant distribution patterns, as mixed herds selected for areas with lengthier fire return intervals, whereas bulls selected areas with shorter fire return intervals, albeit less clearly (Table 4.1). Bulls, being more dependent on grass during the winter

months (Smit *et al.* 2007; Shannon *et al.* 2013), may respond to more frequent fires as they improve grass quality (Trollope 1996). This supports a cause and effect synergy between fires and elephants as seen by Dublin *et al.* (1990) and others (Shannon *et al.* 2011). In an outdoor laboratory like Kruger however, it is difficult to discern the directionality of cause and response, i.e. whether fire is driving elephant distribution and abundance (cause) or if the distribution and abundance of elephants is forming and/or maintaining fire regimes (effect) or both (Asner *et al.* 2015; Levick *et al.* 2015). In other words, are higher fire frequencies changing elephant space-use intensity or are changing elephant distribution and abundance patterns shifting fire frequencies as they alter tree-grass dynamics? Dublin *et al.*'s (1990) work in the Serengeti highlighted both elephants and fire as mechanisms of multiple stable states in their ecosystem. In their study, fire was identified as the catalyst of vegetation change from woodland to grassland but that elephants were the maintenance agents of this state change (Dublin *et al.* 1990). In Kruger, decision makers can use the resource selection functions presented here to glimpse potential future elephant distribution and abundance scenarios under different climate change projections, available surface water changes and/or fire regime shifts. Results may also be used to guide management decisions surrounding possible space-use manipulation experiments described by Ferreira *et al.* (2012).

4.4.3. Elephant space-use intensity change

Long-term distribution and abundance patterns of elephants in Kruger have without question changed from 1985-2012 (Fig. 4.3b). Areas identified as significantly increasing or decreasing in densities are however spatiotemporally dynamic (Fig. 4.3a). Significant changes were strongly associated with distance to rivers, with the majority of marked increases happening < 1km from major rivers (*Fig. S4.4b in Appendix S4*). This could suggest that density dependant changes are being felt more strongly than suggested by Ferreira *et al.* (2017).

Fire is also a potentially significant agent of change, where the magnitude of density increase appears to shrink as fire return intervals shorten (*Fig. S4.4a in Appendix S4*). This may however be an artefact of elephants increasing in riparian areas, which are inherently less likely to burn and therefore have low fire frequencies. Nevertheless, drawing on Fig. 4.3b managers may be able to identify possible 'impact hotspots' and focus research into the more empirical effects of increased elephant densities, like changes to vegetation structure and associated species diversity, and potential ecosystem regime shifts (Kerley *et al.* 2008; Scholes and Mennel 2008; Ferreira *et al.* 2012).

4.4 Elephant group-type distribution change

Considering that over this same period (1985-2012) the probability of encountering bull vs. mixed herd groups also changed noticeably, suggests evidence of more pervasive density-dependent effects. From Fig. 4.5, one can see herd groups moving north of the Olifants River while bulls shift further south. In synchrony, bull groups are now also occupying areas closer to rivers as herds expand outwards into the uplands (Fig. 4.4d; Fig. 4.5). This strongly confirms the hypothesis that as elephant numbers grow, empty-space becomes more limiting and elephants are forced to move into previously unoccupied areas. Added to this, the probability of encountering bull groups is shifting into areas with shorter fire return intervals, while herd groups do so at more intermediate fire frequencies (Fig. 4.4c). Since bull elephants generally cause more damage to larger tree species (Guy 1976; O'Connor *et al.* 2007) and coupled with the impacts of fires, we can only speculate as to the long-term effects these shifts in bull dominance may have on the ecosystem as elephant numbers continue to grow. For example, have elephants and fire acted together to change the system significantly enough to detect changes in elephant distribution patterns, and are these changes in response to changing fire frequencies driven by increasing elephant densities? If this is the case, these interacting effects

may result in similar state-changes as were seen by Dublin *et al.* (1990) in the Serengeti. Further exploration of our results may also help disentangle drivers of tree mortality in Kruger. That is, does tree mortality occur in response to elephant-fire interactions (Shannon *et al.* 2011; van Wilgen *et al.* 2014) or does fire act alone to accelerate tree loss in elephant populated areas (Levick *et al.* 2015)? Either way, tree loss may be more intrinsically linked to changes in elephant space-use intensity than originally expected. A deeper understanding of Fig. 4.5 and the recently bull-dominated areas identified therein, may also help stratify research to answer the question whether these areas are in fact loosing large trees at a faster rate.

4.4.5. Limitations

The entwined nature of the causes and effects phenomena, which is ubiquitous throughout the field of ecology, makes identifying primary drivers or mechanisms almost impossible, especially with simple regression techniques (MacFadyen *et al.* 2016). Future studies may wish to employ techniques like Structural Equation Models (SEM) to help tease apart cause and effect relationships affecting elephant distribution and abundance. The ability to include interaction terms into MPPM's in future, would also allow us to interrogate how these resource selection functions change with increasing densities. Furthermore, the roles played by rivers in elephant distribution patterns could also be explored further by perhaps classifying rivers into functional classes, i.e. source of water versus riparian vegetation resource, and by including artificial waterholes into the analysis.

4.5. CONCLUSION

The challenge going forward lies in digesting these insights into a guiding principle for management action and the prioritisation of finer scale research into the cascading effects of different elephant space-use intensities. Recognising the challenges Southern African protected

areas face to produce practical management solutions for healthy and growing elephant populations, this work aimed to fill some of the biogeographical gaps on what drives the population-level distribution and abundance patterns of elephant in Kruger. Ideally, this work should help guide experimental management action strategies, which aim to alter elephant density and distribution patterns by manipulating artificial water sources (opening/closing windmills), into areas experiencing fewer fires and those further from rivers (Smit and Ferreira 2010; Ferreira *et al.* 2012). Ultimately, we encouraged SANParks to use the spatiotemporal results herein to focus research into the more empirical effects of high elephant densities and perhaps establishing possible refuge areas.

Landscape heterogeneity at the interface of herbivore, fire, climate and landform interactions

© Sandra MacFadyen

Landscape heterogeneity at the interface of herbivore, fire, climate and landform interactions

This chapter has been submitted as:

MacFadyen S, Hui C, Van Teeffelen AJA and Verburg PH (*submitted*) Landscape heterogeneity at the interface of herbivore, fire, climate and landform interactions. *Global Change Biology* [manuscript ID: GCB-18-0279]

ABSTRACT

Protected areas (PA) are strongholds of biodiversity in an epoch of global biodiversity loss. Ecosystem complexity makes managing large PAs and identifying key environmental drivers and responders difficult. This is in part because ecological systems express themselves in complex adaptive ways, with multifarious physical and stochastic components interacting to both form landscape patterns and influence ecosystem processes at different scales. The resulting mosaic of landscape heterogeneity is a product of this complexity, making it an important global biodiversity indicator. The role of heterogeneity as a determinant of species richness is generally accepted, however its relationship with the structural and functional components of biodiversity are less understood. Here we describe how landscape heterogeneity responds to and/or influences interactions between selected drivers in a large African Savanna, the Kruger National Park. Using Piecewise Structural Equation Modelling we examine the local scale (1 km^2) roles of the underlying physical landscape template, rainfall, herbivore densities, and fire in the formation of regional scale (8 km^2) variability of 28-year normalized difference vegetation index observations, as a proxy for landscape heterogeneity. The emergent spatiotemporal patterns of driver dominance are dynamic, varying in effect size across the landscape and over time. Higher rainfall and greater landform diversity generally increase heterogeneity, while higher elephant densities and less frequent fires reduce heterogeneity and drive landscape homogenization. Under climate change projections of reduced rainfall, our results foretell of potentially significant declines in heterogeneity - densification of buffalo herd structures - lengthening of fire return periods - and continued homogenisation of elephant distribution and abundance patterns. In the face of global environmental change, the key to effective and holistic ecosystem conservation may lie in our ability to describe changes to the casual structure of heterogeneity and the environmental drivers that generate and maintain its pattern.

5.1. INTRODUCTION

Conserving biodiversity in dynamic ecosystems is a challenge facing protected area managers worldwide (Mittermeier *et al.* 2003; Brooks *et al.* 2006). Despite global efforts, negative impacts on biodiversity continue to trigger warnings that predict widespread biodiversity declines (Tittensor *et al.* 2014). Measuring biodiversity loss is however no easy task, especially in the face of pervasive ecosystem change and inherent complexity. Landscape pattern is the self-organizing expression of interactions between different evolutionary and ecological processes and mechanisms (Wiens 2002; Chapin *et al.* 2011). The resulting mosaic of landscape heterogeneity could therefore be the key to understanding changes to biodiversity when described in terms of the mechanisms that generate and maintain its derivative pattern (Levin 1992). This means being able to predict or quantify causality in lieu of simply describing the correlation of a mechanism with an observed pattern (Levin 1992; Grace *et al.* 2015). Importantly, the scale at which these phenomena are investigated will influence pattern detection and thus also control what mechanisms emerge as important (Levin 1992). At the regional-local scale, landscape heterogeneity is known to play an important role in healthy ecosystem functioning and is already considered a primary indicator of biodiversity (Christensen 1997; Parrot 2010; MacFadyen *et al.* 2016). Due to the complexity of heterogeneity theory in ecology however, there is a lag in the development of practical solutions for monitoring (Stein *et al.* 2014).

Kolasa and Rollo (1991) descriptively coined the phrase, "the heterogeneity of heterogeneity", in which stochastic and systemic aspects of heterogeneity are discriminated. Pickett *et al.* (2003) developed this idea further into a heterogeneity framework by which the causes of, and responses to, heterogeneity could be understood. Their (Pickett *et al.* 2003) framework describes heterogeneity as the outcome of factor-driven interactions between different key components namely, *agents*; *substrates*; *controllers*; and *responders*. In Protected

Areas (PAs) for example, herbivores will act as *agents* of herbivory to create, maintain, and/or transform the vegetation *substrate* at density-dependent levels of intensity. This in turn will be *controlled* by rainfall driven patterns of herbivore distribution to which fire frequencies will also *respond* (Fig. 5.1). The outcomes of these interactions frame the basis of biodiversity formation, maintenance and flux linked to many global, regional and local conservation objectives. In a complex system like a large PA, components can however also be multiplicitous, acting as both *agents* and/or *controllers* and manifesting as both *substrates* and/or *responders* (Pickett *et al.* 2003). This is the puzzle beclouding the development of standardized implementation strategies for global heterogeneity monitoring (Gergel and Turner 2002).
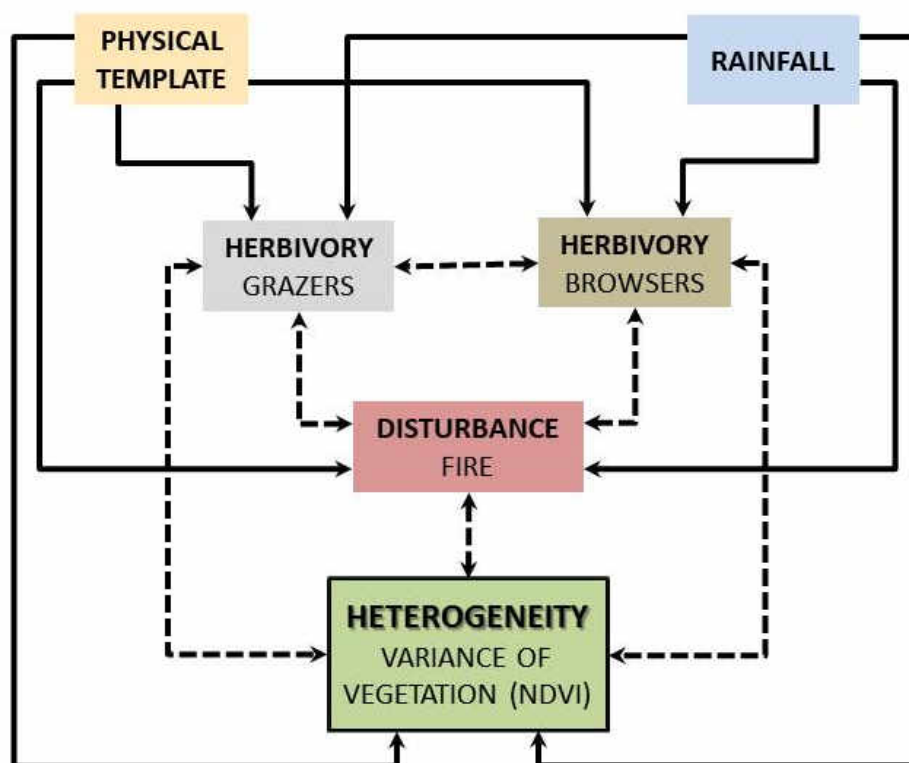
Fig. 5.1: Hypothetical construct of the cause and effect relationships between landscape heterogeneity, the physical landscape template, rainfall, herbivory and disturbance in Kruger National Park. Solid lines represent simple (one-way) interactions and dashed lines complex (two-way) interactions.

Nonetheless, substantial progress has been made towards real-world applications for large-scale biodiversity studies thanks to advancements in remote sensing and the growing base of open source resources (e.g. Rocchini *et al.* 2016; He *et al.* 2015; Petrou *et al.* 2015; Lausch *et al.* 2016). For example, at the global scale the Group on Earth Observations Biodiversity Observation Network (GEO BON) provide a set of key indicators of biodiversity change (Pereira *et al.* 2013). These indicators or Essential Biodiversity Variables (EBVs) are made up of biological measurements, characteristic of different aspects of biodiversity and are used to assess system-level biodiversity trends (Brummitt *et al.* 2016; Proença *et al.* 2016). Many of the EBVs are derived from space-borne sensors using new techniques in remote sensing to detect, assess and predict biodiversity change (Lausch *et al.* 2016, Paganini *et al.* 2016). In a large PA like the Kruger National Park (Kruger), which spans almost 20,000 km^2, remote sensing techniques offer novel approaches to landscape wide biodiversity assessment (e.g. Duro *et al.* 2007; MacFadyen *et al.* 2016). Recognized theories like the spectral diversity hypothesis are central to these advancements, where higher levels of spectral diversity, recorded by satellite sensors, can be indicative of a wider variety of environmental characteristics (Palmer *et al.* 2002; Rocchini *et al.* 2016; MacFadyen *et al.* 2016). From the perspective of the ecological niche theory, a wider range of these characteristics will result in different habitat types which will support a larger diversity of species (Chase 2011). Similarly, the variability in the phenology of vegetation, as measured by the Normalized Difference Vegetation Index (NDVI), can inform our understanding of resource driven animal population dynamics and associated environmental variability (e.g. Wessels *et al.* 2006; Xie *et al.* 2008; Hasan *et al.* 2011; Pettorelli *et al.* 2011; Pettorelli *et al.* 2014). Remote sensing is therefore an ideal tool for biodiversity assessment in large protected areas since it is capable of measuring heterogeneity at multiple scales and over long continuous time periods (Pettorelli *et al.* 2014).

In Kruger some early attempts were made to quantify heterogeneity loss using long-term monitoring data (Margules *et al.* 2003; SANParks 2006; MacFadyen 2010). The limitations of these studies were the lack of spatiotemporal methods to recognize ecosystem dynamics and the ability to discern undesirable change from natural ecosystem flux (Biggs and Rogers 2003; Parrish *et al.* 2003; Scholes and Kruger 2011). The ability to detect this difference can of course be difficult when healthy ecosystems are adaptive, dynamic networks of environmental components interacting at various structural, spatial and temporal scales (Parrot 2010). Change is also an inevitable outcome of these interactions, raising three questions, where and when does this change manifest as landscape pattern and/or ecosystem process, and when should it be considered a negative or positive ecosystem result? To answer these questions, PA managers must first be able to measure change and identify the drivers behind a specific change while separating out their reciprocal causes and effects (Cardinale *et al.* 2006). A major obstacle to this type of holistic ecosystem approach is a lack of understanding of the causal structure of landscape heterogeneity. This requires insights into the directionality of the cause and effect interactions within and between different mechanisms that shape heterogeneity (Gergel and Turner 2002; Lefcheck and Duffy 2015). The objective of this paper is thus to examine the complex array of physical and stochastic components in a PA landscape, where these components interact to both form physical features and influence system processes. In doing so, we examine the magnitude and directionality of the cause and effect relationships of selected drivers on landscape heterogeneity in Kruger using the long-term variability of NDVI as a proxy for heterogeneity from 1985 to 2012 (Vermote *et al.* 2014). Selected drivers include different topographical characteristics, geological classes and soil properties that make up Kruger's physical landscape template or landform (Wessels *et al.* 2006). Herbivory and landscape disturbance, namely grazing (buffalo) and browsing (elephant) herbivore densities and fire frequency, are included as mechanisms of Kruger's heterogeneity response (Asner *et al.* 2015;

Levick *et al.* 2015). In turn we expect these mechanisms will also be influenced by climate, specifically rainfall, in that rainfall will drive NDVI and ultimately herbivore densities, associated herbivory and fire frequency (Zambatis 2003; Vermote *et al.* 2014).

In order to describe the causal links between landscape heterogeneity and the underlying physical landscape template, herbivore density, fire and rainfall, inferences about causal structures need to be made. For this purpose and in place of standard regression techniques, which are ineffective at differentiating causal links in natural systems, we use Structural Equation Modelling (SEM) (Schumacker and Lomax 2016; Shipley 2016). First, we designed a conceptual framework for heterogeneity in Kruger, containing a selection of interacting biological and environmental components and processes of interest (Fig. 5.1). This framework is used to posit the direction and magnitude of the different effects the selected drivers have on heterogeneity using a 'Piecewise' method of SEM (pSEM) (Schumacker and Lomax 2016, Grace *et al.* 2012; Lefcheck 2016). Using Kruger as a model system, we ultimately dissect the causality of landscape heterogeneity to demonstrate how dominant forces in an ecosystem can be identified to aid management and conservation planning in the face of change.

5.2. MATERIALS AND METHODS

5.2.1. Study area

Kruger is a model protected area ecosystem, covering $\sim$ 20,000 km^2 of the Savanna biome in South Africa (SA) between latitudes -22.328°S; -25.529°S and longitudes 30.888°E; 32.033°E (MacFadyen *et al.* 2016). Officially proclaimed in 1926 under a strong protectionist philosophy, the PA has been managed for conservation for almost a century (Carruthers 1995) and supports an impressive array of plant (1980), animal (856) and invertebrate species (SANParks 2017). Kruger's gently undulating topography accommodates an extensive river network, which also gives rise to a highly patchy landscape with both open grasslands and dense woodlands (Venter

et al. 2003). It is recognized as one of the few protected landscapes remaining where 'natural' ecological response can be investigated in the absence of human impacts (Pickett *et al.* 2003).

5.2.2. Data

5.2.2.1. Landscape heterogeneity

Resource driven animal population dynamics and associated environmental variability are attuned to the dynamics of biophysical vegetation properties, as measured by NDVI (Pettorelli *et al.* 2011; Pettorelli *et al.* 2014). Monthly maximum composites of NDVI were thus obtained from version 3 of the Global Inventory Modeling and Mapping Studies' (GIMMS) NDVI3g dataset (Pinzon and Tucker 2014; Detsch 2016). NDVI3g is an 8 km resolution dataset, derived from the National Oceanic and Atmospheric Administration's (NOAA) AVHRR, providing reliable long-term (1981 to 2014) records of vegetation greenness (Vermote *et al.* 2014; Marshall *et al.* 2016). A Coefficient of Variation (CV) of maximum monthly NDVI composites was calculated, at the pixel level for each year, to produce 28 layers describing the long-term regional-scale (8 km^2) dynamics of annual vegetation greenness across Kruger from 1985 to 2012 (Vermote *et al.* 2014; Marshall *et al.* 2016; Hijmans, 2016).

5.2.2.2. Physical landscape template (Landform)

A mosaic of underlying geophysical attributes provide a template on which pattern and processes interact (MacFadyen *et al.* 2016; Levick and Rogers 2011). This physical landscape template, which forms a stable (at the timescale of this study) platform for ecosystem role-players, will vary locally with i) topography, ii) geology, and iii) soil properties.

i)   Topography: Various terrain characteristics were derived from a 30m elevation data provided by the Shuttle Radar Topography Mission (SRTM; USGS 2014). In addition to

elevation; slope; and aspect, a Topographic Position Index (TPI); and a Terrain Ruggedness Index (TRI) were calculated from SRTM (Hijmans 2016).

ii)   Geology: Geological data for South Africa (SA) was obtained from the Council of Geoscience, SA at 1:1 000 000m scale (Council for Geoscience 2016). These data describe SA's geological forms, lithostratigraphic units and principle rock types after Vegter (1995).

iii)   Soils: Different soil property grids were downloaded from the World Soil Information's (ISRIC) online database *SoilGrids* at 250 m pixel resolution (Hengl *et al.* 2017). Layers selected from this dataset included absolute depth to bedrock; soil texture classifications for depths 0 m to 2 m; a soil drainage classification according to the United Nations Food and Agriculture Organization's (FAO) guidelines for profile description; and a soil form/taxonomy classification according to the World Reference Base system (Hengl *et al.* 2017).

The pixel-wise (1 km^2) relative variability of the above properties was then derived from the subsequent raster-stack using CV to represent overall physical landscape variability across Kruger (Hijmans *et al.* 2016; R Core Team 2016; Leutner and Horning 2016).

5.2.2.3. Dynamic components: Climate, fire and herbivores

i)   Climate – Rainfall surfaces: Modelled 1 km^2 resolution monthly rainfall grids, derived from *in situ* rainfall measurements, environmental covariates and the Climate Hazards Infrared Precipitation with Stations (CHIRPS) global climate surfaces (Funk *et al.* 2015), were downloaded from the SANParks data repository (see MacFadyen *et al.* 2018 for detailed description of data). Monthly rainfall surfaces were collated and summed by rainfall year (i.e. July year 1 to June year 2) to produce 1 km^2 annual rainfall grids from 1985 to 2012 for Kruger (MacFadyen *et al.* 2018).

ii)   Fire – Disturbance: Annual cumulative fire return intervals were calculated from binary burn scar data (0 = no burn; 1= burn) captured by SANParks from 1941 to 2012 (Govender *et al.* 2012). The pixel-wide cumulative intervals between fires were then counted (Smit *et al.* 2013b; MacFadyen *et al. in Review*). Results thus describe the 1 km^2 annual cumulative fire return intervals for Kruger from 1941 to 2012 (72 years).

iii)   Herbivores – Species population dynamics: Lastly, density estimates of elephant (browser) and buffalo (bulk grazer) were calculated from annual SANParks winter (July/August) helicopter census counts (Whyte 2001; MacFadyen *et al. in Review*). Data were converted into point patterns and the kernel smoothed intensities calculated annually for each species using a 5 km smoothing bandwidth (sigma^2) and Diggle's edge correction (Baddeley *et al.* 2015; MacFadyen *et al. in Review*). Results describe 1 km^2 mega-herbivore distribution and density trends in Kruger from 1985-2012.

5.2.3. Statistical analyses

5.2.3.1. Causal structure of landscape heterogeneity

The causal structure of landscape heterogeneity in Kruger, and the environmental variables described above, are explored using pSEM (piecewiseSEM package R; Lefcheck 2016). pSEM is particularly well suited to ecological studies in that it has the added ability to deal with non-independence and non-linearity in data, a chronic condition of environmental data (Lefcheck 2016). pSEM was used here specifically to help discern complex multivariate relationships from different observational data that are known to be non-normally distributed, exposed to random effects and have observations in close proximity (over geographic distance and/or time) that are significantly correlated (Lefcheck and Duffy 2015). A preliminary thesis of possible cause and effect relationships between selected environmental drivers of heterogeneity pattern in Kruger is illustrated in Fig. 5.1. Pixel values of the selected drivers, namely heterogeneity of

the underlying physical landscape template; annual rainfall; herbivory (as represented by the long-term distributions and densities of bulk grazing buffalo and browsing elephants); and the annual cumulative fire return periods, were feed into the pSEM. Model optimization was done using *Fisher's C* statistic after Shipley (2016). Results express landscape heterogeneity, as measured by NDVI variability, as the macroscale pattern (8 km^2) formed by the effects of these local scale (1 km^2) processes or drivers. Results further illustrate the degree to which herbivores and fire, for example, cause or simply respond to landscape heterogeneity (Eisenhauer *et al.* 2015).

5.2.3.2. Spatiotemporal dynamics of driver dominance

pSEM path coefficients were standardized by the mean and extracted into a table of coefficients. Using these coefficient values, the magnitude of the effect each variable exerted on heterogeneity was calculated per pixel per year. The maximum value across all years was determined and the dominant driver identified. Pixels were then classified as being driven primarily by the physical template, rainfall, fire return interval, elephant or buffalo activities according to which variable occurred most frequently as the dominant driver for that pixel from 1985 to 2012.

5.3. RESULTS

5.3.1. Response and explanatory variables

Annual monthly variability of NDVI varied considerably from year to year, with extreme low and high rainfall years generally experiencing greater variability (Fig. 5.2). The surface distribution of rainfall also varied from year to year (Fig. 5.3) with roughly 5-yearly fluctuations of wet and dry cycles as described by MacFadyen *et al.* (2018). The physical landscape template varied more within the fertile basaltic regions of the East compared to their granitic counterparts

in the West (Fig. 5.4). Animated maps of buffalo and elephant kernel density estimates from annual census totals in Kruger showed a general increasing trend in the densities of animals as well as obvious distribution changes from 1985 to 2012 (see *Animation S5.1 in Appendix S5*). The return intervals for fires also varied across Kruger, with fires returning most frequently (i.e. smallest return interval) to those areas in the South-West along the Western boundary fence and less frequently (i.e. largest return interval) to those along major rivers (Fig. 5.4; see *Animation S5.2 in Appendix S5* for annual burnt area maps).
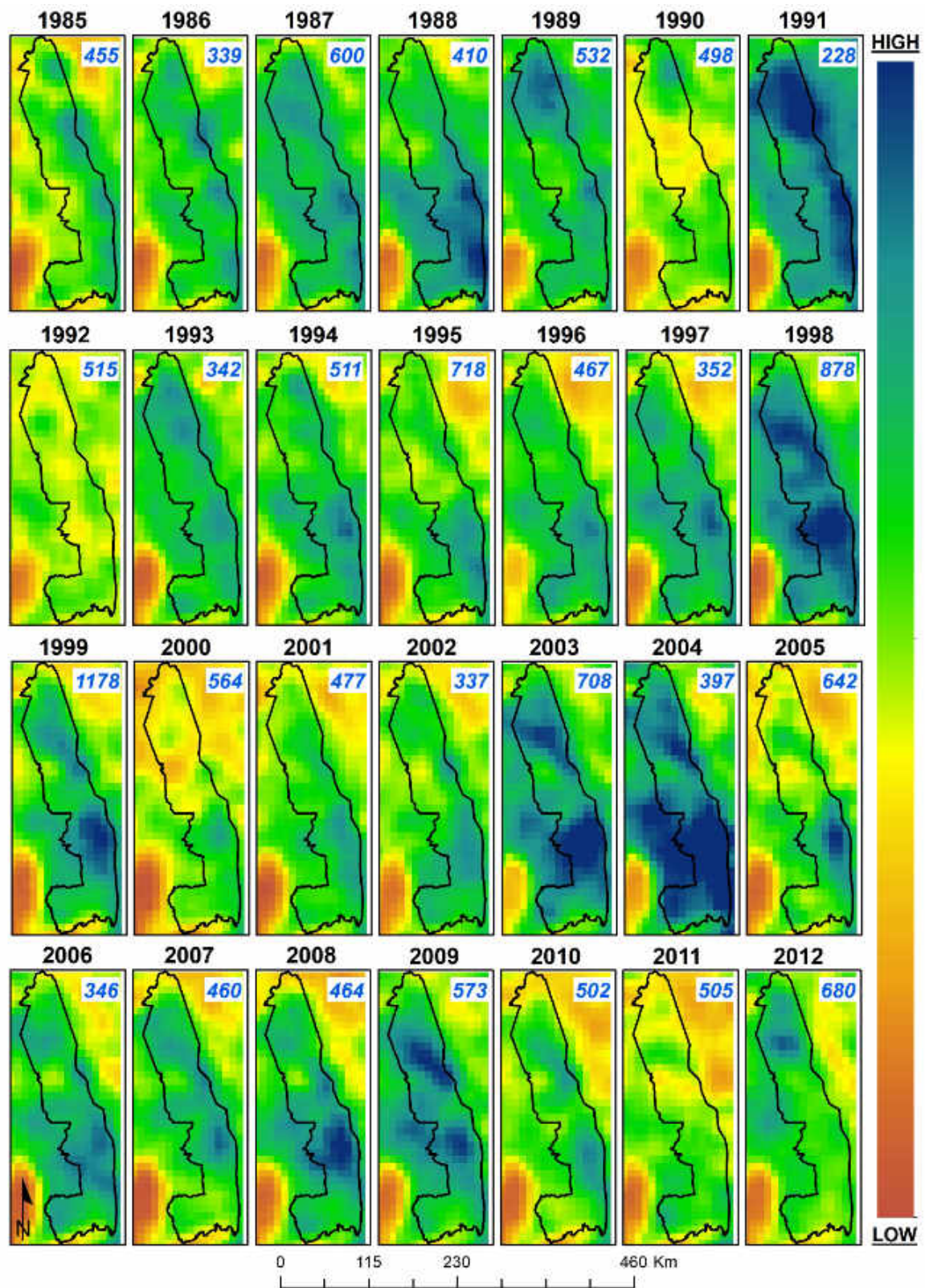
Fig. 5.2: Levelplot of the 8 km^2 annual monthly variability (coefficient of variation) of Advanced Very High Resolution Radiometer (AVHRR) Normalized Difference Vegetation Index (NDVI) values from 1984-2012. Figures in top-right corners represent mean-annual rainfall values for each year.
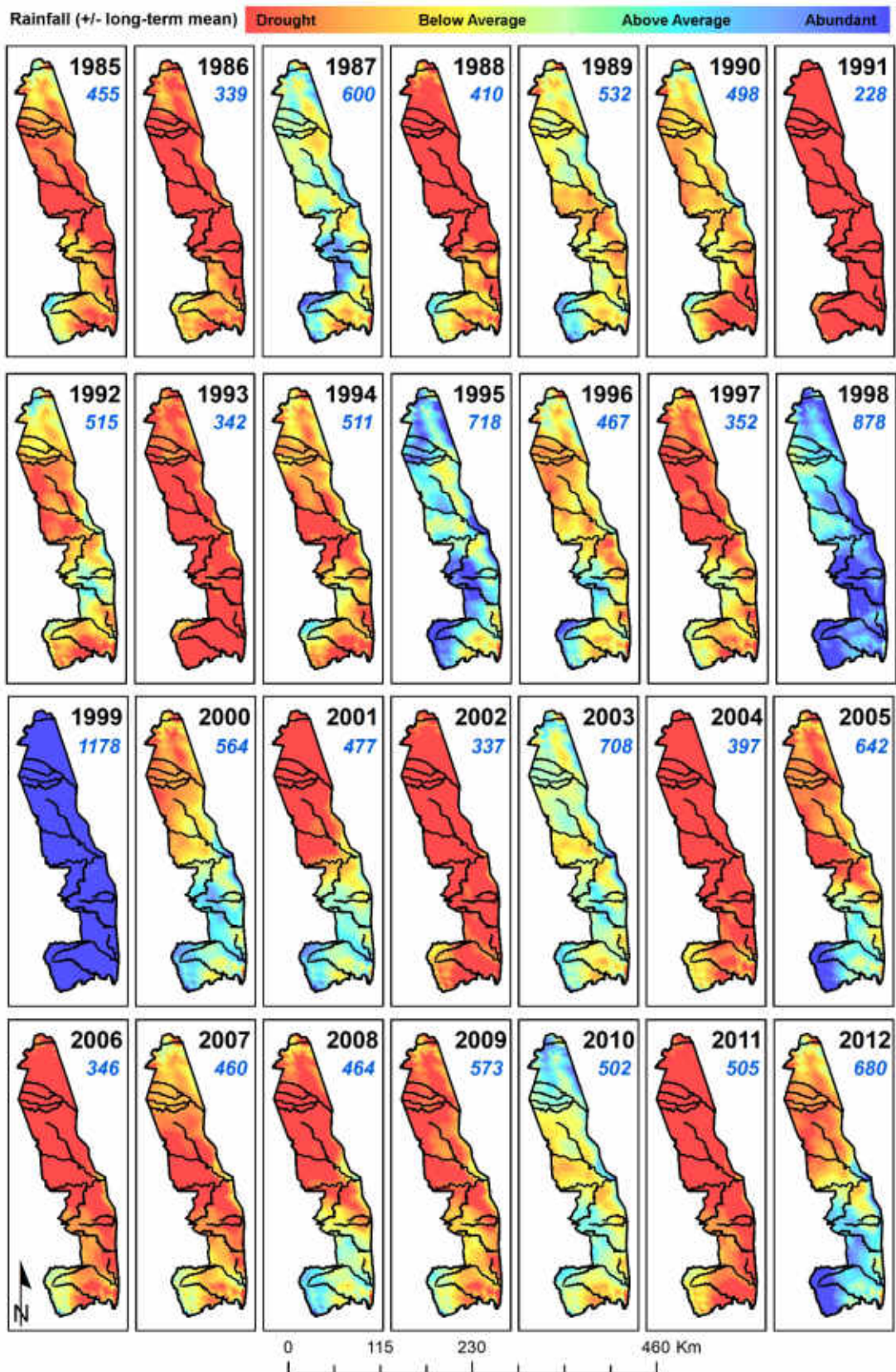
Fig. 5.3: Surface distribution of rainfall above and below the long-term mean for Kruger National Park from 1985 to 2012. Figures in the top-right corners represent mean-annual rainfall values for each year.
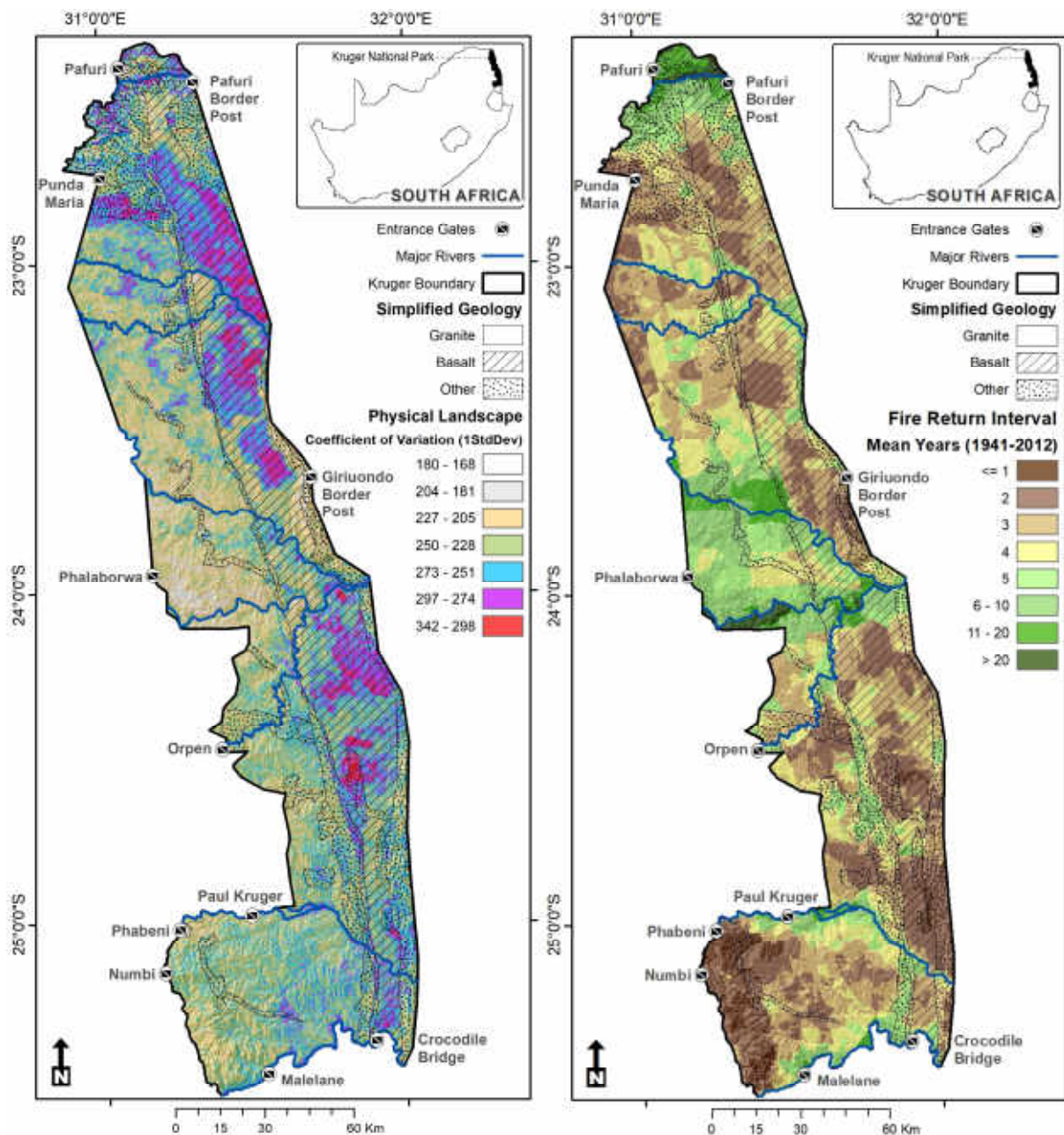
Fig. 5.4: Variability of physical landscape properties and fire return intervals in Kruger National Park. Left panel) Variability of physical landscape properties, geology, soils, terrain and distance to major rivers, displayed as coefficients of variation (CV). Class breaks in the legend above are CV quantiles. Right panel) Mean fire return intervals for Kruger National Park from 1941-2012 (See *Animation S5.2 in Appendix S5* for annual burnt areas maps).

5.3.2. Causal structure of landscape heterogeneity

Based on tests of directed separation, we failed to reject the hypothesized causal structure (Fisher's C $\chi2$ = 0.30, df = 2, p = 0.863, n = 145124, AIC = 100.335, K = 50) and thus feel confident in drawing inferences from the pSEM presented (Fig. 5.5; Table 5.1). In addition, the embedded component models explained much of the variability of the different conditional response variables namely, fire return interval (R^2 = 0.76); elephant density (R^2 = 0.40); heterogeneity (R^2 = 0.34) and buffalo density (R^2 = 0.20).

In order of effect size seen in Fig. 5.5 and Table 5.1, rainfall most distinctly increased heterogeneity (β = 2.782, p < 0.001) followed by increased variability in the physical landscape template (β = 0.746, p < 0.001). Higher elephant densities significantly reduced landscape heterogeneity (β = -0.585, p < 0.001) while lower heterogeneity values caused a less pronounced reduction in elephant density (β = -0.374, p < 0.001). More frequent fires enhanced heterogeneity (β = -0.314, p < 0.001) whereas more heterogeneous landscapes lengthened fire return periods albeit weakly (β = 0.021, p = 0.001). Higher buffalo densities decreased heterogeneity (β = -0.298, p < 0.001) while they also selected for landscapes with lower levels of heterogeneity in almost equal measure (β = -0.276, p < 0.001). Overall Kruger's landscape heterogeneity has moderately increased over time (β = 0. 514, p < 0.001).
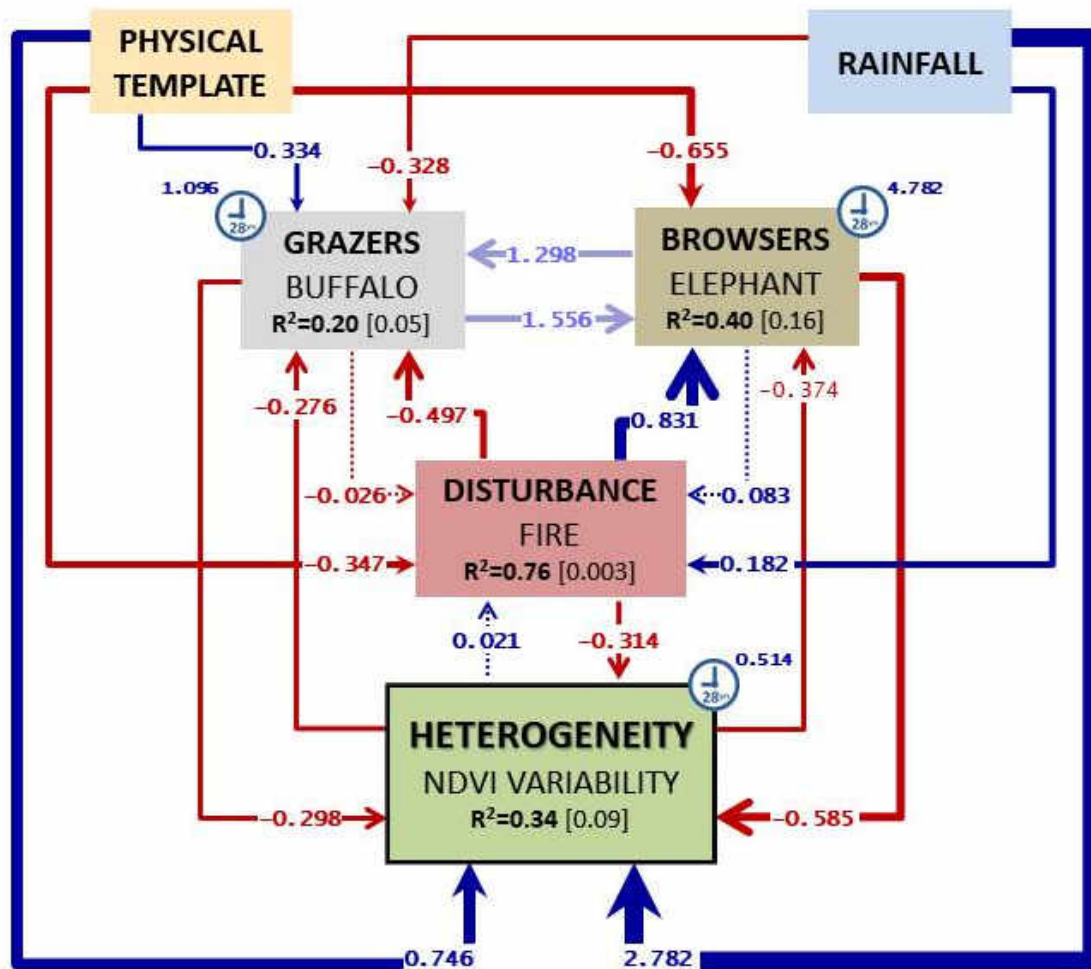
Fig. 5.5: Results of piecewise Structural Equation Model (pSEM) of the cause and effect relationships between landscape heterogeneity, the physical landscape template, rainfall, herbivory and disturbance in Kruger National Park (Fisher's C $\chi^2 = 0.3$, df = 2, p = 0.863, n = 145124, AIC = 100.335, K = 50). Red pathways indicate negative path coefficients. Blue pathways represent positive path coefficients. Thicker lines represent larger effects (positive or negative). Non-significant pathways are removed for clarity (See Table 5.1 for all path coefficients).

Table 5.1: Path coefficients and goodness-of-fit statistics from a piecewise Structural Equation Model (pSEM) of the cause and effect relationships between environmental heterogeneity (HET), the physical landscape template (PHY-CV), rainfall (RAIN), herbivory i.e. buffalo (BUF-DEN) and (ELE-DEN) densities and disturbance i.e. fire return interval (FIRE-RI) in Kruger National Park (Fisher's C χ^2 = 0.30, df = 2, P = 0.863, n = 145124, AIC = 100.335, K = 50). The conditional R^2 (fixed and random effects) are reported in the response column along with the marginal [R^2] (fixed effects only) in brackets.

response	predictor	estimate (unitless)	std-error (unitless)	--> effect	= response
FIRE-RI R^2 = 0.76 [0.003]	PHY-CV	-0.347***	0.081	⬆ PHY	⬆ FIRE
	RAIN	0.182***	0.007	⬆ RAIN	⬇ FIRE
	ELE-DEN	0.083***	0.008	⬆ ELE	⬇ FIRE
	BUF-DEN	-0.026**	0.009	⬆ BUF	⬇ FIRE
	HET	0.021**	0.007	⬆ HET	⬇ FIRE
ELE-DEN R^2 = 0.40 [0.16]	YEAR	4.782***	0.035	⬆ TIME	⬆ ELE
	BUF-DEN	1.556***	0.028	⬆ BUF	⬆ ELE
	FIRE-RI	0.831***	0.043	⬇ FIRE	⬆ ELE
	PHY-CV	-0.655***	0.052	⬆ PHY	⬇ ELE
	HET	-0.374***	0.021	⬆ HET	⬇ ELE
BUF-DEN R^2 = 0.20 [0.05]	ELE-DEN	1.298***	0.024	⬆ ELE	⬆ BUF
	YEAR	1.096***	0.040	⬆ TIME	⬆ BUF
	FIRE-RI	-0.497***	0.041	⬇ FIRE	⬇ BUF
	PHY-CV	0.334***	0.039	⬆ PHY	⬆ BUF
	RAIN	-0.328***	0.020	⬆ RAIN	⬇ BUF
	HET	-0.276***	0.020	⬆ HET	⬇ BUF
HET R^2 = 0.34 [0.09]	RAIN	2.782***	0.024	⬆ RAIN	⬆ HET
	PHY-CV	0.746***	0.059	⬆ PHY	⬆ HET
	ELE-DEN	-0.585***	0.030	⬆ ELE	⬇ HET
	YEAR	0.514***	0.039	⬆ TIME	⬆ HET
	FIRE-RI	-0.314***	0.046	⬇ FIRE	⬇ HET
	BUF-DEN	-0.298***	0.032	⬆ BUF	⬇ HET

Significance levels: *** p < 0.001, ** p < 0.01

The model further revealed different cause-effect relationships between the physical landscape, herbivores and fire frequencies. Specifically, a more variable landscape template shortened fire return intervals (more frequent fires; β = -0.347, p < 0.001) while more rainfall lengthened return intervals (less frequent fires; β = 0.182, p < 0.001). In general both elephant (β = 4.782, p < 0.001) and to a lesser degree buffalo (β = 1.096, p < 0.001) densities increased significantly

over time. Fewer fires (longer return intervals/low fire frequency) however elicited a density decrease response from buffalo (β = -0.497, p < 0.001) and an even stronger density increase response from elephants (β = 0.831, p < 0.001). In return fire return intervals were significantly shortened by higher buffalo densities (β = -0.026, p = 0.002) and lengthened by higher elephants densities (β = 0.083, p < 0.001), although these effects were substantially weaker (Fig. 5.5). Buffalo responded positively to more variability in the underlying landscape template (β = 0.334, p < 0.001) whereas elephants had a stronger negative response to this variability (β = -0.655, p < 0.001). Buffalo densities also decreased with increasing rainfall (β = -0.328, p < 0.001) whereas rainfall had no significant effect on elephant density.

5.3.3. Spatiotemporal dynamics of driver dominance

The variability of driver dominance over heterogeneity change in Kruger from 1985-2012 was spatiotemporally dynamic (see *Animation S5.3 in Appendix S5* for annual driver dominance maps). However, on average heterogeneity is largely affected by rainfall (30%) and physical landscape variability (27%), followed by fire frequency (22%) and elephant density (17%), and to a lesser degree buffalo density (3%) (Fig. 5.6). Rainfall appears to dominate as a driver of heterogeneity in the Southern Granites (Fig. 5.6). While physical landscape variation dominates the Western Basalts often in coalition with fire (Fig. 5.6). Similarly, elephants and fire appear to act together as dominant drivers of heterogeneity in the Northern Granites (Fig. 5.6), while buffalo dominate isolated Granitic patches in the Phalaborwa area along the Olifants and Letaba Rivers (Fig. 5.6).
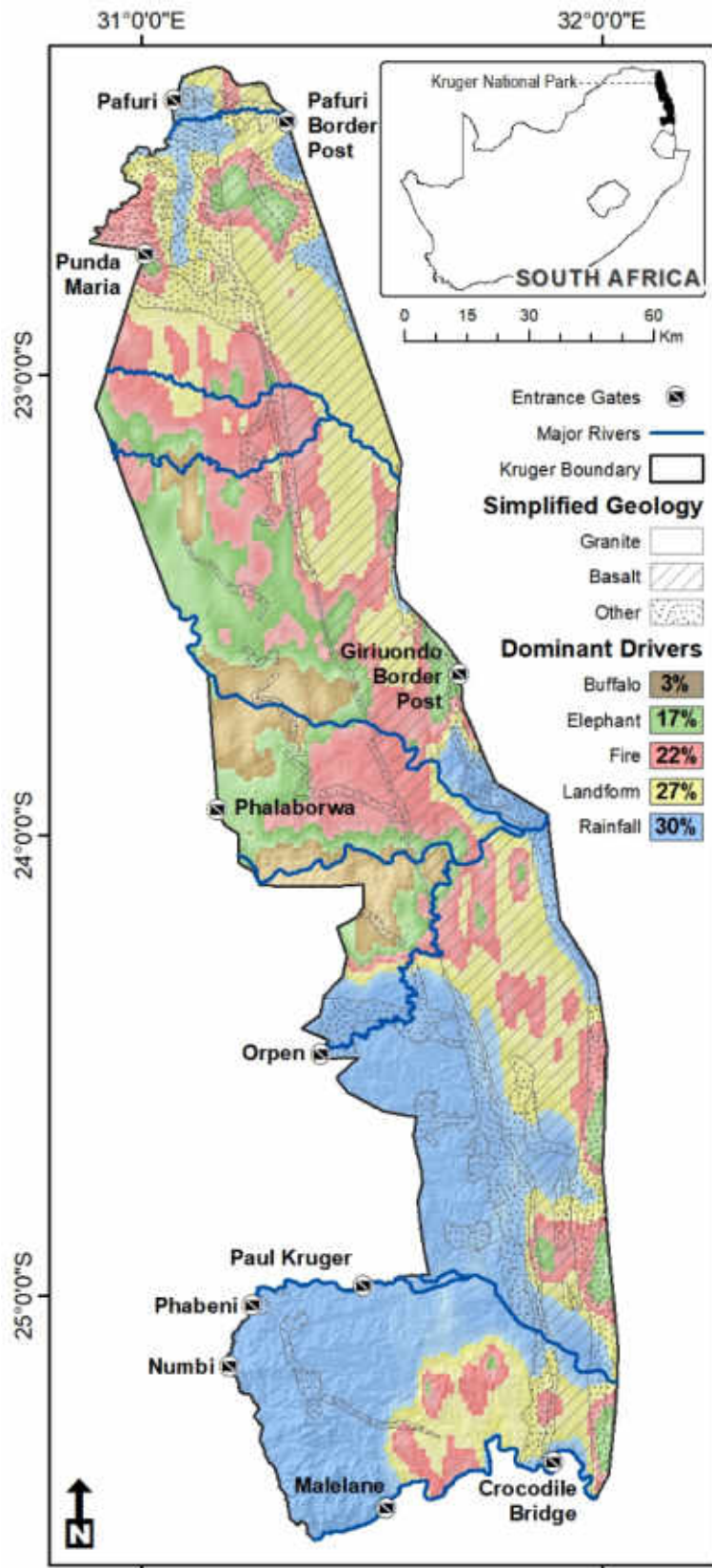
Fig. 5.6: Spatiotemporal arrangement of significant drivers of heterogeneity in the Kruger National Park. The map and percent values in its legend represent the area a specific driver dominated overall (See *Animation S5.3 in Appendox S5* for time series animation).

5.4. DISCUSSION

Landscape heterogeneity in Kruger, as measured by the annual monthly variability of NDVI, is strongly driven by rainfall, variations in the physical landscape template, elephant density and fire. This aligns well with the results of Sankaran *et al.* (2005) who correspondingly found rainfall, herbivory and fire to be key drivers of tree-grass dynamics across African savannas but at a continental scale. At a local scale (Kruger), higher rainfall elicited a strong positive response from heterogeneity as did a more diverse underlying physical landscape template. In contrast, heterogeneity significantly decreased in areas with longer fire return intervals (less frequent fires). Fundamentally this supports the hypothesis of Parr and Andersen (2006) who describe fire as an agent of biodiversity formation and maintenance. Conversely more heterogeneous landscapes generally experienced fewer fires, which we expect may also be a product of the patch mosaic burning model. That is, mosaic burning allows fire to move freely through the landscape, burning at varied levels of intensity as a function of different barriers (e.g. rivers or roads), fuel content, soil moisture conditions and/or topographic features in the landscape (Duncan *et al.* 2015). Heterogeneous environments would typically have a greater diversity of such barriers and/or physical landscape features, thus resulting in the more patchy fire history or longer return intervals. Smit *et al.* (2013b) correspondingly found granitic areas and those closer to rivers less prone to fire. Heterogeneity responded to higher elephant densities with a significant decrease, even though as ecosystem engineers they are often credited to enhance landscape heterogeneity (Pringle 2008). Using pSEM we were able to distinguish a stronger negative response of heterogeneity to increased elephant density from the weaker negative response of elephants to heterogeneity in the landscape. If a standard regression model had been run instead of pSEM, we would be less able to distinguish this cause and effect, or answer the question whether elephants are selecting for areas with less heterogeneity or are they actually causing a reduction in heterogeneity. Guldemond and van Aarde (2008) and others

(Loarie *et al.* 2009; Vanak *et al.* 2010) have suggested the presence of fences may further compound negative effects of elephants on savanna vegetation by altering movement patterns and resulting densities. Our results suggest that at their current densities and within a confined space like Kruger, elephants are having a potentially large scale homogenizing effect on the landscape.

We expect the effect of fire on vegetation structure may also be responsible for different herbivore density and distribution patterns. For example, higher buffalo densities were found in areas with shorter fire return intervals whereas higher elephant densities were found in areas experiencing fewer fires. Grazers like buffalo, favor open grassland areas maintained by high fire frequencies, whereas browsing elephants occur in higher densities in less fire prone areas like those along rivers and more wooded areas (MacFadyen *et al. in Review*; Skinner and Chimimba 2005). In return, fire return intervals were significantly shortened by higher buffalo densities and lengthen by higher elephants densities, although these effects were considerably weaker (Fig. 5.5). The higher grazing pressure of buffalo may therefore be responsible for maintaining fire-prone grassland states as suggested by Ripple *et al.* (2015) when they described globally under recognized ecosystem effects of large herbivores. In contrast, higher elephant densities may reduce fire frequencies as they have been shown to alter tree-grass dynamics and stimulate woody shrub encroachment in many woodland areas of northern Botswana (Fullman and Bunting 2014; Teren 2016). Rainfall is also known to influence animal behavior in Kruger, with herbivores dispersing more in wetter seasons compared to dry seasons, as they are no longer forced to concentrate around limited food and water resources (Chirima *et al.* 2012). We found this pattern in buffalo, as densities decreased with increasing rainfall, but not for elephants. We expect buffalo may be responding to an increase in surface water availability, as well as a grass biomass production response to increased rainfall rather than a direct density response. Elephants however showed no significant response to rainfall, a result supported by

MacFadyen *et al.* (*in Review*) who found herd elephant densities did not change significantly from the mean under higher rainfall conditions.

The role played by different drivers of heterogeneity change in Kruger from 1985-2012 is spatiotemporally variable (Fig. 5.6; *Animation S5.3 in Appendix S5*). Rainfall tends to dominate the Southern Basalts and patches in the Far North described by MacFadyen *et al.* (2018) as extreme-high rainfall areas. Fire is a key driver throughout the park, although elephants and fire also appear to have a strong synergistic relationship in that elephants (green in Fig. 5.6) are often associated with fire driven areas (pink in Fig. 5.6). The combination of these two drivers affects almost 40% of Kruger's surface area. While the underlying physical landscape, as a driver of heterogeneity, only dominates 27% of Kruger. We believe the diverse range of drivers, responders and consequent processes interact with Kruger's physical landscape template to produce a highly dynamic system (Munyati and Ratshibvumo 2010; Smit *et al.* 2013b). This is supported by MacFadyen *et al.* (2016), who showed the proportion of environmental heterogeneity explained by stable physical landscape properties in Kruger is spatiotemporally dynamic.

It is however important to also consider the dynamic nature of heterogeneity, which clearly fluctuates from year to year as seen in Fig. 5.2. We illustrate this using an animation (*Animation S5.3 in Appendix S5*) of the spatiotemporal variability of drivers in terms of those that dominated from 1985 to 2012. How these drivers have moved or changed in the landscape and how they interact remains an interesting question, one which could perhaps be answered with time series analysis and the inclusion of latent variables into pSEM functionality in future. Likewise, the inclusion of new higher resolution datasets into this framework may also provide more local detail for adaptive park management. For example, the 5 km^2 Leaf Area Index and Fraction of Absorbed Photosynthetically Active Radiation product (AVH15C1) available from NOAA's National Centers for Environmental Information, Climate Data Record from 1981 to

the present (Claverie *et al.* 2014; Claverie *et al.* 2016). New solutions for measuring diversity using remotely sensed imagery, like Rao's quadratic entropy (Q), could also be explored further to investigate potential pattern and process links (Rocchini *et al.* 2017). Until then future scenario can also be mapped using the results presented here, for example, should the effects of climate change result in 200 mm less rainfall per year, i) heterogeneity will decrease; ii) buffalo with cluster into larger herds; iii) and fire return periods will lengthen iv) while elephant distribution and abundance patterns will remain largely unchanged (Fig. 5.5).

In conclusion, we stress that while it may be difficult to separate system drivers and their reciprocal cause and effects from complex interacting ecosystem processes, pSEM produces compelling results for holistic biodiversity conservation. Coupled with remotely sensed NDVI data, the cause and effect relationships of drivers known to be either direct or indirect mechanisms of ecosystem change can now be quantified. Reciprocal cause and effect relationships clearly exist, although the significance of one will often overshadow the other over the long-term. For example, climate change predictions of decreased rainfall across African savannas (DEA 2013; IPCC 2014) may directly affect only 30% of Kruger's PA landscape (Fig. 5.6) but its compound effects on fire frequencies and herbivore distribution and abundance patterns will stimulate a domino effect that could shift ecosystem states and have long-term, ecosystem wide consequences. Globally, these results therefore add to efforts to discern ecosystem structure and functioning and assess conservation outcomes by quantifying heterogeneity and visualizing its causal relationships with key environmental drivers. Locally, these results provide insight into the role, and magnitude of each driver's impact on Kruger ecosystem properties and functioning to help gain an understanding of heterogeneity and the dynamic drivers thereof. Protected areas managers may as a result be able to critically review, and where necessary adapt, policies and plans. For Kruger these results may cultivate a better understanding of i) rainfall as a dynamic driver of heterogeneity, which can help steer national

park planning and land reclamation policies based on projected climate change impacts; ii) how fire interacts with rainfall and herbivory to affect heterogeneity, which can now support current and future fire management policies; and iii) the importance of large mammal management plans that acknowledge and offer mitigation strategies for the spatial and temporal impacts of herbivore distribution and density patterns on heterogeneity. Conclusively, our analysis has shown that heterogeneity is formed and maintained by different interacting ecosystem processes. Incorporating heterogeneity into the EBV may therefore also provide interesting insights into global biodiversity dynamics specifically for protected areas.

Global Heterogeneity Tracker

Beta 1.0

Global Heterogeneity Tracker for Protected Areas ≡

UNIVERSITEIT STELLENBOSCH UNIVERSITY — Department of Botany and Zoology — VU VRIJE UNIVERSITEIT AMSTERDAM — Faculty of Earth and Life Sciences

Heterogeneity Tracker Beta 1.0

Sandra MacFadyen - Cang Hui - Peter Verburg - Astrid Van Teeffelen

Biodiversity conservation is an accelerating global concern, as illustrated by the growing need for globalised biodiversity protection strategies. However, for globalised initiatives to work they need to be interactive and easily assessable to collaborators across continents. We therefore explore the graphical and statistical power of R combined with the web-sharing ability of Shiny and mapping capabilities of Leaflet , to provide an interactive system for biodiversity planning in Protected Areas (PA). Landscape heterogeneity is considered an important indicator for biodiversity, described as a duplicitous cause and consequence of ecological processes and environmental pattern {Turner 1989 ; Pereira et al. 2013 ; MacFadyen et al. inPrep). In the relatively unaltered landscapes of PAs, increased heterogeneity is thus indicative of an accompanying increase in habitat diversity, resulting in greater species diversity and improved ecosystem resilience (Tews et al. 2004 ; MacFadyen et al. inPrep). The underlying heterogeneity template is made up of a mosaic of different topographies; climates; geologies; soil types; and vegetation phenology which interact to create, maintain or influence these available habitats and supported species assemblages (MacFadyen et al. 2016) The key to effective ecosystem conservation therefore lies in the ability to describe landscape heterogeneity in terms of the environmental drivers that generate and maintain this relationship (Levin 1992 ; MacFadyen et al. inPrep).

○ Esri.WorldStreetMap
○ Esri.NatGeoWorldMap
○ Esri.WorldImagery

① Protected Areas

Leaflet | Tiles © Esri — Source: Esri, DeLorme, NAVTEQ, USGS, Intermap, iPC, NRCAN, Esri Japan, METI, Esri China (Hong Kong), Esri (Thailand), TomTom, 2012

Input shapefile [PROJ. WGS84]

Browse... No file selected

6

Heterogeneity Tracker: Knowledge sharing using Shiny R to monitor global landscape heterogeneity differences across protected areas

This chapter is to be submitted as:

MacFadyen S, Hui C, Verburg PH and Van Teeffelen, AJA (To be submitted) Heterogeneity Tracker: Shiny monitoring of global landscape heterogeneity differences for protected areas. *International Journal of Digital Earth*. https://heterogeneity.shinyapps.io/globalheterogeneity

ABSTRACT

Biodiversity conservation is an accelerating global concern driving a need for international biodiversity protection strategies. Globalised initiatives will however need spatial information that is interactive and easily accessible to collaborators across continents and conservation agencies. To facilitate this we explore the graphical and statistical power of R, combined with the web-sharing ability of Shiny and mapping capabilities of Leaflet, to illustrate the effectiveness of such an approach for global biodiversity planning and protected areas management. Specifically, we develop an interactive interface to evaluate biodiversity features using an index of landscape heterogeneity and dissimilarity. In Protected Area (PA) landscapes, increased heterogeneity is often indicative of an accompanying increase in habitat diversity, resulting in greater species diversity and improved ecosystem resilience. Underlying this heterogeneity is an environmental template made up of a mosaic of different topographies, climates, geologies, soil types, and vegetation variables. These variables interact to create, maintain and influence available habitats and the range of species assemblages they can support. How these patterns differ across PAs is summarised across global subregions (n = 19) to explore potential gaps in existing delineations of biodiversity hotspots. Central, South and East Asian PAs were ranked highest in overall heterogeneity, despite the fact they represent a relative low proportion of the worlds recognised biodiversity hotspots (3-6%). Northern European and Central American PAs were also identified as being environmentally diverse. Using these results we begin to operationalise the heterogeneity-biodiversity theory with a Heterogeneity Tracker App (https://heterogeneity.shinyapps.io/globalheterogeneity) to explore underlying environmental drivers of global landscape heterogeneity patterns. Heterogeneity Tracker Beta 1.0 provides a method of exploring these patterns at different scales across ~ 8 000 PAs globally.

6.1. INTRODUCTION

Biodiversity conservation is a global priority for the maintenance of ecosystem health and the protection of ecosystem services (Egoh *et al.* 2009; Hooper *et al.* 2012). In response to accelerated declines in the global biodiversity estate, the Conference of the Parties (COP) of the Convention on Biological Diversity (CBD) introduced 20 Aichi Biodiversity Targets in a revised Strategic Plan for Biodiversity 2011-2020 (CBD 2010; UNEP-WCMC and IUCN 2016). The targets aim to track the state and trends of biodiversity through the use of global, national and regional indicators (Han *et al.* 2014). A number of these indicators are described in the Group on Earth Observations Biodiversity Observation Network's (GEOBON) list of Essential Biodiversity Variables (EBV; Mace and Baillie 2007; Pereira *et al.* 2013; Brummitt *et al.* 2016). Each EBV class contains a set of candidate variables derived from either *in-situ* monitoring or remote sensing measurements that gauge the effectiveness of implementation strategies and assess progress (Pereira *et al.* 2013).

Absent from this list is landscape heterogeneity, despite its recognised links to biodiversity outcomes (Stein *et al.* 2014; Tuanmu and Jetz 2015; MacFadyen *et al.* 2016). The ability to describe and visualise the patterns of the constituent parts of landscape heterogeneity is however well positioned to become an important support tool for biodiversity conservation in large PAs (Levin 1992). Large PAs in particular play an important role in the long-term maintenance of biodiversity, including the generation and sustention of its compositional, structural and functional forms (Cantú-Salazar and Gaston 2010). Such areas also afford ecologists the opportunity to develop and test different ecological theories by exploring models across natural-degraded gradients upon highly heterogeneous physical and functional templates. This underlying template is comprised of a mosaic of different topographies,

climates, geologies, soil and vegetation types and conditions which interact to create, maintain and influence landscape heterogeneity and its dependant species (MacFadyen *et al.* 2016).

The development of practical tools to quantify, monitor and track heterogeneity can therefore be of particular importance to conservation managers (Levin 1992). This need is echoed in the 2005 Millennium Ecosystem Assessment (MEA 2005) and 2014 Global Biodiversity Outlook 4 (CBD 2014) reports for globalised biodiversity protection strategies. Globalised conservation initiatives require data and knowledge sharing agreements, which are interactive and easily accessible to collaborators across continents. Han *et al.* (2014) recognised this need and developed the Biodiversity Indicators Dashboard using disaggregated global data to "track progress toward the Aichi Targets, support national monitoring and reporting, and inform outcome-based policy-making for the protection of natural resources" (Han *et al.* 2014). Taking Han *et al.*'s (2014) approach a step further, we explore the graphical and statistical power of R (R Core Team 2016) combined with the web-sharing ability of Shiny (Beeley 2013; Chang *et al.* 2015) and mapping capabilities of Leaflet (Cheng and Xie 2016), to develop an application (App) that can support collaborative and interactive exploration of heterogeneity in protected areas across the world. Heterogeneity Tracker Beta 1.0 is presented here as an open access spatial tool to demonstrate the ability of these technologies to serve large scale information for collaborative conservation management and research. The interactive interface allows users to visualise indices of global landscape variability as different map layers and interrogate consequent results. This Beta 1.0 release is a proof of concept, analysis and visualisation tool to begin understanding the role heterogeneity may play in global biodiversity conservation strategies. We conclude with a discussion of possible version shortcomings and highlight plans for future developments to ultimately produce a practical, implementable, tool for PA managers.

6.2. MATERIALS AND METHODS

6.2.1. Building Heterogeneity Tracker Beta 1.0

All analyses were carried out in R version 3.3.1 (R Core Team, 2016). All raster processing

and analyses were done using R's {raster} package (Hijmans 2016) unless otherwise stated.

Shiny R package version 1.0.0 (Chang *et al*. 2015) and Leaflet version 1.0.1 (Cheng and Xie

2016) were used to compile a web interface to interactively explore and visualise landscape

heterogeneity using freely available global data sources. The Shiny framework was used to

provide a graphical user interface for the interactive Leaflet map, with additional R functions

driving statistical analysis and plot generation (Beeley 2013). Three separate map tile layers,

provided by ESRI (WorldStreetMap; NatGeoWorldMap; WorldImagery), were embedded into

the App, allowing users to zoom in and out with scalable cartographic detail (Karambelkar

2017). The ability to add user defined shapefiles from a local directory was also added to afford

users the opportunity to explore results in the context of their own studies. The Heterogeneity

Tracker App and associated R code was then served online using the free version of

shinyapps.io (2017). The free plan is however limited to only one application instance and one

worker process (shinyapps.io team 2017). This means only one user at a time may fully utilize

the App and that multiple concurrent users may result in a system reloaded or refresh request.

Starter, basic, standard and professional plans are also available to purchase. For example, the

basic plan would allow "unlimited applications, 500 active hours, multiple workers processes

and the ability to add additional instances to keep the App responsive as more people use them"

(shinyapps.io team 2017). See the shinyapps.io user guide for detailed setting descriptions

(shinyapps.io team 2017).

6.2.2. Data Input

To define the earth's physical landscape template we needed global spatial information to describe the underlying mosaic of different topographies, geologies, soils, vegetation (types and conditions) and climates, across all terrestrial protected areas. These components interact to create, maintain and influence landscape heterogeneity and its associated suite of dependant species (MacFadyen *et al*. 2016). Thus, the patterns generated by the unique combination of these components are expected to provide some insight into the diversity of environmental conditions and, by proxy, biodiversity. Global data sources incorporated here include:

6.2.2.1. *Protected areas*

The World Database on Protected Areas (WDPA) is an open source global spatial database of marine and terrestrial protected areas, with associated regional, national and international details on IUCN classifications, designations and management plan standings (UNEP-WCMC 2016). All terrestrial protected areas greater than 200 km^2 (n = 7927) were extracted from the WDPA (UNEP-WCMC 2016) and used to create a mask for further analyses.

6.2.2.2. *Topography*

The Global Multi-resolution Terrain Elevation Data (GMTED) is an enhanced elevation model produced by the U.S. Geological Survey (USGS) and the National Geospatial-Intelligence Agency (NGA) specifically for global and continental scale applications (Danielson and Gesch 2011). The 1 km^2 resolution version of this product was downloaded and resampled to 5 km^2 using a nearest neighbour assignment (Hijmans 2016). A Topographic Roughness Index (TRI) was then calculated (Evans 2016) from GMTED and the results reclassified into seven categories of terrain surface ruggedness, as described by Riley *et al*. (1999).

6.2.2.3. *Geology*

A new spatial representation of global lithology and geology (GLiM), developed by Hartmann and Moosdorf (2012), was downloaded as a polygon shapefile indicating the distribution of 15 different rock types across the Earth's surface. These were later converted into a global 5 km^2 grid, classified into dominant rock types (Hijmans 2016).

6.2.2.4. *Soil Properties: Depth to bedrock and soil form*

The International Soil Reference and Information Centre (ISRIC) administers an online database of soil properties (SoilGrids) derived from machine learning algorithms using global soil profile data and environmental covariates (Hengl *et al*. 2014). The absolute depth to bedrock (in cm) and the predicted soil class according to the World Reference Base for soils and the U.S. Department of Agriculture key to soil taxonomy (Hengl *et al*. 2014) were downloaded as 1 km^2 grids and then resampled to 5 km^2 (Hijmans 2016).

6.2.2.5. *Land Cover*

The Food and Agriculture Organization of the United Nations (FAO) produced a harmonized Global Land Cover product (GLC-SHARE) based on national, regional and global land cover datasets (Latham *et al*. 2014). The 1 km^2 GLC-SHARE grids were downloaded, stacked and assigned a dominant 'natural' (excluding artificial surfaces and croplands) landcover class per pixel. That is, the maximum percentage cover value per pixel was identified from categories: grassland; tree covered areas; shrub covered areas; herbaceous vegetation, aquatic or regularly flooded areas; mangroves; sparse vegetation; bare soil; snow and glaciers and; inland water bodies (FAO 2014). The resulting dominant natural landcover layer was then resampled to 5 km^2 (Hijmans 2016).

6.2.2.6. *Climate: Temperature and rainfall*

Bioclimatic variables representing the long-term seasonality (i.e. annual range) of temperature (bio4) and precipitation (bio15) were downloaded from the global climate dataset WorldClim version 1.4 as $\pm$ 5 km^2 grids (Hijmans *et al.* 2005). These variables characterise the long-term inter-annual variability of temperature and rainfall in units of standard deviation[*100] and coefficients of variation respectively (Hijmans *et al.* 2005).

6.2.2.7. *Vegetation phenology*

Satellite derived Normalised Difference Vegetation Indexes (NDVI) provide estimates of vegetation biomass and vigour by measuring vegetation 'greenness' (Marshall *et al.* 2016). Long-term global NDVI datasets are therefore often used to study vegetation dynamics and examine resource variability (Wessels *et al.* 2006; Marshall *et al.* 2016). Monthly maximum composites of NDVI were downloaded from the Global Inventory Modelling and Mapping Studies' (GIMMS) dataset version 3 (NDVI$_{3g}$; Detsch 2016). The inter-annual standard deviation (SD) of NDVI was then calculated at the pixel level for each year (n = 33), resulting in a *rasterStack* with 33 layers distinguishing NDVI variability (Hijmans 2016). The long-term mean of this inter-annual variability of NDVI was then calculated to smooth out any confounding climate change effects.

6.2.2.8. *Globally recognised biodiversity hotspots*

Global biodiversity hotspots represent those areas which support a significant number of unique or endemic species (Noss *et al.* 2015). Each of the 36 biodiversity hotspots, as defined by Meyers *et al.* (2000), are nested within an outer limit zone, which acts as a buffer to potential impacts from adjacent land uses (Myers *et al.* 2000). Forest landscapes form a large portion of these biodiversity hotspots and are considered some of the most biologically diverse landscapes

(Potapov *et al*. 2008). The boundaries of 'intact' forest landscapes are therefore of special interest for conservation planning as they include all forest expanses not yet significantly fragmented by human activity (Potapov *et al*. 2008). The boundaries of these areas (biodiversity hotspots and intact forests) were downloaded as polygon shapefiles and used as overlays for comparing results.

6.2.3. Analysis of Environmental Heterogeneity and Dissimilarity

For each layer, all values falling outside of protected areas were masked (assigned as NA) from further analyses. A heterogeneity index was then determined for each layer using a Grey Level Co-occurrence Matrix (GLCM), which computes the anisotropic distribution of co-occurring values in a 3 x 3 pixel moving window (Lu and Batistella 2005).

$$P_{i,j} = V_{i,j} / \sum_{i,j=0}^{N-1} V_{i,j} \qquad \text{[1]}$$

Where $V_{i,j}$ is the value in the cell with row i and column j of the moving window and N is the total number unique values in each layer. In this way the matrix is normalised to approximate the probability tables of how often a pixel value of 1, for example, occurs either horizontally (0°), vertically (90°), or diagonally adjacent (45°, 135°) to a value other than 1 (Zvoleff 2016). The dissimilarity of GLCM was then calculated as follows:

$$D = \sum_{i,j=0}^{N-1} P_{i,j} \; (i-j) \qquad \text{[2]}$$

Where $P_{i,j}$ is given above [1] and dissimilarity D increases linearly as $(i - j)$ increases. Larger D values therefore depict pixels highly dissimilar to their neighbours in all four directions (Zvoleff 2016). In this way dissimilarity was estimated for topographic roughness (TRI), geology

(GEO), bedrock depth (RDEP), soil type (SOIL), landcover type (LNDC) and long-term mean variability of temperature (TEMP), rainfall (RAIN) and vegetation 'greenness'(NDVI). The area-weighted mean of each dissimilarity estimate was then calculated for all protected areas (n = 7927) and compared across continents and subregions (ISO 3166-1 2006) using Kruskal-Wallis rank sum tests and box plots (R Core Team 2016). An overall heterogeneity index was derived from the sum of all component dissimilarities and presented as different choropleth or thematic maps by continent (Sarkar and Andrews 2016; Tennekes 2017).

6.3. RESULTS

6.3.1. Heterogeneity Tracker Beta 1.0: Structural and functional outline

The resulting Global Heterogeneity Tracker for Protected Areas App is available from https://heterogeneity.shinyapps.io/globalheterogeneity/. Fig. 6.1 describes the five different tab items and their associated functions:

❷ **Introduction:** Provides a brief outline to the rationale behind the development of the Heterogeneity Tracker App along with a world map displaying all PAs as points. The user can select from three possible background map layers namely streets, NatGeo or satellite imagery, as well as add their own shapefile (point, line or polygon) to the map. Numbers represent the number of PAs nested behind a particular point at a particular scale. A left-mouse click on one of these numbered points will zoom the user closer to those PAs within the boundary area indicated by the pop-up blue polygon. Numbers will change as one zooms closer to the centre-point of a particular PA, leaving a green marker with pop-up labels giving the PA's name.

❷ **Custom analysis:** Allows users to run the analyses, described in 6.2.3 of the methods section above, for a PA of their choice. When no PA is selected, the boxplot below depicts the distribution of PA size across world regions. Users may zoom directly into the map and select a PA (green marker), or select a country from the drop-down list provided and then choose from the filtered list of PAs for that country. Once a PA is selected, the boxplot will update to display the dissimilarities of the various environmental variables. Users can also add their own shapefile (point, line or polygon) layers to the map by browsing to their selected .shp, .shx and .dbf files. In addition, a layer control menu will appear on the top-right of the map allowing the user to turn the different base and/or result layers on or off. Specifics of these results are summarised in section 6.3.2 below.

Fig. 6.1: Composite screen view of Heterogeneity Tracker Beta 1.0 structure and functionality, designed using a Shiny framework with embedded Leaflet maps and various summary and graphing functions. Available from https://heterogeneity.shinyapps.io/globalheterogeneity/.

❸ **Continental summary:** Summarises the results of the different environmental dissimilarity weights for PAs across continents, as described in methods section 6.2.3. The user may select the desired environmental variable from the drop-down list to change the associated thematic map and boxplot. Specifics of these results are summarised in section 6.3.2 below.

❹ **Data citations:** Includes the references and online repositories for all global data, referred to in methods section 6.2.2, used in the development of the Heterogeneity Tracker App. All data are open access or used within specific restrictions described by relevant use agreements.

❺ **Acknowledgements:** Acknowledges the contributions of financial institutions and individuals who provided data or other support for the development of the Beta 1.0 release of Heterogeneity Tracker.

6.3.2. Environmental Heterogeneity and Dissimilarity

Dissimilarity weights of the environmental layers, namely TRI; GEO; RDEP; SOIL; LNDC; TEMP; RAIN and NDVI varied significantly ($P < 0.0001$) within PAs between world subregions (Fig. 6.2). The sum of all dissimilarities represents the overall heterogeneity score for a particular PA. The distribution of these scores across world subregions is illustrated in Fig. 6.3.

On average, Southern Asia and parts of South America have the highest levels of environmental dissimilarities (i.e. highly heterogeneous) across their PAs, while Middle Africa and Australia had the lowest. This may be an artefact of the large number of PAs designated in similar environments, for example, forests in South America or arid regions in Australia. Moreover, South America as a subregion had surprisingly low levels of dissimilarities considering the high levels of biodiversity known to occur in its Amazonian rain forests.
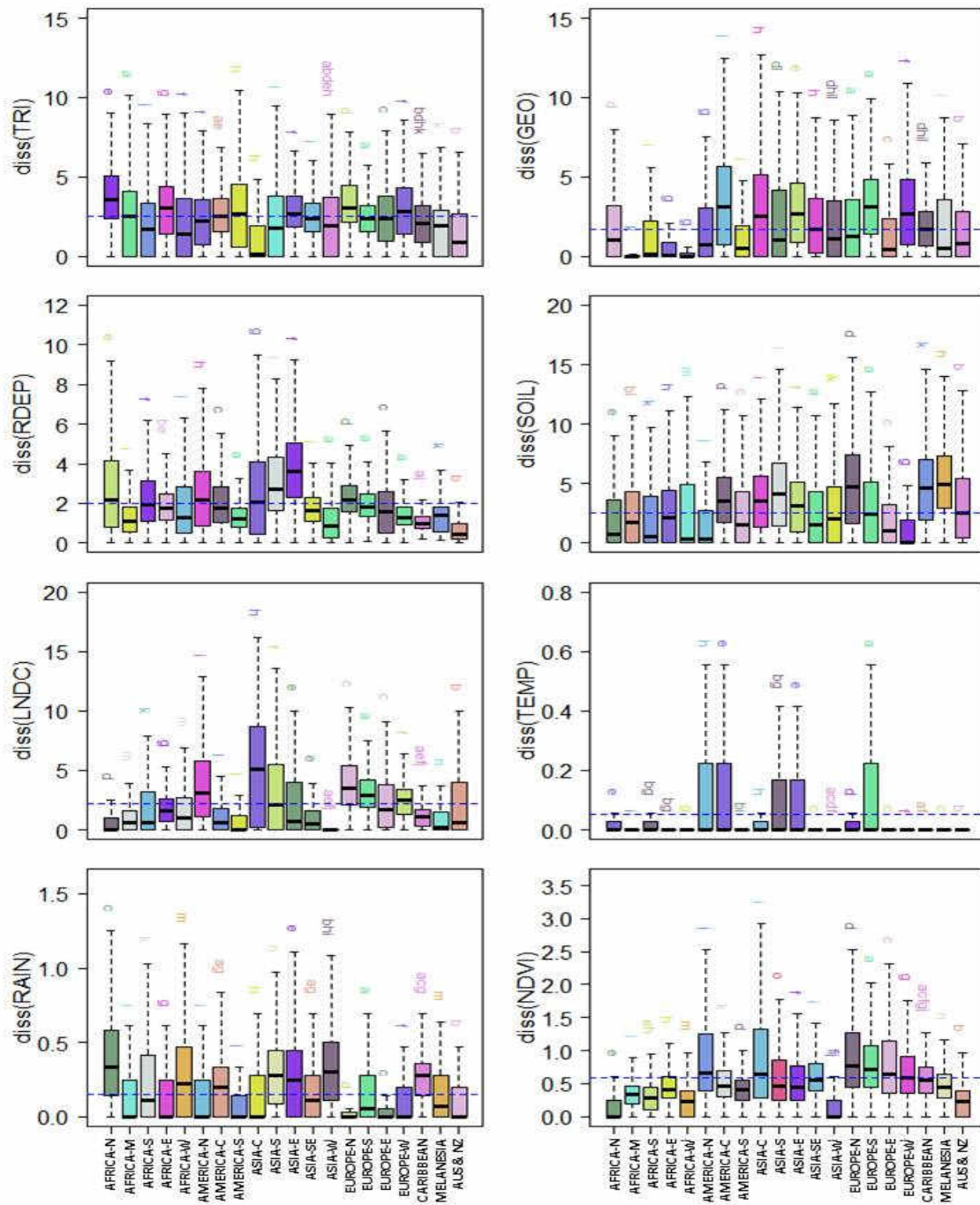
Fig. 6.2: Distribution of dissimilarity (diss) weights of environmental layers, topography (TRI); geology (GEO); depth to bedrock (RDEP); soil type (SOIL); landcover type (LNDC) and the mean inter-annual variability of long-term temperature (TEMP); rainfall (RAIN) and vegetation greenness (NDVI), in protected areas between world subregions. Letters and associated colours in each plot represent a summary of similarities and differences between subregions based on TukeyHSD results (Graves *et al*. 2015). Common characters identify subregions that are not significantly different (P < 0.05). Abbreviations: N-North; M-Middle; S-South; E-East; W-West; C-Central; AUS-Australia; NZ-New Zealand.

We posit that while rainforests themselves are species rich (Myers *et al.* 2000), the underlying environmental variables may not necessarily be highly dissimilar across PAs. That is, the majority (74%) of areas protected across South America are classified as Tropical Moist Broad-leaf Forests (UNEP-WCMC 2016; Sayre *et al.* 2014) with intrinsically similar geology, climate and vegetation greenness. This suggests the simple summation of all component dissimilarities produces a skewed view of heterogeneity as an indicator for biodiversity. However these preliminary results do also suggest potentially significant gaps in existing delineations of biodiversity hotspots. For example, Central, South and East Asian PAs were ranked highest in overall heterogeneity although they represent relative low percentages of Myers *et al.* (2000) biodiversity hotspots (3-6%). Similarly, Northern European and Central American PAs were also identified as being environmentally diverse. From a PA point of view, diversity clearly varies across substrates (Fig. 6.2) and between global subregions (Fig. 6.3), future revisions should investigate the use of weighted sums, with certain ecosystem types weighing higher than others (e.g. forests versus deserts or tundra). Of course other component dissimilarities could also be included to better reflect the complexity of landscape heterogeneity and its composite relationship with biodiversity. These and other future developments are discussed in more detail below.
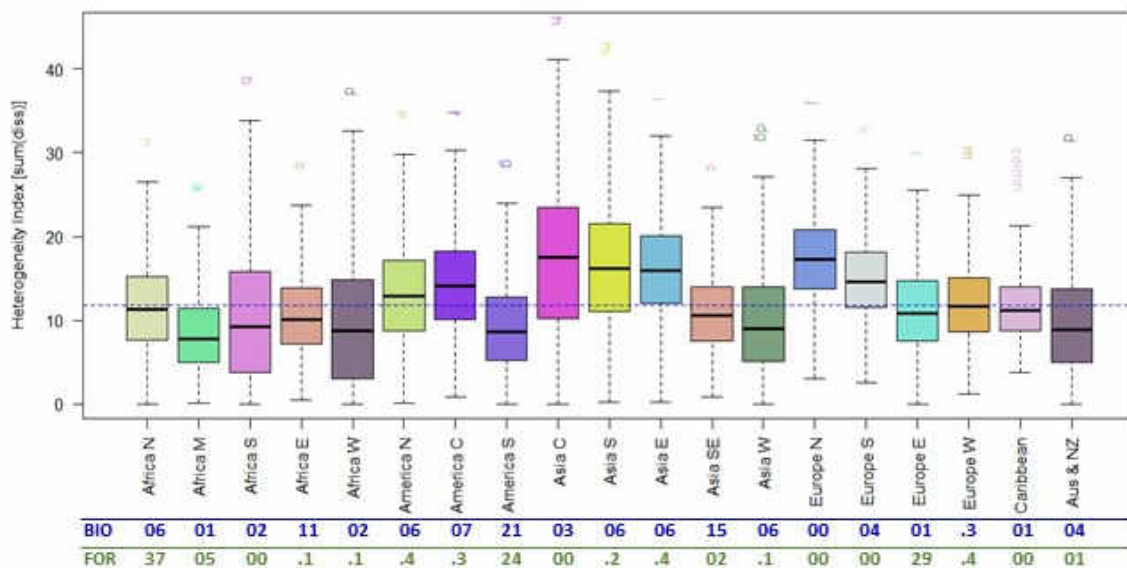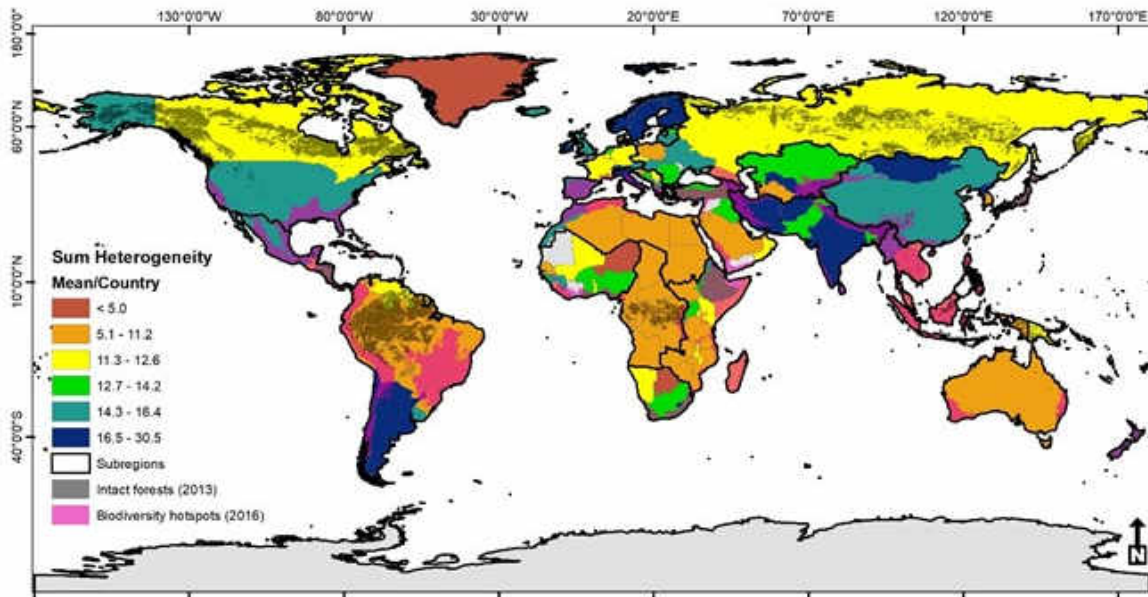
Fig. 6.3: Distribution of overall heterogeneity scores derived from the sum of all environmental dissimilarity weights, normalised by the total area of protected areas for each subregion. Top panel: Map shows results summarised by country overlaid by biodiversity hotspots (Myers *et al.* 2000) and intact forest landscapes (Potapov *et al.* 2008). Bottom panel: Boxplot illustrating how heterogeneity scores differ significantly across world subregions (Kruskal-Wallis χ^2 = 1312.7, df = 19, P < 0.0001). Blue (BIO) and green (FOR) values indicate the percent of the global biodiversity hotspots and intact forest landscapes falling within each subregion respectively. Abbreviations: BIO-Biodiversity Hotspots (Myers *et al.* 2000); FOR-Intact Forests (Potapov *et al.* 2008); N-North; M-Middle; S-South; E-East; W-West; C-Central; AUS-Australia; NZ-New Zealand.

6.4. DISCUSSION

Heterogeneity Tracker Beta 1.0 illustrates how being able to interrogate results at multiple scales can give researchers and managers unique perspectives to help effect sound management decisions. In this way the user can interact with results, zooming in and out and panning across areas of interest in lieu of trying to interpret a static map or broad regional summaries. Regional summaries can also sometimes be misleading as we saw in our Fig 6.3 results for South America. In this case when PA heterogeneity scores were averaged across large subregions, much of the small-scale details were smoothed out and lost in the summarised outputs. This is a common challenge when presenting global or large-scale results (Sievert 2017). However, advancements in data sharing and interactive data visualisations are fast resolving these problems with JavaScript graphing libraries like *plotly.js* and interfacing packages like R's *plotly* (Sievert *et al.* 2016). In future we hope to add more of *plotly's* web visualisation functions to our App. In the meantime, the user has the freedom to interpret patterns of heterogeneity in a specific area in more/less detail in the context of a particular management question. Repeating this type of analysis at a national scale could assist the development of regional conservation strategies and support park expansion plans.

Future releases of the App will explore for example i) the inclusion of ecologically meaningful weights for different landcover types, ecosystem classes or specific PAs; ii) expanding the list of environmental variables or biodiversity proxies to include variables such as vegetation structure [e.g. MODIS continuous vegetation field (NASA LP DAAC 2017) or the new 1 km^2 Worldclim datasets (Fick and Hijmans 2017)]; iii) provide the ability to access user-defined datasets, either from a local directory or online with OPeNDAP (Garcia *et al.* 2009), or PA specific data e.g. Kruger National Park (MacFadyen *et al. submitted*); iv) the ability to intersect user-input species locality or diversity data with heterogeneity results to begin developing a universal understanding of the heterogeneity-biodiversity relationship

(Stein *et al.* 2014; Schluter and Pennell 2017); and v) expand its application to include different climate change models, enabling easy visualisation of potential scenarios in comparison with current patterns (MacFadyen *et al*. 2018).

6.5. CONCLUSION

Due to technological advancements in the worldwide web, social media and data sharing platforms, global communication networks have become collaborative highways along which researchers can share ideas and interact. The data sharing opportunities facilitated through these networks provide a platform for protected area research to become more multi-scale, interactive and adaptive. As big data becomes more freely available, the effective communication of results will grow into a more visual and interactive arena. The freedom to interrogate graphs, plots and maps will no longer fall solely with statistician and Geographic Information Science (GIS) specialists but to conservation managers and decision makers. Our global Heterogeneity Tracker App provides an example of how R, Shiny and Leaflet can be integrated to make valuable knowledge relevant to a broader audience while still maintaining its local scale application. Since Heterogeneity Tracker was developed using only open source software (R, Shiny, Leaflet) and data, the possibilities for improvement and expansion are manifold.

SYNTHESIS

7

SYNTHESIS

The thesis aimed to differentiate the cause and effect relationships between landscape heterogeneity and its key environmental drivers and/or responders. The environmental components selected were chosen based on their expected links with long-term patterns of landscape heterogeneity and changing ecosystem processes in Kruger between 1985 and 2012. They included the underlying physical landscape template (landform), rainfall, large herbivore distribution and density patterns, and fire return periods. This chapter provides a synthesis of the research findings, summarised by initial research questions (by chapter) and more broadly (general synthesis):

1. How does the **UNDERLYING PHYSICAL LANDSCAPE TEMPLATE** affect environmental heterogeneity and the detection thereof?

2. As a dynamic ecosystem driver, what are the long-term (1981-2015) spatiotemporal patterns of **RAINFALL**?

3. As dynamic ecosystem drivers, how do **LARGE HERBIVORES** (specifically elephants) respond to the long-term (1985-2012) spatiotemporal distribution of rainfall, fire and the availability of surface water?

4. How do all of the above (herbivores, climate, landform) and fire interact to generate and maintain **LANDSCAPE HETEROGENEITY**?

5. How can the heterogeneity-biodiversity theory be operationalised into a **HETEROGENEITY TRACKER** to help globalise biodiversity protection strategies in future?

MAIN FINDINGS BY CHAPTER

Underlying influence of the physical landscape

The underlying influence of the physical landscape (landform) on environmental heterogeneity is spatiotemporally dynamic, with rainfall and season driving the strength and directionality of effects. In general, the explanatory power of landform decreased from summer to winter and from high to low rainfall conditions. These results and the spatial arrangement of model disagreement (Fig. 2.3) suggested more dynamic agents, not explained by landform alone, were playing an important role in shaping Kruger's environmental heterogeneity. The new measure of *Landscape complexity*, based on the spatial arrangement of model disagreement ($1-R^2$), produced compelling evidence of spatiotemporal variability in driver dominance and was strongly related to plant species richness. Even within broad rainfall classes (image selection based on low-average-high rainfall conditions), rainfall emerged as a significant driver of heterogeneity. This prompted a finer scale investigation into the long-term spatiotemporal patterns of Kruger's rainfall in chapter 3.

Spatiotemporal patterns of rainfall

Although Kruger has a long history of climate data collection, no gridded rainfall datasets were available. Consequently, these were generated in chapter 3 using local rainfall measurements modelled against CHIRPS, elevation and distance to the Ocean to produce 1 km^2 monthly gridded rainfall surfaces from July 1981 to June 2015 (http://dataknp.sanparks.org/sanparks/metacat/judithk.111609.2/sanparks). The resulting spatiotemporal trends showed Kruger's rainfall is shifting both spatially and temporally as dry/wet seasons move outside of historical ranges and archetypal extremes (Fig. 3.5). These changes may indicate early-onset effects of climate change, which should help guide adaptive conservation strategies and climate-change conscious spatial planning. For example, the development or corridor systems and land

expansion plans may give species the fundamental ability to move in response to climate induced niche shifts when necessary. Moreover, the knowledge gained in this chapter and the precept that rainfall is intrinsically linked to vegetation and species distributions dynamics, pressed the need for deeper insights into rainfall effects on different environmental role-players, like large herbivores. Understanding the spatiotemporal dynamics of Kruger's largest herbivores (elephants) therefore became an important next step in developing a truly holistic understanding of landscape heterogeneity and cognate ecosystem dynamics.

Spatiotemporal dynamics of elephants

Results from chapter 4 showed Kruger's patterns of elephant group-type (bulls vs. herds) dimorphism, distribution and abundance have shifted in response to increasing space limitations and possible elephant-fire induced regime shifts. Specifically, bull and herd groups are no longer clearly segregated and available empty-space has become limited. Despite this, bull and herd elephants have dichotomous resource selection functions, in that bulls concentrate in areas receiving lower rainfall but more frequent fires while herds concentrate in higher rainfall areas experiencing less frequent fires. However, both bull and herd groups concentrate closer to major rivers, emphasizing rivers as important spatial drivers. Overall, densities increased most significantly closer to rivers and in areas experiencing fewer fires. Fire was also identified as a strong agent of group-type change, as the probability of finding bulls, instead of herds, significantly increased as fire return periods shortened. Recognising the challenges Southern African protected areas face to produce practical management solutions for healthy and growing elephant populations, this work aimed to fill some of the biogeographical gaps on what drives the population-level distribution and abundance patterns of elephant in Kruger. Ideally, this work should help guide experimental management action strategies, which aim to alter elephant density and distribution patterns by manipulating artificial water sources (opening/closing

windmills), into areas experiencing fewer fires and those further from rivers (Smit and Ferreira 2010; Ferreira *et al.* 2012). The challenge identified following this chapter, was how to tease apart synergistic relationships (like elephants and fire) in the presence of other environmental factors like rainfall, vegetation dynamics and topography. This boils down to the "correlation does not equal causation" argument, which prompted the inclusion of chapter 5.

The causal structure of landscape heterogeneity

Chapter 5 thus attempted to evaluate the roles played by different ecosystem components to define the causal structure of landscape heterogeneity. Using piecewise Structural Equation Modelling, results uncovered a spatiotemporally dynamic interplay between different heterogeneity drivers (Fig. 5.6). In general, landscape heterogeneity was enhanced by landform variability and increased rainfall. Landscapes were, in contrast, homogenised by higher elephant densities and less frequent fires. The long-term patterns of driver dominance also varied both spatially and temporally, with landform, rainfall, herbivory and fire fluctuating in their effect size (Animation S5.3). On average however, rainfall was spatially dominant, with fire frequency governing the formation and maintenance of landscape heterogeneity in higher rainfall areas while elephants dominated the lower rainfall granitic areas (Fig. 5.6). This chapter culminates in an understanding that ecosystems express themselves in complex adaptive ways, with multifarious physical and stochastic components interacting to both form landscape patterns and influence ecosystem processes at different scales. The ability to describe the resulting patchwork of landscape heterogeneity in terms of its environmental drivers is key to effective ecosystem conservation. Based on the results of Chapter 5, I caution against managing for 'benchmark states' (e.g. historical snapshots of 'pristine' conditions), under which any ecosystem change is labelled 'undesirable'. Instead healthy ecosystems are complex and adaptive (Christensen 1997; SCBD 2004; Parrot 2010) and should be managed as such.

Managing for change avoids disrupting natural system dynamics by allowing landscapes to continue evolving as they are shaped by varying types and magnitudes of natural disturbances, such as herbivory, wildfire, drought and flooding (Parminter and Daigle 1997). Conclusions arrived at here propose that it is not change itself but the homogeneity of the change that should raise concern for conservationists. The maintenance of heterogeneity and the endurance of related spatiotemporal dynamics should therefore be prioritised.

Heterogeneity Tracker Beta 1.0

The development of Heterogeneity Tracker Beta 1.0 was realised in chapter 6 (https://heterogeneity.shinyapps.io/globalheterogeneity). The App attempted to operationalise the heterogeneity-biodiversity theory by exploring patterns of underlying environmental heterogeneity at a global scale across > 8000 protected areas. Heterogeneity Tracker provides a method of exploring global results at different scales using the graphical and statistical power of R, combined with the web-sharing ability of Shiny and mapping capabilities of Leaflet. The interactive interface is to be developed further into a practical tool for protected area managers to evaluate biodiversity features using an index of landscape heterogeneity and dissimilarity in future.

RESULTS IN SYNTHESIS

The results across the chapters demonstrate that in large savanna protected areas, the interactions of physical landscape properties, rainfall, herbivores and fire produce complex spatiotemporal patterns and alter processes that form and maintain landscape heterogeneity (Groen 2007; Folke *et al.* 2004; Bond and Midgley 2012). This emphasizes the importance of designing spatially explicit management strategies that take a holistic view of protected area ecosystems for biodiversity protection (Tscharntke *et al.* 2012; Brambilla *et al.* 2017). In Kruger

for example, climate change projections of decreased rainfall (DEA 2013; IPCC 2014) may manifest and affect 30% of the protected area's landscape (Fig. 5.6). However, "everything is connected" (Commoner 1971) and thus the compound effects reduced rainfall will have on fire frequencies and herbivore distribution and abundance patterns cannot be discounted (Fig. 5.6). Alarmingly, chapter 3's assessment of the short to medium term (35 years) changes to Kruger's rainfall patterns already shows evidence of spatiotemporal rainfall shifts in seasonality and extremes. This means that SANParks will need to consider climate change scenarios for future conservation and land acquisition planning (Ackerly *et al.* 2010).

Results further present strong evidence that Kruger's elephant density and distribution patterns are homogenising as available empty space rapidly declines. Moreover, there are also clear shifts in historical patterns of elephant distribution and abundance and relative likelihoods of elephant male versus female occupancies. Considering the spatial distribution of organisms in protected landscapes is largely in response to resource availability and the spatial heterogeneity thereof (Murwira 2003), Kruger is already experiencing significant landscape changes since 1985. Coupled to this, the synergistic relationship of elephants and fire (Shannon *et al.* 2011, Pringle *et al.* 2015) illustrated in Fig. 4.4 and Fig. 5.6, suggests tree-grass dynamics may also be affected as a result of these reciprocal cause and effects (Fullman and Bunting 2014; Teren 2016). This was confirmed in chapter 5, where pSEM results uncovered a strong positive response of elephants to fire and a weaker positive response of fire to elephants (Fig. 5.5). This confirms that fire is driving elephant distribution and abundance more so than elephants are altering fire regimes. This does not discount the results of chapter 4, in that bulls may have localised effects on fire frequencies. Ultimately Kruger will need to develop and refine spatially explicit elephant management strategies that are cognisant of the spatiotemporal dynamics of water and fire in the landscape (Ferreira *et al.* 2012). These may include strategies that will disperse resources like water, and disturbances like fire, differently across the

landscape (Smit and Ferreira 2010; Shannon *et al.* 2011; van Wilgen *et al.* 2014; Hilbers *et al.* 2015). In a summary report to park management, I encouraged SANParks to use the spatiotemporal results presented to focus research into the more empirical effects of high elephant densities and perhaps develop the concept of refuge in more detail. The resource selection functions presented here can also be used to glimpse potential future elephant distribution and abundance scenarios under different climate change projections, available surface water changes and/or fire regime shifts.

In combination with the results from chapter 5, using the methods developed and results presented here, any conservation agency may delve into the causal structure of landscape heterogeneity in their specific area of interest. In Kruger, for example, understanding that a decrease in landscape heterogeneity is indicative of system change (whether that be less rainfall / more elephants / more buffalo / less fire; Fig. 5.5) will allow managers to focus field monitoring and decipher agents of change. Future scenarios can also be mapped this way, for example, should the effects of climate change result in 200 mm less rainfall per year, i) heterogeneity will decrease; ii) buffalo with cluster into large herds; iii) and fire return periods will lengthen iv) while elephant distribution and abundance patterns will remain largely unchanged (Fig. 5.5).

METHODILOGICAL ADVANCES AND LIMITATIONS

To assess drivers of landscape heterogeneity, this thesis combined and analysed extensive datasets, with spatially explicit time series data spanning 28 years (annual elephant distribution records: 1985-2012), 72 years (annual fire records: 1941-2012), and 408 months (monthly rainfall records: 1981-2012) over an area of ~ 20,000 km^2. The use of such extensive datasets is not yet commonplace in ecology, but with recent advances in parallel computing and availability of High Performance Computing facilities, this may change as their use becomes

more widely publicised in this age of information sharing and 'big data' era (Hampton *et al.* 2013; LaDeau *et al.* 2017). By using these extensive spatiotemporal datasets, this thesis has been able to test the efficacy of different spatiotemporal methods to understand the nature and relationships of various ecosystem components and their interactions. Such data are invaluable in their ability to use 'repeated measures' to distinguish hard-and-fast long-term patterns and trends in the place of single snapshots, as demonstrated throughout the different chapters. However, dealing with vast quantities of complicated spatiotemporal data requires novel applications of interdisciplinary and sometimes heterodox methods to understand patterns and trends in the presence of computational and natural ecosystem complexity.

Many of the methods applied here moved beyond the state of the art, in search of techniques that could be applied in an 'outdoor laboratory' setting where complex adaptive feedback loops abound. Unlike controlled laboratory experiments, in ecology and accompanying 'outdoor labs', all variables cannot always be held constant or explicitly accounted for. The methods explored and the results presented here expand on the laws of Commoner (1971) and Tobler (1970) to suggest that in ecology, "everything is in fact related to everything else but relative to spatiotemporal proximity". Until recently however, ecology papers rarely applied explicit spatiotemporal techniques, partly because of data resource limitations and limited capacity to run complex models. Or perhaps regression models have become emblematic of ecological studies because if all you have is a hammer everything looks like a nail? I sympathise with this challenge facing fellow ecologists, having tested many more methods than presented here in search of techniques that could i) deal with such vast quantities of data; ii) account for inherent multicollinearity; iii) account for spatiotemporal autocorrelation; iv) identify long-term spatiotemporal patterns and trends v) and expound the complication of correlation vs. causation.

Chapter 2 began by applying Geographically Weighted Regression (GWR), perhaps because it looks like a 'hammer' but allows relationships (and β coefficients) to vary over space

(Brunsdon *et al.* 1996; Fotheringham *et al.* 2002). It has typically been used as an exploratory technique (Bivand and Yu 2015) but shows promise for both spatial and potentially temporal applications. General Additive Mixed Effects Models (GAMM) were later explored in chapter 3 since they allow relationships to change smoothly across continuous levels of covariates (spatial) over time (temporal). In this way a response variable can be explained by its non-linear relationship with covariates over space and time, including both fixed and random effects (Zuur *et al.* 2009). In ecology, where almost nothing is linear, it is surprising these techniques are not more mainstream. In the same chapter, spatiotemporal regression kriging was initially explored as a geostatistical means to interpolate or predict a response variable between and/or beyond measured geographic locations and observation intervals (Gräler *et al.* 2016). It was specifically chosen become of its ability to analyse the spatial-temporal correlation structure of a continuous variable, like rainfall, in relation to explanatory covariates, like CHIRPS and elevation (Liu *et al.* 2016). The methodologies are still actively being developed and refined and should offer some exciting new avenues for spatiotemporal research in the new future.

Breaks in Seasonality and Trend (BFAST), which is typically used in remote sensing studies to detect change in time series products like NDVI (Verbesselt *et al.* 2012), was uniquely applied to elephants in chapter 4 to identify long-term distribution and abundance pattern changes. Exploring the application of different methods from other fields requires lateral thinking but will ensure science and management continues to be adaptive. In the same chapter, a relative risk assessment was applied to elephant groups to estimate the spatially-varying probabilities of finding bull vs. herd groups (Baddeley *et al.* 2015). Until now this technique was traditionally only used in epidemiological studies to identify the relative risk of disease spread using infected vs. non-infected patient reports (Lucca *et al.* 2013; Baddeley *et al.* 2015), but we showed that it can be successfully used to identify changes in the demographics of species distribution and abundance patterns.

The application of piecewise Structural Equation Modelling (SEM) was arguably the most exciting new methodology tested here. The notorious inability to separate cause and effect in ecology can potentially be overcome by using SEM. The piecewise version of SEM (pSEM) further allows mixed-effects and different correlation structures to be included in these models. However, the inclusion of latent variables into pSEM's capabilities in future would vastly help improve our understanding of the complexity behind causal structures in the ecosystem. Specifically, the ability to represent landscape heterogeneity as an ecosystem construct rather than a directly observable landscape feature would be a major step forward.

There remain a few caveats to be addressed in future as software and technologies advance and research theories evolve. Firstly, chapters 2 and 5 used Landsat spectral variation and long-term monthly variability of AVHRR NDVI respectively as a proxy for heterogeneity. Landsat imagery was initially selected because of its higher spatial and longer temporal resolutions (80-30 m spatial resolution; 1972-present). However the processing requirements necessary to calibrate five different scenes, across potentially seven sensors, at least twice a year (winter and summer), over the whole park for a 35 year period proved too intensive. In contrast, the lower resolution AVHRR imagery (~ 1-8 km spatial resolution; 1979-present) covered Kruger in one scene and provided a continuous time series of pre-calibrated, cleaned data from 1981 to 2015 making it more appropriate for long-term large-scale monitoring. Unfortunately however, this means the resulting map of complexity (Fig. 2.5) is not directly comparable with that of the dominant driver map (Fig. 5.6). Notwithstanding this discrepancy, the concept of using model disagreement to map landscape complexity is a compelling one that should be explored further.

Additional research opportunities lie in exploring alternative, or complementary, proxies of remotely sensed landscape heterogeneity to infer ecosystem complexity. Likewise the temporal dynamics of heterogeneity is an increasingly important area for future research to assess and predict biodiversity and ecosystem response to environmental change. Environmental change,

using landscape heterogeneity as an indicator of interest, can thus also potentially be evaluated between hypothesised limits of acceptable change to identify areas that are on a trajectory to exceed predetermined limits of acceptable homogenisation or change, thereby warning managers of possible state changes in the system. Further development of the Heterogeneity Tracker App is hoped to encourage further research into the development of a universal understanding of the heterogeneity-biodiversity relationship (Stein *et al.* 2014; Schluter and Pennell 2017).

IMPLICATIONS AND OUTLOOK

Each chapter of this thesis makes its own independent contribution to conservation science and ecosystem understanding in the different fields of landscape ecology, climate modelling, species biogeography, holistic ecosystem modelling and computer programming for interactive data visualisation. Taken together these results encapsulate a deeper understanding of ecosystem structure and function for the management of complex adaptive systems like large protected areas. At the outset of this thesis, the role of heterogeneity as a determinant of species richness (biodiversity-composition) was generally accepted (see Stein *et al.* 2014 for a synthesis). However, there was still much debate over its application to the structural and functional components of biodiversity (Schluter and Pennell 2017). Iterating through each chapter, the roles of the different key ecosystem drivers namely, landform, rainfall, large herbivores and fire, were unpacked and linked back to landscape heterogeneity. In this way, its application to the compositional, structural and functional dimensions of biodiversity was articulated. In essence landscape heterogeneity is the expression of stable ecosystem properties (e.g. landform) and dynamic ecosystem features (e.g. climate) and role players (e.g. fauna) interacting to maintain ecosystem processes. In an African savanna, these include landform (topography, geology, and soil), rainfall, large herbivores and fire. Therefore, if heterogeneity

is considered a proxy for biodiversity, under a biodiversity conservation paradigm, reductions in heterogeneity should at the very least sound alarm bells.

The work presented here attests to the natural complexity of ecosystem dynamics, which dictates change to be part of all healthy, functioning ecosystems but which also introduces uncertainty. The non-linear interactions among the different components across chapters points to the inherent uncertainty and unpredictability of ecosystems and the need for an adaptive management approach to decision making (Allen *et al.* 2011). However, in recognising that ecosystem management involves understanding complex systems to be able to apply intervention strategies to problems that are often unstructured, open ended, multidimensional, systemic and potentially without a definitive solution, suggests ecosystem management is more likely a 'wicked problem' (DeFries and Nagendra 2017). In the business world, this is called a VUCA environment where the predictability of action outcomes and understanding or system knowledge interact to form different levels of Volatility, Uncertainty, Complexity and Ambiguity (Mack and Khare 2016). Results from this thesis have helped reduce the uncertainty around selected ecosystem drivers while uncovering more complexity in their interactions. To apply this knowledge globally, emphasis should be placed on understanding and maintaining the spatiotemporal dynamics of heterogeneity as an important conservation goal (Sinclair and Byrom 2006). Locally, SANParks managers should use the results herein to critically review, and where necessary adapt, policies and plans while cultivating a better understanding of, for example i) rainfall as a dynamic driver of heterogeneity, which can help steer national park planning and land reclamation policies based on projected climate change impacts; ii) how fire interacts with rainfall and herbivory to affect heterogeneity, which can support current and future fire management policies and strategies; and iii) the importance of large mammal management plans that acknowledge and offer mitigation strategies for the spatial and temporal impacts of herbivore distribution and abundance patterns on heterogeneity. Sharing this

knowledge, through interactive data visualisation will come out of the exciting and ongoing developments in the fields of knowledge exploration and information sharing (i.e. worldwide web, social media and data clearinghouses). These type of developments will provide the scope for truly globalised conservation initiatives that are more interactive and collaborative in future (Han *et al*. 2014; Scholes *et al.* 2017). Ideally, Heterogeneity Tracker may provide a platform for this, allowing protected area research to become more multi-scale, interactive and adaptive in the near future.

REFERENCES

Aalto J, Pirinen P, Heikkinen J and Venäläinen A (2013) Spatial interpolation of monthly climate data for Finland: comparing the performance of kriging and generalized additive models. *Theoretical and Applied Climatology* 112: 99–111. doi:10.1007/s00704-012-0716-9

Ackerly DD, Loarie SR. Cornwell WK, Weiss SB, Hamilton H, Branciforte R and Kraft NJB (2010) The geography of climate change: implications for conservation biogeography. Diversity and Distributions 16: 476–487. doi:10.1111/j.1472-4642.2010.00654.x

Allen CR, Fontaine JJ, Pope KL and Garmestani AS (2011) Adaptive management for a turbulent future. *Journal of Environmental Management* 92: 1339-1345. doi:10.1016/j.jenvman.2010.11.019

Allouche O, Kalyuzhny M, Moreno-Rueda G, Pizarro M and Kadmon R (2012) Area–heterogeneity tradeoff and the diversity of ecological communities. *Proceedings of the National Academy of Sciences* 109: 17495–17500. doi:10.1073/pnas.1208652109

Archibald S, Roy DP, van Wilgen BW and Scholes RJ (2009) What limits fire? An examination of drivers of burnt area in Southern Africa. *Global Change Biology* 5: 613–630. doi:10.1111/j.1365-2486.2008.01754.x

Asner GP and Levick SR (2012) Landscape-scale effects of herbivores on treefall in African savannas. *Ecology Letters* 15: 1211–1217. doi:10.1111/j.1461-0248.2012.01842.x

Asner GP, Vaughn N, Smit IPJ and Levick S (2015) Ecosystem-scale effects of megafauna in African savannas. *Ecography* 38: 1–13. doi:10.1111/ecog.01640

Baddeley A, Rubak E and Turner R (2015) *Spatial Point Patterns: Methodology and Applications with R*. CRC Press. Taylor & Francis Group, USA. ISBN: 9781482210200 - CAT# K21641

Bar-Massada A and Wood EM (2014) The richness–heterogeneity relationship differs between heterogeneity measures within and among habitats. *Ecography* 37: 528–535. doi:10.1111/j.1600-0587.2013.00590.x

Beeley C (2013) *Web Application Development with R Using Shiny*. Packt Publishing Ltd. Birmingham, UK

Berry RS and Kulmatiski A (2017). A savanna response to precipitation intensity. PLoS ONE 12 (4):e0175402. doi:10.1371/journal.pone.0175402.

Biggs HC and Rogers KH (2003) An adaptive system to link science, monitoring and management in practice. In: du Toit JT, Biggs H and Rogers KH (eds.) *The Kruger experience: ecology and management of savanna heterogeneity*. Island Press, Washington, DC. pp. 59–80

Birkett PJ, Vanak AT, Muggeo VMR, Ferreira SM and Slotow R (2012) Animal perception of seasonal thresholds: changes in elephant movement in relation to rainfall patterns. *PLoS ONE* 7: e38363. doi:10.1371/journal.pone.0038363

Bond WJ and Midgley GF (2012) Carbon dioxide and the uneasy interactions of trees and savannah grasses. *Philosophical Transactions of the Royal Society B* 367: 601–612. doi:10.1098/rstb.2011.0182

Brambilla M, Caprio E, Assandri G, Scridel D, Bassi E, Bionda R, *et al.* (2017) A spatially explicit definition of conservation priorities according to population resistance and resilience, species importance and level of threat in a changing climate. Diversity and Distributions 23: 727–738. doi:10.1111/ddi.12572

Brooks TM, Mittermeier RA, da Fonseca GAB, Gerlach J, Hoffmann M, Lamoreux JF, *et al.* (2006) Global biodiversity conservation priorities. *Science* 313: 58–61. doi:10.1126/science.1127609

Brummitt N, Regan EC, Weatherdon LV, Martin CS, Geijzendorffer IR, Rocchini D, *et al.* (2016) Taking stock of nature: essential biodiversity variables explained. *Biological Conservation* 213(B): 252–255. doi:10.1016/j.biocon.2016.09.006

Brunsdon C, Fotheringham AS and Charlton M (1996) Geographically weighted regression: a method for exploring spatial nonstationarity. *Geographical Analysis* 28: 281–298. doi:10.1111/j.1538-4632.1996.tb00936.x

Brunsdon C, Fotheringham AS and Charlton M (2002) Geographically weighted summary statistics - a framework for localised exploratory data analysis. *Computers, Environment and Urban Systems* 26: 501–524. doi:10.1016/S0198-9715(01)00009-6

Brynard HJ (2006) Managing geoscience information in an African context. *Position IT* March/April: 13–16. Available from http://www.geoscience.org.za/index.php/publication/downloadable-material (accessed 01 December 2010)

Bunn A, Korpela M, Biondi F, Campelo F, Mérian P, Qeadan F and Zang C (2016) dplR: Dendrochronology Program Library in R. R package version 1.6.4. https://CRAN.R-project.org/package=dplR (accessed 25 October 2016)

Cantú-Salazar L and Gaston K (2010) Very large protected areas and their contribution to terrestrial biological conservation. *Bioscience* 60: 808–818. doi:10.1525/bio.2010.60.10.7

Cardinale BJ, Weis JJ, Forbes AE, Tilomn KJ and Ives AR (2006) Biodiversity as both a cause and consequence of resource availability: a study of reciprocal causality in a predator-prey system. *Journal of Animal Ecology* 75: 497–505. doi:10.1111/j.1365-2656.2006.01070.x

Carruthers J (1995) The Kruger National Park: A social and political history. Natal University Press, Pietermaritzburg, South Africa. ISBN: 978-0869809150

Celesia GG, Townsend Peterson A, Kerbis Peterhans JC and Gnoske TP (2010) Climate and landscape correlates of African lion *(Panthera leo)* demography. *African Journal of Ecology* 48: 58–71. doi:10.1111/j.1365-2028.2009.01082.x

Chamaillé-Jammes S, Valeix M and Fritz H (2007) Managing heterogeneity in elephant distribution: interactions between elephant population density and surface-water availability. *Journal of Applied Ecology* 44: 625–633. doi:10.1111/j.1365-2664.2007.01300.x

Chan A (2000) Wavelet techniques for the analysis and synthesis of rainfall data. *Journal of Water Management Modeling* 206–208. doi:10.14796/JWMM.R206-08.

Chang W, Cheng J, Allaire JJ, Xie Y, McPherson J, RStudio, jQuery Foundation, *et al*. (2015) *shiny: Web Application Framework for R*. R package version 0.11.1

Chapin III FS, Matson PA and Vitousek PM (2011) Principles of Terrestrial Ecosystem Ecology. Springer Science, New York, NY. doi:10.1007/978-1-4419-9504-9.

Chase JM (2011) Ecological niche theory. In: Scheiner SM and Willig MR (eds.) *The theory of ecology*. University of Chicago Press. pp. 93–107

Chen D and Chen HW (2013) Using the Köppen classification to quantify climate variation and change: an example for 1901–2010. *Environmental Development* 6: 69–79. doi:10.1016/j.envdev.2013.03.007

Cheng J and Xie Y (2016) leaflet: Create Interactive Web Maps with the JavaScript 'Leaflet' Library. R package version 1.0.1. Available from https://CRAN.R-project.org/package=leaflet (accessed 01 December 2017)

Chirima GJ, Owen-Smith N and Erasmus BFN (2012) Changing distributions of larger ungulates in the Kruger National Park from ecological aerial survey data. *Koedoe* 54(1), 11 pages. doi:10.4102/koedoe.v54i1.1009

Christensen NL (1997) Managing for heterogeneity and complexity on dynamic landscapes. In: Pickett STA, Ostfeld RS, Shachak M and Likens GE (eds.) *The ecological basis of conservation: Heterogeneity, ecosystems, and biodiversity*. Springer, Dordrecht. pp. 167–186. doi:10.1007/978-1-4615-6003-6_17

CITES (2016*a*) CITES CoP17 Proposals for the amendment of Appendices I and II. Available from https://cites.org/sites/default/files/eng/cop/17/Proposals_for_amendment_of _Appendices_I_II.pdf_ (accessed 31 Oct 2016)

CITES (2016*b*) CITES CoP17 votes in committee against the proposal to include all African elephant populations in Appendix I. Available from https://twitter.com/CITES/status/ 78292396624 7755778/photo/1 (accessed 31 Oct 2016)

CITES (2016*c*) African elephants still in decline due to high levels of poaching. Available from https://cites.org/eng/news/pr/african_elephants_still_in_decline_due_to_high_ levels_of_poaching_03032016 (accessed 03 May 2015)

Claverie M, Matthews JL, Vermote EF and Justice CO (2016) A 30+ Year AVHRR LAI and FAPAR Climate Data Record: Algorithm Description and Validation. *Remote Sensing* 8(3): 263. doi:10.3390/rs8030263

Claverie M, Vermote E and NOAA CDR Program (2014) NOAA Climate Data Record (CDR) of Leaf Area Index (LAI) and Fraction of Absorbed Photosynthetically Active Radiation (FAPAR), Version 4. [AVH15C1-LAI]. *NOAA National Centers for Environmental Information*. doi:10.7289/V5M043BX

Codron J, Lee-Thorp JA, Sponheimer M, Codron D, Grant RC and de Ruiter DJ (2006) Elephant (*Loxodonta africana*) diets in the Kruger National Park, South Africa: spatial and landscape differences. *Journal of Mammalogy* 87: 27–34. doi:10.1644/05-MAMM-A-017R1.1

Colgan MS, Asner GP, Levick SR, Martin RE and Chadwick OA (2012) Topo-edaphic controls over woody plant biomass in South African savannas. *Biogeosciences* 9: 1809–1821. doi:10.5194/bg-9-1809-2012

Colón-González FJ, Tompkins AM, Biondi R, Bizimana JP and Namanya DB (2016) Assessing the effects of air temperature and rainfall on malaria incidence: an epidemiological study across Rwanda and Uganda. *Geospatial Health* 11(s1) 379: 18–37. doi:10.4081/gh.2016.379

Commoner B (1971) The Closing Circle: Nature, Man, and Technology. Random House Inc, New York. ISBN: 978-0-394-42350-0

Cressie N, Calder CA, Clark JS, Ver Hoef JM and Wilke CK (2009) Accounting for uncertainty in ecological analysis: the strengths and limitations of hierarchical statistical modelling. *Ecological Applications* 19: 553–570. doi:10.1890/07-0744.1

Cullum C and Rogers K (2011) A framework for the classification of drainage networks in savanna landscapes. Report to the Water Research Commission, South Africa. WRC Project No K5/1790

Cushman SA, Gutzweiler K, Evans JS and McGarigal K (2010) The gradient paradigm: a conceptual and analytical framework for landscape ecology. In: Cushman SA and Huettmann F (eds.) *Spatial complexity, informatics, and wildlife conservation*. Springer, Dortrecht. pp. 83–108. doi:10.1007/978-4-431-87771-4_5

Danielson JJ and Gesch DB (2011) *Global multi-resolution terrain elevation data 2010 (GMTED2010)*. U.S. Geological Survey Open-File Report, 2011-1073, 1-26.

DeFries R and Nagendra H (2017) Ecosystem management as a wicked problem. *Science* 356: 265–270. doi:10.1126/science.aal1950

de Knegt HJ (2010) Beyond the here and now- herbivore ecology in a spatial-temporal context. PhD thesis, Wageningen University, The Netherlands

de Knegt HJ, van Langevelde F, Skidmore AK, Delsink A, Slotow R, Henley S, *et al.* (2011) The spatial scaling of habitat selection by African elephants. *Journal of Animal Ecology* 80: 270–281. doi:10.1111/j.1365-2656.2010.01764.x

de Jongh ILM, Verhoest NEC and de Troch FP (2006) Analysis of a 105-year time series of precipitation observed at Uccle, Belguim. *International Journal of Climatolo*gy 26: 2023–2039. doi:10.1002/jpc.1352.

de Lucca T, Rodrigues RCA, Castagna C, Presotto D, De Nadai DV, Fagre A, *et al.* (2013) Assessing the rabies control and surveillance systems in Brazil: an experience of measures toward bats after the halt of massive vaccination of dogs and cats in Campinas, Sao Paulo. *Preventive Veterinary Medicine* 111: 126–133. doi:10.1016/j.prevetmed.2013.03.007

de Rosario-Martinez H (2015) phia: post-hoc interaction analysis. R package version 0.2-0. Available from http://CRAN.R-project.org/package=phia (accessed June 2015)

DEA (Department of Environmental Affairs) (2013) *Long-term adaptation scenarios flagship research programme (LTAS) for South Africa.* Climate Trends and Scenarios for South Africa. Pretoria, South Africa

Dedekind Z, Engelbrecht FA and van der Merwe J (2016) Model simulations of rainfall over southern Africa and its eastern escarpment. *Water SA* 42(1): 129–143. doi:10.4314/wsa.v42i1.13

Detsch F (2016) gimms: download and process GIMMS NDVI3g Data. R package version 0.6.0. doi:10.13140/RG.2.1.4824.2962

DeVries B, Verbesselt J, Kooistra L and Herold DM (2015) Robust monitoring of small-scale forest disturbances in a tropical montane forest using landsat time series. *Remote Sensing of Environment* 161: 107–121. doi:10.1016/j.rse.2015.02.012

Doebeli M and Dieckmann U (2003) Speciation along environmental gradients. *Nature* 421: 259–264. doi:10.1038/nature01274

du Toit JT, Biggs HC and Rogers KH (eds.) (2003) *The Kruger experience: ecology and management of savanna heterogeneity.* Island Press, Washington, DC

Dublin HT, Sinclair ARE and McGlade J (1990) Elephants and fire as causes of multiple stable states in the serengeti-mara woodlands. *Journal of Animal Ecology* 59: 1147–1164

Duncan BW, Schmalzer PA, Breininger DR and Stolen ED (2015) Comparing fuels reduction and patch mosaic fire regimes for reducing fire spread potential: a spatial modeling approach. *Ecological Modelling* 314: 90–99. doi:10.1016/j.ecolmodel.2015.07.013

Dunham KM, Robertson EF and Grant CC (2004) Rainfall and the decline of a rare antelope, the tsessebe (*Damaliscus lunatus lunatus*), in Kruger National Park, South Africa. *Biological Conservation* 117: 83–94. doi:10.1016/S0006-3207(03)00267-2

Duro DC, Coops NC, Wulder MA and Han T (2007) Development of a large area biodiversity monitoring system driven by remote sensing. *Progress in Physical Geography* 31: 235–260. doi:10.1177/0309133307079054

Duro DC, Girard J, King DJ, Fahrig L, Mitchell S, Lindsay K, *et al.* (2014) Predicting species diversity in agricultural environments using Landsat TM imagery. *Remote Sensing of Environment* 144: 214–225. doi:10.1016/j.rse.2014.01.001

Dutrieux LP, DeVries B and Verbesselt J (2014) bfastSpatial: Utilities to monitor for change on satellite image time-series. R package version 0.6.1

Egoh B, Reyers B, Rouget M, Bode M and Richardson DM (2009) Spatial congruence between biodiversity and ecosystem services in South Africa. *Biological Conservation* 142: 553–562. doi:10.1016/j.biocon.2008.11.009

Eisenhauer N, Bowker MA, Grace JB and Powell JR (2015) From patterns to causal understanding: structural equation modelling (SEM) in soil ecology. *Pedobiologia* 58: 65–72. doi:10.1016/j.pedobi.2015.03.002

Ekblom A, Gillson L, Risberg J, Holmgren K and Chidoub Z (2012) Rainfall variability and vegetation dynamics of the lower Limpopo Valley, Southern Africa, 500 AD to present. *Palaeogeography, Palaeoclimatology, Palaeoecology* 363–634: 69–78. doi:10.1016/j.palaeo.2012.08.015

ESPA Ordering Interface (2013) US Geological Survey's (USGS) on demand interface for the Earth Resources Observation and Science's (EROS) Centre Science Processing Architecture (ESPA). Available from http://espa.cr.usgs.gov/index/ (accessed November 2013)

Evans JS (2016) spatialEco. R package version 0.0.1-4. Available from http://CRAN.R-project.org/ package=spatialEco (accessed 01 December 2017)

Fahrig L (2013) Rethinking patch size and isolation effects: the habitat amount hypothesis. *Journal of Biogeography* 40: 1649–1663. doi:10.1111/jbi.12130

Fahrig L, Baudry J, Brotons L, Burel FG, Crist TO, Fuller RJ, *et al.* (2011) Functional landscape heterogeneity and animal biodiversity in agricultural landscapes. *Ecology Letters* 14: 101–112. doi:10.1111/j.1461-0248.2010.01559.x

Favre A, Philippon N, Pohl B, Kalognomou EA, Lennard C, Hewitson B, Nikulin G, Dosio A, Panitz JJ and Cerezo-Mota R (2016) Spatial distribution of precipitation annual cycles over South Africa in 10 CORDEX regional climate model present-day simulations. *Climate Dynamics* 46: 1799–1818. doi:10.1007/s00382-015-2677-z

Ferreira S, Freitag-Ronaldson S, Pienaar DJ and Hendriks H (2012) *Elephant management plan - Kruger National Park 2013-2022.* South African National Parks, Scientific Services, November 2012

Field R, Hawkins BA, Cornell HV, Currie DJ, Diniz-Filho JAF, Guégan J, *et al.* (2009) Spatial species-richness gradients across scales: a meta-analysis. *Journal of Biogeography* 36: 132–147. doi:10.1111/j.1365-2699.2008.01963.x

Fick SE and Hijmans RJ (2017) Worldclim 2: New 1-km spatial resolution climate surfaces for global land areas. *International Journal of Climatology.* Available from http://worldclim.org/version2 (accessed 01 December 2017)

Folke C, Carpenter S, Walker B, Scheffer M, Elmqvist T, Gunderson L and Holling CS (2004) Regime shifts, resilience, and biodiversity In ecosystem management. *Annual Review of Ecology, Evolution and Systematics* 35: 557–81. doi:10.1146/ annurev.ecolsys.35.021103.105711

Fotheringham AS, Brunsdon C and Charlton M (2002) *Geographically Weighted Regression: the analysis of spatially varying relationships*. John Wiley & Sons Ltd

Fullman TJ and Bunting EL (2014) Analyzing Vegetation Change in an Elephant-Impacted Landscape Using the Moving Standard Deviation Index. *Land* 3: 74–104. doi:10.3390/land3010074.

Funk C, Peterson P, Landsfeld M, Pedreros D, Verdin I, Shukla S, *et al.* (2015) The climate hazards infrared precipitation with stations - a new environmental record for monitoring extremes. *Scientific Data* 2: 150066. doi:10.1038/sdata.2015.66 2015

Garcia RA, Cabeza M, Rahbek C and Araújo MB (2014) Multiple dimensions of climate change and their implications for biodiversity. *Science* 344(6183): 1247579. doi:10.1126/science.1247579

Garonna I, de Jong R, de Wit AJW, Mücher CA, Schmid B and Schaepman ME (2014) Strong contribution of autumn phenology to changes in satellite-derived growing season length estimates across Europe (1982–2011). *Global Change Biology* 20: 3457–3470. doi:10.1111/gcb.12625

Garstang M, Davis RE, Leggett K, Frauenfeld OW, Greco S, Zipser E and Peterson M (2014) Response of African elephants (*Loxodonta africana*) to seasonal changes in rainfall. *PLoS ONE* 9(10): e108736. doi:10.1371/journal.pone.0108736

Gaylard A (2015) *Adopting a heterogeneity paradigm for understanding and managing elephants for biodiversity: a case study in riparian woodlands in Kruger National Park.* PhD Thesis, University of the Witwatersrand, Johannesburg

Gergel SE and Turner MG (2002) *Learning landscape ecology: a practical guide to concepts and techniques.* Springer-Verlag, New York. doi:10.1007/978-1-4939-6374-4

Gertenbach WPD (1980) Rainfall patterns in the Kruger National Park. *Koedoe* 23:35–43. doi:10.4102/koedoe.v23i1.634

Giraudoux P (2015) pgirmess: data analysis in ecology. R package version 1.6.0. Available from http://CRAN.R-project.org/package=pgirmess (accessed June 2015)

Gollini I, Lu B, Charlton M, Brunsdon C and Harris P (2015) GWmodel: an R package for exploring spatial heterogeneity using geographically weighted models. *Journal of Statistical Software* 63: 1–50. doi:10.18637/jss.v063.i17

González-Megías A, Gómez JM and Sánchez-Piñero F (2011) Spatiotemporal change in the relationship between habitat heterogeneity and species diversity. *Acta Oecologica* 37: 179–186. doi:10.1016/j.actao.2011.01.011

Gould W (2000) Remote sensing of vegetation, plant species richness, and regional biodiversity hotspots. *Ecological Applications* 10: 1861–1870. doi:10.2307/2641244

Govender N, Mutanga O and Ntsala D (2012) Veld fire reporting and mapping techniques in the Kruger National Press, South Africa, from 1941 to 2011. *African Journal of Range and Forage Science* 29: 63–73. doi:10.2989/10220119.2012.697918

Grace JB, Schoolmaster Jr DR, Guntenspergen GR, Little AM, Mitchell BR, Miller KM and Schweiger EW (2012) Guidelines for a graph-theoretic implementation of structural equation modelling. *Ecosphere* 3(8): 1–44. doi:10.1890/ES12-00048.1

Grainger M, van Aarde RJ and Whyte IJ (2005) Landscape heterogeneity and the use of space by elephants in the Kruger National Park, South Africa. *African Journal of Ecology* 43: 369–375. doi:10.1111/j.1365-2028.2005.00592.x

Gräler B, Pebesma E and Heuvelink G (2016) Spatiotemporal Interpolation using gstat. The R Journal. Available from: https://journal.r-project.org/archive/accepted/na-pebesma-heuvelink.pdf

GRASS (2014) GRASS Development Team. GRASS GIS 7.1.svn Reference Manual. Available from http://grass.osgeo.org/grass71/manuals/index.html (accessed November 2014)

Graves S, Piepho H-P, Selzer L and Dorai-Raj S (2015) multcompView: Visualizations of Paired Comparisons. R package version 0.1-7. Available from https://CRAN.R-project.org/package=multcompView (accessed 01 December 2017)

Groen TA (2007) *Spatial matters: how spatial patterns and processes affect savanna dynamics.* PhD Dissertation, Wageningen University, The Netherlands

Guisan A and Thuiller W (2005) Predicting species distribution: offering more than simple habitat models. *Ecology Letters* 8: 993–1009. doi:10.1111/j.1461-0248.2005.00792.x

Guldemond R and van Aarde R (2008) A meta-analysis of the impact of African elephant on savanna vegetation. *Journal of Wildlife Management* 72(4): 892–899. doi:10.2193/2007-072

Guo L, Ma Z and Zhang L (2008) Comparison of bandwidth selection in application of geographically weighted regression: a case study. *Canadian Journal of Forest Research* 38: 2526–2534. doi:10.1139/X08-091

Guy PR (1976) The feeding behaviour of elephant (*Loxodonta africana)* in the Sengwa area, Rhodesia. *South African Journal of Wildlife Research* 6: 55–63

Haerter, JO, Eggert B, Moseley C, Piani C and Berg P (2015) Statistical precipitation bias correction of gridded model data using point measurements. *Geophysical Research Letters* 42: 1919–1929. doi:10.1002/2015GL063188

Hampton SE, Strasser CA, Tewksbury JJ, Gram WK, Budden AE, Batcheller AL, Duke CS and Porter JH (2013) Big data and the future of ecology. *Frontiers in Ecology and the Environment* 11(3): 156–62. doi:10.1890/120103

Han X, Smyth RL, Young BE, Brooks TM, de Lozada AS, Bubb P, *et al*. (2014) A Biodiversity indicators dashboard: addressing challenges to monitoring progress towards the Aichi Biodiversity Targets using disaggregated global data. *PLoS ONE* 9(11): e112046. doi:10.1371/journal.pone.0112046

Hannah L, Midgley G, Andelman S, Araújo M, Hughes G, Martinez-Meyer E, *et al.* (2007) Protected area needs in a changing climate. *Frontiers in Ecology and Environment* 5(3): 131–138. doi:10.1890/1540-9295(2007)5[131:PANIAC]2.0.CO;2

Hartmann J and Moosdorf N (2012) The new global lithological map database GLiM: A representation of rock properties at the Earth surface. *Geochemistry, Geophysics, Geosystems* 13: Q12004. doi:10.1029/2012GC004370

Hasan KF, Ali MS, Nessa M, Aditya SK and Mazumder RK (2011) Retrieval of Surface Reflectance from NOAA-AVHRR Satellite Data. *Dhaka University Journal of Engineering and Technology* 1(2): 121–124

He KS, Bradley BA, Cord AF, Rocchini D, Tuanmu M-N, Schmidtlein S, *et al*. (2015) Will remote sensing shape the next generation of species distribution models? *Remote Sensing in Ecology and Conservation* 1: 4–18. doi:10.1002/rse2.7

Hefley TJ, Broms KM, Brost BM, Buderman FE, Kay S, Scharf HR, Tipton JR, Williams PJ and Hooten MB (2017) The basis function approach for modeling autocorrelation in ecological data. *Ecology* 98(3): 632–646. doi:10.1002/ecy.1674

Hengl T, Mendes de Jesus J, MacMillan RA, Batjes NH, Heuvelink GBM *et al.* (2014) SoilGrids1km - Global Soil Information Based on Automated Mapping. *PLoS ONE* 9(8): e105992. doi:10.1371/journal.pone.0105992

Hengl T, Mendes de Jesus J, Heuvelink GBM, Ruiperez Gonzalez M, Kilibarda M, *et al.* (2017) SoilGrids250m: global gridded soil information based on Machine Learning. *PLOS One* 12(2). doi:10.1371/journal.pone.0169748

Heritage GL and van Niekerk AW (1995) Drought conditions and sediment transport in the Sabie River. *Koedoe* 38(2): 1–9. doi:10.4102/koedoe.v38i2.311

Hernández-Stefanoni JL, Gallardo-Cruz JA, Meave JA, Rocchini D, Bello-Pineda J and López-Martínez JO (2012) Modeling Alpha and Beta diversity in a tropical forest from remotely sensed and spatial data. *International Journal of Applied Earth Observation and Geoinformation* 19: 359–368. doi:10.1016/j.jag.2012.04.002

Hewitt JE, Thrush SF, Dayton PK and Bonsdorff E (2007) The effect of spatial and temporal heterogeneity on the design and analysis of empirical studies of scale-dependent systems. *The American Naturalist* 169: 398–408. doi:10.1086/510925

Hijmans RJ (2015). raster: Geographic Data Analysis and Modeling. R package version 2.3-40. Available from http://CRAN.R-project.org/package=raster (accessed June 2015)

Hijmans RJ (2016) raster: Geographic Data Analysis and Modeling. R package version 2.5-8. Available from https://CRAN.R-project.org/package=raster (accessed December 2016)

Hijmans RJ, Cameron SE, Parra JL, Jones PG and Jarvis A (2005) Very high resolution interpolated climate surfaces for global land areas. *International Journal of Climatology* 25: 1965–1978. doi:10.1002/joc.1276

Hilbers JP, van Langevelde F, Prins HHT, Grant C, Peel MJS, Coughenour MB, *et al.* (2015) Modeling elephant-mediated cascading effects of water point closure. *Ecological Applications* 25(2): 402–415. doi:10.1890/14-0322.1

Hitz S and Smith J (2004) Estimating global impacts from climate change. *Global Environmental Change* 14: 201–218. doi:10.1016/j.gloenvcha.2004.04.010

Hooper DU, Adair EC, Cardinale BJ, Byrnes JEK, Hungate BA, Matulich KL, *et al.* (2012) A global synthesis reveals biodiversity loss as a major driver of ecosystem change. *Nature* 486: 105–108. doi:10.1038/nature11118

Huang B, Thorne APW, Banzon VF, Boyer T, Chepurin G , Lawrimore JH, *et al.* (2017) Extended Reconstructed Sea Surface Temperature, Version 5 (ERSSTv5): Upgrades, Validations, and Intercomparisons. Journal of Climate 30:8179-8205. doi:10.1175/JCLI-D-16-0836.1. Available from http://origin.cpc.ncep.noaa.gov/products/analysis_ monitoring/ensostuff/ONI_v5.php (accessed 20 October 2016)

International Standard ISO 3166-1 (2006) Codes for the representation of names of countries and their subdivisions. International Organization on Standardization. Available from http://www.iso.org/iso/home/standards/country_codes.htm (accessed September 2017)

IPCC (Intergovernmental Panel on Climate Change) (2014) Climate Change 2014: Impacts, adaptation, and vulnerability. In: Field CB, Barros VR, Dokken DJ, Mach KJ, Mastrandrea MD, Bilir TE, *et al.* (eds.) *Part A: global and sectoral aspects. Contribution of Working Group II to the Fifth Assessment Report of the Intergovernmental Panel on Climate Change.* Cambridge University Press. pp. 1–32

Irish RR (2000) Landsat 7 Science Data User's Handbook. Report 430-15-01-003-0, National Aeronautics and Space Administration. Available from http://ltpwww.gsfc.nasa.gov /IAS/handbook/handbook_toc.html (accessed November 2014)

IUCN (2015) Updated African Elephant Database reveals declining elephant populations. News Report. Available from https://www.iucn.org/news_homepage/all_news_by_theme/world_heritage_news/?21925/Updated-African-Elephant-Database-reveals-declining-elephant-populations. (accessed 03 May 2016)

IUCN (2016) Position Paper: Convention on Biological Diversity Thirteenth Meeting of the Conference of the Parties (COP13). Available from https://www.iucn.org/sites/dev/files/iucn_position_paper_for_cop13_-_en.pdf (accessed 9 January 2017)

IUCN, UNEP-WCMC. 2016. The World Database on Protected Areas. WDPA. Cambridge, UK: UNEP-WCMC. Available from https://www.protectedplanet.net (accessed 03 May 2016)

Johnson NF (2007) *Simply Complexity: A Clear Guide to Complexity Theory*. One world Publications

Jongman RHG, Skidmore AK, Mücher CA, Bunce RGH and Metzger MJ (2017) In Walters M and Scholes RJ (eds.) *The GEO Handbook on Biodiversity Observation Networks.* Springer Open. Pages 19-38. doi:10.1007/978-3-319-27288-7

Joubert S (2007) *The Kruger National Park: a history*. High Branching (Pty) Ltd, Johannesburg, South Africa

Karambelkar B (2017) leaflet.extras: Extra Functionality for 'leaflet' Package. R package version 0.2. Available from https://CRAN.R-project.org/package=leaflet.extras (accessed 01 December 2017)

Katayama N, Amano T, Naoe S, Yamakita T, Komatsu I, Takagawa S, *et al.* (2014) Land scape heterogeneity–biodiversity relationship: effect of range size. *PLoS ONE* 9: e93359. doi:10.1371/journal.pone.0093359

Kearney MR, Shamakhy A, Tingley R, Karoly DJ, Hoffmann AA, Briggs PR and Porter WP (2014) Microclimate modelling at macro scales: a test of a general microclimate model integrated with gridded continental-scale soil and weather data. *Methods in Ecology and Evolution* 5: 273–286. doi:10.1111/2041-210X.12148

Kemp MU, van Loon EE, Shamoun-Baranes J and Bouten W (2012) RNCEP: global weather and climate data at your fingertips. *Methods in Ecology and Evolution* 3: 65–70. doi:10.1111/j.2041-210X.2011.00138.x

Kerley GIH, Landman M, Kruger L, Owen-Smith N, Balfour D, de Boer WF, *et al.* (2008) Effects of elephants on ecosystems and biodiversity. In: Scholes RJ and Mennell KG (eds.). *Elephant management: a scientific assessment for South Africa.* pp. 146–205. Wits University Press, South Africa

Kiker GA, Scholtz R, Smit IPJ and Venter FJ (2014) Exploring an extensive dataset to establish woody vegetation cover and composition in Kruger National Park for the late 1980s. *Koedoe* 56: 1–10. doi:10.4102/koedoe.v56i1.1200

Kilibarda M, Hengl T, Heuvelink GBM, Gräler B, Pebesma E, Perčec Tadić M and Bajat B (2014) Spatiotemporal interpolation of daily temperatures for global land areas at 1 km resolution. *Journal of Geophysical Research: Atmosphere* 119: 2294–2313. doi:10.1002/2013JD020803

Knapp AK, Smith MD, Hobbie SE, Collins SL, Fahey TJ, Hansen GJA, *et al.* (2012) Past, present, and future roles of long-term experiments in the LTER network. *BioScience* 62: 377–389. doi:10.1525/bio.2012.62.4.9

Knight J and Evans M (2017) The sediment stratigraphy of a flood event: An example from the Sabie River, South Africa. *Catena* 151: 87–87. doi:10.1016/j.catena.2016.12.015

Kolasa J and Rollo CD (1991) Introduction: the heterogeneity of heterogeneity: a glossary. In: Kolasa J and Pickett STA (eds.) *Ecological heterogeneity*. Springer-Verlag, New York. pp. 1–23

Köppen W (1930) Das geographisca System der Klimate. In: Köppen W and Geiger R (eds.) *Handbuch der Klimatologie*. Gebrueder Borntraeger, Berlin. pp. 1–44

Kruger AC and Nxumalo MP (2017) Historical rainfall trends in South Africa: 1921-2015. *Water SA* 43(2): 285–297. doi:10.4314/wsa.v43i2.12

LaDeau SL, Han BA, Rosi-Marshall EJ and Weathers KC (2017) The Next Decade of Big Data in Ecosystem Science. *Ecosystems* 20: 274–283. doi:10.1007/s10021-016-0075-y

Latham J, Cumani R, Rosati I and Bloise M (2014) FAO Global Land Cover (GLC-SHARE) Beta-Release 1.0 Database, Land and Water Division

Lausch A, Bannehr L, Beckmann M, Boehm C, Feilhauer H, Hacker JM, *et al.* (2016) Linking earth observation and taxonomic, structural and functional biodiversity: local to ecosystem perspectives. *Ecological Indicators* 70: 317–339. doi:10.1016/j.ecolind.2016.06.022

Lechner AM, Langford WT, Bekessy SA and Jones SD (2012) Are landscape ecologists addressing uncertainty in their remote sensing data? *Landscape Ecology* 27: 1249–1261. doi:10.1007/s10980-012-9791-7

Lefcheck JS (2016) piecewiseSEM: Piecewise structural equation modelling in R for ecology, evolution, and systematics. *Methods in Ecology and Evolution* 7: 573–579. doi:10.1111/2041-210X.12512

Lefcheck JS and Duffy JE (2015) Multitrophic functional diversity predicts ecosystem functioning in experimental assemblages of estuarine consumers. *Ecology* 96(11): 2973–2983. doi:10.1890/14-1977.1

Lengyel S, Kobler A, Kutnar L, Framstad E, Henry P, Babij V, *et al.* (2008) A review and a framework for the integration of biodiversity monitoring at the habitat level. *Biodiversity Conservation* 17: 3341–3356. doi:10.1007/s10531-008-9359-7

Leung Y, Mei C-L and Zhang W-X (2000) Statistical tests for spatial nonstationarity based on the geographically weighted regression model. *Environment and Planning* 32: 9–32. doi:10.1068/a3162

Leutner B and Horning N (2016) RStoolbox: Tools for Remote Sensing Data Analysis. R package version 0.1.5. Available from https://CRAN.R-project.org/package=RStoolbox (accessed 01 December 2017)

Levick SR and Rogers KH (2011) Context-dependent vegetation dynamics in an African savanna. *Landscape Ecology* 26: 515–528. doi:10.1007/s10980-011-9578-2

Levick SR, Baldeck CA and Asner GP (2015) Demographic legacies of fire history in an African savanna. *Functional Ecology* 29: 131–139. doi:10.1111/1365-2435.12306

Levin SA (1992) The problem of pattern and scale in ecology: The Robert H. MacArthur Award Lecture. *Ecology* 73(6): 1943–1967. doi:10.2307/1941447

Lin M, Lucas HC and Shmueli G (2013) Too big to fail: large samples and the *p*-Value problem. *Information Systems Research* 24(4): 906–917. doi:10.1287/isre.2013.0480

Liu M, Lei L, Liu Da and Zeng ZC (2016) Geostatistical Analysis of CH4 Columns over Monsoon Asia Using Five Years of GOSAT Observations. *Remote Sensing* 8(361). doi:10.3390/rs8050361

Loarie SR, van Aarde RJ and Pimm SL (2009) Fences and artificial water affect African savannah elephant movement patterns. *Biological Conservation* 142: 3086–3098. doi:10.1016/j.biocon.2009.08.008

Low AB and Rebelo G (1996) *Vegetation of South Africa, Lesotho and Swaziland*. Department of Environmental Affairs & Tourism, Pretoria

Lu D and Batistella M (2005) Exploring TM Image Texture and its Relationships with Biomass Estimation in Rondônia, Brazilian Amazon. *Acta Amazonica* 35: 249–257. doi:10.1590/S0044-59672005000200015

MacArthur RH and MacArthur JW (1961) On Bird Species Diversity. *Ecology* 42: 594–598. doi:10.2307/1932254

MacArthur RH and Pianka ER (1966) On optimal use of a patchy environment. *The American Naturalist* 100: 603–609. doi:10.1086%2F282454

Mace GM and Baillie JEM (2007) The 2010 Biodiversity Indicators: Challenges for Science and Policy. *Conservation Biology* 21: 1406–1413. doi:10.1371/journal.pone.0062180

MacFadyen S (2010) Identifying priority protection zones within protected areas: a biodiversity sensitivity-value analysis of the Kruger National Park, South. MSc. Thesis, Vrije Universiteit, Amsterdam, The Netherlands. Available from https://spinlab.vu.nl/websites/unigis/downloads/msc/Sandra%20MacFadyen.pdf

MacFadyen S, Hui C, Verburg PH and Van Teeffelen AJA (2016) Quantifying spatiotemporal drivers of environmental heterogeneity in Kruger National Park, South Africa. *Landscape Ecology* 31: 2013–2029. doi:10.1007/s10980-016-0378-6

MacFadyen S, Hui C, Verburg PH and Van Teeffelen AJA (*in Review*) Space is not 'irrelephant': Spatiotemporal distribution dynamics of elephants in response to density, rainfall, rivers and fire in Kruger National Park, South Africa. *Diversity and Distributions*

MacFadyen S, Smit IPJ, Foxcroft LC, Grant-Biggs R, Freitag-Ronaldson S, Zambatis N, *et al.* (2013) A spatial plan for elephant management in Kruger National Park, South Africa. South African National Parks. Scientific Report 02/2013

MacFadyen S, Verburg PH, Van Teeffelen AJA, Hui C (*submitted*) Landscape heterogeneity at the interface of herbivore, fire, climate and landform interactions. *Global Change Biology*

MacFadyen S, Zambatis N, Verburg PH, Van Teeffelen AJA, Hui C (2018) Long-term rainfall regression surfaces for the Kruger National Park, South Africa: A spatiotemporal review of patterns from 1981-2015. *International Journal of Climatology*. doi:10.1002/joc.5394

Mack O and Khare A (2016) Perspectives on a VUCA World. In: Mack O, Khare A, Krämer A and Burgartz T (eds.) *Managing in a VUCA world*. Springer International Publishing, Switzerland. pp. 3-19. doi:10.1007/978-3-319-16889-0

Margules C, Grant CC, Poon E, Deacon A, MacFadyen S, Biggs HC and Sithole H (2003) *A suggested biodiversity survey and monitoring program for Kruger National Park.* Scientific Report 02/03, South African National Parks

Marshall M, Okuto E, Kang Y, Opiyo E and Ahmed M (2016) Global assessment of Vegetation Index and Phenology Lab (VIP) and Global Inventory Modeling and Mapping Studies (GIMMS) version 3 products. *Biogeosciences* 13: 625–639. doi:10.5194/bg-13-625-2016

Martin J, Benhamou S, Yoganand K and Owen-Smith N (2015) Coping with spatial heterogeneity and temporal variability in resources and risks: adaptive movement behaviour by a large grazing herbivore. *PLoS ONE* 10(2): e0118461. doi:10.1371/journal.pone.0118461

Matthews S and Yang T (2012) Mapping the results of local statistics: using geographically weighted regression. *Demographic Research* 26: 151–166. doi:10.4054/DemRes.2012.26.6

McGarigal K, Tagil S and Cushman SA (2009) Surface metrics: an alternative to patch metrics for the quantification of landscape structure. *Landscape Ecology* 24: 433–450. doi:10.1007/s10980-009-9327-y

MEA (2005) *Millennium Ecosystem Assessment - Ecosystems and Human Well-being: Biodiversity Synthesis.* World Resources Institute, Washington, DC

Menne MJ, Durre I, Korzeniewski B, McNeal S, Thomas K, Yin X, *et al.* (2012) Global Historical Climatology Network - Daily (GHCN-Daily), Version 3. NOAA National Climatic Data Center. doi:10.7289/V5D21VHZ (accessed January 2016)

MIKE (2016) MIKE: Subregional trends from CITES MIKE Programme. Available from https://www.google.com/fusiontables/DataSource?docid=1Q-Kl4PcUJNe_a466-v9wlrJbKzczSnRGbwsWLnGc#rows:id=1 (accessed 3 May 2016)

Mittermeier RA, Mittermeier CG, Brooks TM, Pilgrim JD, Konstant WR, da Fonseca GAB and Kormos C (2003) Wilderness and biodiversity conservation. *Proceedings of the National Academy of Sciences* 100(18): 10309–10313. doi:10.1073/pnas.1732458100

Muñoz E, Álvarez C, Billib M, Arumí JL and Rivera D (2011) Comparison of gridded and measured rainfall data for basin-scale hydrological studies. *Chilean Journal of Agricultural Research* 71(3): 459–468. doi:10.4067/S0718-58392011000300018

Munyati C and Ratshibvumo T (2010) Differentiating geological fertility derived vegetation zones in Kruger National Park, South Africa, using Landsat and MODIS imagery. *Journal for Nature Conservation* 18(3): 169–179. doi:10.1016/j.jnc.2009.08.001

Murwira A (2003) *Scale Matters! A new approach to quantifying spatial heterogeneity for predicting the distribution of wildlife.* PhD Thesis, Wageningen University, The Netherlands

Myers N, Mittermeier RA, Mittermeier CG, da Fonseca GAB and Kent J (2000) Biodiversity hotspots for conservation priorities. *Nature* 403: 853–858. doi:10.1371/ journal.pone.0034459

Nagendra H, Lucas R, Honrado JP, Jongmand RHG, Tarantinoe C, Adamoe M and Mairota P (2013) Remote sensing for conservation monitoring: assessing protected areas, habitat extent, habitat condition, species diversity, and threats. *Ecological Indicators* 33: 45–59. doi:10.1016/j.ecolind.2012.09.014

Naimi B (2015) usdm: Uncertainty analysis for species distribution models. R package version 1.1-12. Available from http://CRAN.R-project.org/package=usdm (accessed June 2015)

NASA LP DAAC (2017) MOD44B: MODIS/Terra Vegetation Continuous Fields Global Yearly L3 250m. Version 6. NASA EOSDIS Land Processes DAAC, USGS Earth Resources Observation and Science (EROS) Center, Sioux Falls, South Dakota. DOI:10.5067/MODIS/MOD44B.006

Noss RF, Platt WJ, Sorrie BA, Weakley AS, Means DB, Costanza J and Peet RK (2015) How global biodiversity hotspots may go unrecognized: lessons from the North American Coastal Plain. *Diversity and Distributions* 21: 236–244. doi:10.1111/ddi.12278

O'Connor GT, Goodman PS and Clegg B (2007) A functional hypothesis of the threat of local extirpation of woody plant species by elephant in Africa. *Biological Conservation* 136: 329–345. doi:10.1016/j.biocon.2006.12.014

Odiyo JO, Makungo R and Nkuna TR (2015) Long-term changes and variability in rainfall and streamflow in Luvuvhu River Catchment, South Africa. *African Journal of Science* 111(7/8): 1–9. doi:10.17159/sajs.2015/20140169

Oksanen J, Blanchet FG, Kindt R, Legendre P, Minchin PR, O'Hara RB, Simpson GL, *et al.* (2015) vegan: Community Ecology Package. R package version 2.3-0. Available from http://CRAN.R-project.org/package=vegan (accessed June 2015)

Oldeland J, Wesuls D, Rocchini D, Schmidt M and Jürgens N (2010) Does using species abundance data improve estimates of species diversity from remotely sensed spectra l heterogeneity? *Ecological Indicators* 10: 390–396. doi:10.1016/j.ecolind.2009.07.012

Oliveira S, Pereira JMC, San-Miguel-Ayanz J and Luciano Lourenço L (2014) Exploring the spatial patterns of fire density in Southern Europe using geographically weighted regression. *Applied Geography* 51: 143–157. doi:10.1016/j.apgeog.2014.04.002

Owen-Smith NO and Ogutu J (2003) Rainfall influences on ungulate population dynamics. In: du Toit JT, Rogers KH and Biggs HC (eds.) *The Kruger Experience: Ecology and Management of Savanna Heterogeneity*. Island Press, Washington, DC. pp. 310–331

Paganini M, Leidner AK, Geller G, Turner W and Wegmann M (2016) The role of space agencies in remotely sensed essential biodiversity variables. *Remote Sensing in Ecology and Conservation* 2(3): 132–140. doi:10.1002/rse2.29

Palmer MW, Earls P, Hoagland BW, White PS and Wohlgemuth T (2002) Quantitative tools for perfecting species lists. *Environmetrics* 13: 121–137. doi:10.1002/env.516

Parminter J and Daigle P (1997) *Landscape ecology and natural disturbances: relationships to biodiversity*. British Columbia, Ministry of Forests Research Program

Parr CL and Andersen AN (2006) Patch mosaic burning for biodiversity conservation: a critique of the pyrodiversity paradigm. *Conservation Ecology* 20(6): 1610–1619. doi:10.1111/j.1523-1739.2006.00492.x

Parrish JD, Braun DP and Unnasch RS (2003) Are we conserving what we say we area? Measuring ecological integrity within protected areas. *BioScience* 53(9): 851–860. doi:10.1641/0006-3568(2003)053[0851:AWCWWS]2.0.CO;2

Parrot L (2010) Measuring ecological complexity. *Ecological Indicators* 10: 1069–1076. doi:10.1016/j.ecolind.2010.03.014

Parsons M, Mcloughlin CA, Rountree MW and Rogers KH (2006) The biotic and abiotic legacy of a large infrequent flood disturbance in the Sabie River, South Africa. *River Research and Applications* 22: 187–201. doi:10.1002/rra.905

Pereira HM, Ferrier S, Walters M, Geller GN, Jongman RHG, *et al*. (2013) Essential biodiversity variables. *Science* 339: 277–278. doi:10.1126/science.1229931

Petrou ZI, Manakos I and Stathaki T (2015) Remote sensing for biodiversity monitoring: a review of methods for biodiversity indicator extraction and assessment of progress towards international targets. *Biodiversity Conservation* 24: 2333–2363. doi:10.1007/s10531-015-0947-z

Pettorelli N, Laurance WF, O'Brien TG, Wegmann M, Nagendra H and Turner W (2014a) Satellite remote sensing for applied ecologists: opportunities and challenges. *Journal of Applied Ecology* 51: 839–848. doi:10.1111/1365-2664.12261

Pettorelli N, Ryan S, Mueller T, Bunnefeld N, Jędrzejewska B, Lima M and Kausrud K (2011) The Normalized Difference Vegetation Index (NDVI): unforeseen successes in animal ecology. *Climate Research* 46: 15–27. doi:10.3354/cr00936

Pettorelli N, Safi K and Turner W (2014b) Satellite remote sensing, biodiversity research and conservation of the future. *Philosophical Transactions of the Royal Society B* 369: 20130190. doi:10.1098/rstb.2013.0190

Philippon N, Martiny N and Camberlin P (2014) Timing and Patterns of the ENSO Signal in Africa over the Last 30 Years: Insights from Normalized Difference Vegetation Index Data. *Journal of Climate* 27: 2509–2532. doi:10.1175/JCLI-D-13-00365.1

Pickett STA, Ostfeld R, Shachak M and Likens G (eds.) (1997). *The ecological basis of conservation: Heterogeneity, ecosystems, and biodiversity.* Chapman & Hall, xxi + 466 pages. ISBN 0412 09851 2

Pickett STA (1998) Natural Processes. In: Mac MJ, Opler PA, Puckett Haecker CE and Doran PD (eds.) *Status and trends of the nation's biological resources.* 2 vols. U.S. Department of the Interior, U.S. Geological Survey, VA. pp. 1–22

Pickett STA, Cadenasso ML and Benning TL (2003) Biotic and abiotic variability as key determinants of savanna heterogeneity at multiple spatiotemporal scales. In: du Toit JT, Rogers KH and Biggs HC (eds.) *The Kruger Experience: Ecology and management of savanna heterogeneity.* Island Press, Washington DC. pp 22–40

Pienaar U de V (1977) Research objectives in South African National Parks. *Koedoe* 20: 38–48. doi:10.4102/koedoe.v20i2.1266

Pienaar U de V, Wyk P van and Fairall N (1966) An aerial census of elephant and buffalo in the Kruger National Park, and the implications thereof on intended management schemes. *Koedoe* 9:40–107. doi:10.4102/koedoe.v9i1.781

Pinzon JE and Tucker CJ (2014) A Non-Stationary 1981-2012 AVHRR NDVI3g Time Series. *Remote Sensing* 6: 6929–6960. doi:10.3390/rs6086929

Plouffe CCF, Robertson C and Chandrapala L (2015) Comparing interpolation techniques for monthly rainfall mapping using multiple evaluation criteria and auxiliary data sources: a case study of Sri Lanka. *Environmental Modelling and Software* 67: 57e71. doi:10.1016/j.envsoft.2015.01.011

Pohl B, Macron C and Monerie PA (2017) Fewer rainy days and more extreme rainfall by the end of the century in Southern Africa. *Scientific Reports 7*: 46466. doi:10.1038/srep46466

Potapov P, Yaroshenko A, Turubanova S, Dubinin M, Laestadius L, *et al.* (2008) Mapping the world's intact forest landscapes by remote sensing. *Ecology and* Society 13(2): 51. Available from http://www.ecologyandsociety.org/vol13/iss2/art51/ (accessed 01 December 2017)

Pringle RM (2008) Elephants as agents of habitat creation for small vertebrates at the patch scale. *Ecology* 89(1): 26–33. doi:10.1890/07-0776.1

Pringle RM, Kimuyu DM, Sensenig RL, Palmer TM, Riginos C, Veblen KE and Young TP (2015) Synergistic effects of fire and elephants on arboreal animals in an African savanna. *Journal of Animal Ecology* 84: 1637–1645. doi:10.1111/1365-2656.12404

Proença V, Martin LJ, Pereira HM, Fernandez M, McRae L, Belnap J, *et al.* (2016) Global biodiversity monitoring: From data sources to Essential Biodiversity Variables. *Biological Conservation* 213: 256–263. doi:10.1016/j.biocon.2016.07.014

Propastin PA (2009) Spatial non-stationarity and scale-dependency of prediction accuracy in the remote estimation of LAI over a tropical rainforest in Sulawesi, Indonesia. *Remote Sensing of Environment* 113: 2234–2242. doi:10.1016/j.rse.2009.06.007

R Core Team (2013) R: A language and environment for statistical computing. R Foundation for Statistical Computing, Vienna, Austria. Available from http://www.R-project.org/ (accessed October 2013)

R Core Team (2016) R version 3.3.1: A language and environment for statistical computing. R Foundation for Statistical Computing, Vienna, Austria. Available from http://www.R-project.org/ (accessed October 2016)

Redon M, Bergès L, Cordonnier T and Luque S (2014) Effects of increasing landscape heterogeneity on local plant species richness: how much is enough? *Landscape Ecology* 29: 773–787. doi:10.1007/s10980-014-0027-x

Reyers B and McGeoch MA (2007) A biodiversity monitoring framework for South Africa: progress and directions. *South African Journal of Science* 103: 295–300. doi:10019.1/9643

Rhasatsha HPC (2016) High Performance Computing System – Stellenbosch University, South Africa. Available from http://www.sun.ac.za/hpc (accessed 20 June 2016)

Riley SJ, DeGloria SD and Elliot R (1999) A terrain ruggedness index that quantifies topographic heterogeneity. *Intermountain Journal of Sciences* 5: 23–27

Ringnér M (2008) What is principal component analysis? *Nature Biotechnology* 26: 303–304. doi:10.1038/nbt0308-303

Ripple WJ, Newsome TM, Wolf C, Dirzo R, Everatt KT, Galetti M, *et al.* (2015) Collapse of the world's largest herbivores. *Science Advances* 1(4): e1400103. doi:10.1126/sciadv.1400103

Rocchini D and Neteler M (2012) Let the four freedoms paradigm apply to ecology. *Trends in Ecology & Evolution* 27: 310–311. doi:10.1016/j.tree.2012.03.009

Rocchini D, Balkenhol N, Carter GA, Foody GM, Gillespie TW, He KS, *et al.* (2010) Remotely sensed spectral heterogeneity as a proxy of species diversity: recent advances and open challenges. *Ecological Informatics* 5: 318–329. doi:10.1016/j.ecoinf.2010.06.001

Rocchini D, Marcantonio M and Ricotta C (2017) Measuring Rao's Q diversity index from remote sensing: an open source solution. *Ecological Indicators* 72: 234–238. doi:1016/j.ecolind.2016.07.039

Rocchini, D, Delucchi L, Bacaro G, Cavallini P, Feilhauer H, Foody GM, *et al.* (2013) Calculating landscape diversity with information-theory based indices: a GRASS GIS solution. *Ecological Informatics* 17: 82–93. doi:10.1016/j.ecoinf.2012.04.002

RStudio (2013) RStudio: Integrated development environment for R (Version 0.96.122). Boston, MA. Available from http://www.rstudio.org/ (accessed February 2014)

RStudio (2016) RStudio: Integrated development environment for R (Version 1.0.136). Boston, MA. Available from http://www.rstudio.org/ (accessed October 2016)

Rubel F, Brugger K, Haslinger K and Auer I (2017) The climate of the European Alps: Shift of very high resolution Köppen-Geiger climate zones 1800-2100. *Meteorologische Zeitschrift* 26: 115–125

Ruckstuhl KE (2007) Sexual segregation in vertebrates: proximate and ultimate causes. *Integrative and Comparative Biology* 47: 245–257. doi:10.1093/icb/icm030

Rutherford MC and Westfall RH (1986) Biomes of southern Africa – an objective categorization. *Memoirs of the Botanical Survey of South Africa* 54, National Botanical Institute, Pretoria, South Africa

Sankaran M, Hanan NP, Scholes RJ, Ratnam J, Augustine DJ, Cade BS, *et al.* (2005) Determinants of woody cover in African savannas. *Nature* 438: 846-849. doi:10.1038/nature04070

SANParks (2006) Setting Thresholds of Potential Concern for Heterogeneity-Aggregation. South African National Parks. Available from http://www.sanparks.org/parks/kruger/ conservation/scientific/mission/TPC_Heterogeneity.pdf (accessed 09 August 2011)

SANParks (2008) Kruger National Park Management Plan. South African National Parks. Available from https://www.sanparks.org/assets/docs/conservation/park_man/knp-management-plan1.pdf (accessed 05 May 2016)

SANParks (2009) Management Plan for the Kruger National Park. In: Freitag-Ronaldson S. (ed.) An Objectives Hierarchy for SANParks. South African National Parks, Scientific Services

SANParks (2016) South African National Parks Geospatial Database. South African National Parks. Unpublished data. Available from http://www.knb.ecoinformatics.org /knb/metacat (accessed December 2014)

SANParks (2017) Kruger National Park: Biodiversity Statistics. South African National Parks. Available from https://www.sanparks.org/parks/kruger/conservation/scientific/ff/ biodiversity_ statistics.php (accessed 18 December 2017)

Sarewitz D (2016) The pressure to publish pushes down quality. *Nature* 533: 147. doi:10.1038/533147a

Sarkar D and Andrews F (2016) latticeExtra: Extra Graphical Utilities Based on Lattice. R package version 0.6-28. Available from https://CRAN.R-project.org/ package=latticeExtra (accessed 01 December 2017)

SAWS (South African Weather Services) (1986) Climate of South Africa. Weather Bureau Publication 40. Department of Environmental Affairs, Pretoria, South Africa

SAWS (South African Weather Services) (2012) Climate data policy. Policy document: CLS-POL-CLIMATE-DATA 2.2, South African Weather Services

Sayre R, Dangermond J, Frye C, Vaughan R, Aniello P, Breyer S, Cribbs D, *et al.* (2014) *A New Map of Global Ecological Land Units — An Ecophysiographic Stratifcation Approach.* Washington, DC: Association of American Geographers. 46 pages

SCBD (Secretariat of the Convention on Biological Diversity) (2004) The Ecosystem Approach, (CBD Guidelines) Montreal: Secretariat of the Convention on Biological Diversity 50 pages. ISBN: 92-9225-023-x

SCBD (Secretariat of the Convention on Biological Diversity) (2008) Protected areas in today's world: their values and benefits for the welfare of the planet. Montreal, Technical Series no. 36, i–vii + 96 pages

SCBD (Secretariat of the Convention on Biological Diversity) (2010) COP-10 Decision X/2. Secretariat of the convention on biological diversity. UNEP/CBD/COP/DEC/X/2, 29 October 2010

SCBD (Secretariat of the Convention on Biological Diversity) (2014) *Global Biodiversity Outlook 4*. Montréal, 155 pages. Available from www.cbd.int/GBO4 (accessed 01 December 2017)

Schluter D and Pennell MW (2017) Speciation gradients and the distribution of biodiversity. *Nature* 546: 48–55. doi:10.1038/nature22897

Scholes RJ and Kruger JM (2011) A framework for deriving and triggering thresholds for management intervention in uncertain, varying and time-lagged systems. *Koedoe* 53(2). doi:10.4102/koedoe.v53i2.987

Scholes RJ and Mennell KG (2008) *Elephant management: a scientific assessment for South Africa.* Wits University Press, South Africa

Scholes RJ, Gill MJ, Costello MJ, Sarantakos G and Walters M (2017) Working in networks to make biodiversity data more available. In Walters M and Scholes RJ (eds.) *The GEO handbook on biodiversity observation networks.* Springer Open. pp. 1–17. doi:10.1007/978-3-319-27288-7

Schumacker RE and Lomax RG (2016) *A beginner's guide to structural equation modeling.* Taylor & Francis, New York. ISBN:1841698911

Schutte (1986) The general geology of the Kruger National Park. *Koedoe* 29: 13–37. doi:10.4102/koedoe.v29i1.517

Seiferling I, Proulx RL and Wirth C (2014) Disentangling the environmental-heterogeneity-species-diversity relationship along a gradient of human footprint. *Ecology* 95: 2084–2095. doi:10.1890/13-1344.1

Seydack AH, Grant CC, Smit IP, Vermeulen WJ, Baard J and Zambatis N (2012) Large herbivore population performance and climate in a South African semi-arid savanna. *Koedoe* 54(1): 20 pages. doi:dx.doi.org/10.4102/koedoe.v54i1.1047

Shannon G, Mackey RL and Slotow R (2013) Diet selection and seasonal dietary switch of a large sexually dimorphic herbivore. *Acta Oecologica* 46: 48e55. doi:10.1016/j.actao.2012.10.013

Shannon G, Page BR, Mackey RL, Duffy KJ and Slotow R (2008) Activity budgets and sexual segregation in African elephants (*Loxodonta Africana*). *Journal of Mammalogy* 89: 467–476. doi:10.1644/07-mamm-a-132r.1

Shannon G, Thaker M, Vanak AT, Page BR, Grant CC and Slotow R (2011) Relative impacts of elephant and fire on large trees in a savanna ecosystem. *Ecosystems* 14: 1372–1381. doi:10.1007/s10021-011-9485-z

Shi C and Wang L (2014) Incorporating spatial information in spectral unmixing: a review. *Remote Sensing of Environment* 149: 70–87. doi:10.1016/j.rse.2014.03.034

Sievert C, Parmer C, Hocking T, Chamberlain S, Ram K, Corvellec M and Despouy P (2016). plotly: Create Interactive Web Graphics via 'plotly.js'. R package version 3.6.0. Available from https://CRAN.R-project.org/package=plotly (accessed 01 December 2017)

Sievert C (2017) Plotly for R: The plotly book. Bookdown. Creative Commons Attribution-NonCommercial-NoDerivs 3.0, United States. Available from https://plotly-book.cpsievert.me/index.html (accessed 01 December 2017)

Shipley B (2016) *Cause and Correlation in Biology: A user's guide to path analysis, structural equations and causal inference with R.* Cambridge University Press, United Kingdom. ISBN:0521529212

shinyapps.io (2017) shinyapps.io by RStudio. RStudio Inc. Available from http://www.shinyapps.io/ (accessed 01 December 2017)

shinyapps.io team (2017) shinyapps.io user guide. RStudio Inc. Available from http://docs.rstudio.com/ shinyapps.io/ (accessed 01 December 2017)

Short (2005) The remote sensing tutorial. Available from http://www.fas.org/irp/imint/docs/ rst/Homepage/ Homepage.html (accessed March 2014)

Sinclair ARE and Byrom AE (2006) Understanding ecosystem dynamics for conservation of biota. *Journal of Animal Ecology* 75: 64–79. doi:10.1111/j.1365-2656.2006.01036.x

Skinner JD and Chimimba CT (2005) *The mammals of the Southern African Subregion.* Cambridge University Press, Cambridge, 872 pp. doi:0.1017/CBO9781107340992

Smit IJP and Ferreira SM (2010) Management intervention affects river-bound spatial dynamics of elephants. *Biological Conservation* 143: 2172–2181. doi:10.1016/ j.biocon.2010.06.001

Smit IPJ (2013) Systems approach towards surface water distribution in Kruger National Park, South Africa. *Pachyderm* 53: 91–98

Smit IPJ, Grant CC and Whyte IJ (2007) Landscape-scale sexual segregation in the dry season distribution and resource utilization of elephants in Kruger National Park, South Africa. *Diversity and Distributions* 13: 225–236. doi:10.1111/j.1472-4642.2007.00318.x

Smit IPJ, Riddell ES, Cullum C and Petersen R (2013a) Kruger National Park research supersites: establishing long-term research sites for cross-disciplinary, multiscaled learning. *Koedoe* 55(1), Art. #1107, 7 pages. doi.org/10.4102/koedoe.v55i1.1107

Smit IPJ, Smit CF, Govender N, van der Linde M and MacFadyen S (2013b) Rainfall, geology and landscape position generate large-scale spatiotemporal fire pattern heterogeneity in an African savanna. *Ecography* 36(4): 447–459. doi:10.1111/j.1600-0587.2012.07555.x

Smith MD, van Wilgen BW, Burns CE, Govender N, Potgieter ALF, Andelman S, Biggs HC, Botha J and Trollope WSW (2013) Long-term effects of fire frequency and season on herbaceous vegetation in savannas of the Kruger National Park, South Africa. *Journal of Plant Ecology* 6: 71–83. doi:10.1093/jpe/rts014

Somers B, Asner GP, Tits L and Coppin P (2011) Endmember variability in spectral mixture analysis: a review. *Remote Sensing of Environment* 115: 1603–1616. doi:10.1016/j.rse.2011.03.003

Stein A, Gerstner K and Kreft H (2014) Environmental heterogeneity as a universal driver of species richness across taxa, biomes and spatial scales. *Ecology Letters* 17: 866–880. doi:10.1111/ele.12277

Stekhoven DJ (2013) missForest: Nonparametric Missing Value Imputation using Random Forest. R package version 1.4. Available from https://cran.r-project.org/web/packages/missForest/index.html (accessed 15 May 2017)

Stekhoven DJ and Buehlmann P (2012) MissForest - non-parametric missing value imputation for mixed-type data. *Bioinformatics* 28(1): 112–118. doi:10.1093/bioinformatics/btr597

Stokke S and du Toit JT (2002) Sexual segregation in habitat use by elephants in Chobe National Park, Botswana. *African Journal of Ecology* 40: 360–371. doi:10.1046/j.1365-2028.2002.00395.x

Stoklosa J, Daly C, Foster SD, Ashcroft MB and Warton DI (2015) A climate of uncertainty: accounting for error in climate variables for species distribution models. *Methods in Ecology and Evolution* 6: 412–423. doi:10.1111/2041-210X.12217

Strauch AM (2013) Interactions between soil, rainfall, and wildlife drive surface water quality across a savanna ecosystem. *Ecohydrology* 6: 94–103. doi:10.1002/eco.1246

Tamme R, Hiiesalu I, Laanisto L, Szava-Kovats R and Pärtel M (2010) Environmental heterogeneity, species diversity and co-existence at different spatial scales. *Journal of Vegetation Science* 21: 796–801. doi:10.1111/j.1654-1103.2010.01185.x

Tennekes M (2017) tmap: Thematic Maps. R package version 1.10. Available from https://CRAN.R-project.org/package=tmap (accessed 01 December 2017)

Teren G (2016) *Elephants and Woody Plant Diversity: spatiotemporal dynamics of the Linyanti woodland, northern Botswana.* University of the Witwatersrand, Johannesburg. PhD thesis. Available at http://hdl.handle.net/10539/21647 (accessed 02 October 2017)

Tews J, Brose U, Grimm V, Tielbörger K, Wichmann MC, Schwager M and Jeltsch F (2004) Animal species diversity driven by habitat heterogeneity/diversity: the importance of keystone structures. *Journal of Biogeography* 31: 79–92. doi:10.1046/j.0305-0270.2003.00994.x

Thomas B, Holland JD and Minot EO (2012) Seasonal home ranges of elephants (*Loxodonta africana*) and their movements between Sabi Sand Reserve and Kruger National Park. *African Journal of Ecology* 50: 131–139. doi:10.1111/j.1365-2028.2011.01300.x

Thomsen MS, Garcia C, Bolam SG, Parker R, Godbold JA and Solan M (2017) Consequences of biodiversity loss diverge from expectation due to post-extinction compensatory responses. *Scientific Reports* 7:43695. doi:10.1038/srep43695

Tittensor DP, Walpole M, Hill SLL, Boyce DG, Britten GL, Burgess ND, *et al.* (2014) A mid-term analysis of progress toward international biodiversity targets. *Science* 346(6206): 241–244. doi:10.1126/science.1257484

Tobler W (1970) A computer movie simulating urban growth in the Detroit region. *Economic Geography* 46: 234–240.

Trabucco A and Zomer RJ (2009) Global Aridity Index (Global-Aridity) and Global Potential Evapo-Transpiration (Global-PET) Geospatial Database. CGIAR Consortium for Spatial Information. Available from http://www.csi.cgiar.org/ (accessed 13 June 2016)

Trollope W, van Wilgen BW, Trollope LA, Govender N and Potgieter ALF (2014) The long-term effect of fire and grazing by wildlife on range condition in moist and arid savannas in the Kruger National Park. *African Journal of Range & Forage Science* 31(3): 199–208. doi:10.2989/10220119.2014.884511

Tscharntke T, Tylianakis JM, Rand TA, Didham RK, Fahrig L, Batáry P, *et al.* (2012) Landscape moderation of biodiversity patterns and processes - eight hypotheses. *Biological Reviews* 87: 661–685. doi:10.1111/j.1469-185X.2011.00216.x

Tuanmu M and Jetz W (2015) A global, remote sensing-based characterization of terrestrial habitat heterogeneity for biodiversity and ecosystem modelling. *Global Ecology and Biogeography* 24: 1329–1339. doi:10.1111/geb.12365

Turner MG (1989) Landscape ecology: the effect of pattern on process. *Annual Review of Ecology and Systematics* 20: 171–197. doi:10.1146/annurev.es.20.110189.001131

Unal YS, Deniz A, Toros H and Incecik S (2012) Temporal and spatial patterns of precipitation variability for annual, wet, and dry seasons in Turkey. *International Journal of Climatology* 32: 392–405. doi:10.1002/joc.2274

UNEP-WCMC (2016) *World Database on Protected Areas User Manual* 1.3. UNEP-CMC Cambridge, UK. Available from http://wcmc.io/WDPA_Manual (accessed 01 December 2017)

UNEP-WCMC, IUCN (2016) *Protected Planet Report 2016.* UNEP-WCMC and IUCN Cambridge UK and Gland, Switzerland

USGS (2014) Shuttle Radar Topography Mission, 1 Arc-Second Global, Global Land Cover Facility, University of Maryland, College Park, Maryland. Available from http://dwtkns.com/srtm30m (accessed 01 December 2017)

Valeix M, Fritz H, Sabatier R, Murindagomo F, Cumming D and Duncan P (2011) Elephant-induced structural changes in the vegetation and habitat selection by large herbivores in an African savanna. *Biological Conservation* 144: 902–912. doi:10.1016/j.biocon.2010.10.029

van Aarde R, Whyte IJ and Pimm S (1999) Culling and the dynamics of the Kruger National Park African elephant population. *Animal Conservation* 2: 287–294. doi:10.1017/s1367943099000621

van Niekerk A (2012) Developing a high resolution DEM of South Africa. *Position IT* Nov-Dec: 55–60. EE Publishers (Pty) Ltd, Muldersdrift, South Africa

van Rij J, Wieling M, Baayen RH and Van Rijn H (2015) itsadug: Interpreting Time Series and Autocorrelated Data Using GAMMs. R package version 2.2. Available from https://cran.r-project.org/web/packages/itsadug/index.html (accessed 15 May 2016)

van Wilgen BW, Govender N, Smit IPJ and MacFadyen S (2014) The ongoing development of a pragmatic and adaptive fire management policy in a large African savanna protected area. *Journal of Environmental Management* 132: 358–368. doi:10.1016/j.jenvman.2013.11.003

van Wilgen NJ, Goodall V, Holness S, Chown SL and McGeoch MA (2016) Rising temperatures and changing rainfall patterns in South Africa's national parks. *International Journal of Climatology* 36: 706–721. doi:10.1002/joc.4377

Vanak AT, Thaker M and Slotow R (2010) Do fences create an edge-effect on the movement patterns of a highly mobile mega-herbivore? *Biological Conservation* 143: 2631–2637. doi:10.1016/j.biocon.2010.07.005

Vegter JR (1995) Geology map of South Africa with simplified lithostratigraphy for geohydrological use. *Water Research Commission* TT 74/95

Venter FJ (1990) *A classification of land for management planning in the Kruger National Park.* PhD Dissertation, University of South Africa, South Africa

Venter FJ, Naiman RJ, Biggs HC and Pienaar DJ (2008) The evolution of conservation management philosophy: science, environmental change and social adjustments in Kruger National Park. *Ecosystems* 11: 173–192. doi:10.1007/s10021-007-9116-x

Venter FJ, Scholes RJ and Eckhardt HC (2003) The abiotic template and its associated vegetation pattern. In: du Toit JT, Rogers KH and Biggs HC (eds.) *The Kruger Experience: Ecology and Management of Savanna Heterogeneity*. Island Press, Washington, DC, USA. pp. 83–129

Verbesselt J, Hyndman R, Newnham G and Culvenor D (2010) Detecting trend and seasonal changes in satellite image time series. *Remote Sensing of Environment* 114: 106–115. doi:10.1016/j.rse.2009.08.014

Verbesselt J, Zeileis A and Herold M (2012) Near real-time disturbance detection using satellite image time series. *Remote Sensing of Environment* 123: 98–108. doi:10.1016/j.rse.2012.02.022

Verdin A, Funk C, Rajagopalan B and Kleiber W (2016) Kriging and local polynomial methods for blending satellite-derived and gauge precipitation estimates to support hydrologic early warning systems. *IEEE Transactions on Geoscience and Remote Sensing* 54(5): 2552–2562. doi:10.1109/TGRS.2015.2502956

Vermote E, Justice C, Csiszar I, Eidenshink J, Myneni R, Baret F, Masuoka E, Wolfe R, Claverie M and NOAA CDR Program (2014) NOAA Climate Data Record (CDR) of AVHRR Surface Reflectance, Version 4. [AVH09C1]. NOAA National Climatic Data Center. doi:10.7289/V5TM782M

Viljoen AJ (1995) The influence of the 1991/92 drought on the woody vegetation of the Kruger National Park. *Koedoe* 38(2): 85–97. doi:10.4102/koedoe.v38i2.316

Wagner PD, Fiener P, Wilken F, Kumar S and Schneider K (2012) Comparison and evaluation of spatial interpolation schemes for daily rainfall in data scarce regions. *Journal of Hydrology* 464: 388–400. doi:10.1016/j.jhydrol.2012.07.026

Walpole M, McGeoch MA, Budd P and Brummitt N (2017) Using data for decision-making: from observations to indicators and other policy tools. In Walters M and Scholes RJ (eds.) *The GEO Handbook on Biodiversity Observation Networks*. Springer Open. Pages 293-308. doi:10.1007/978-3-319-27288-7

Warren SD, Alt M, Olson KD, Irl SDH, Steinbauer MJ and Jentsch A (2014) The relationship between the spectral diversity of satellite imagery, habitat heterogeneity, and plant species richness. *Ecological Informatics* 24: 160–168. doi:10.1016/j.ecoinf.2014.08.006

Wessels KJ, Prince SD, Zambatis N, MacFadyen S, Frost PE and Van Zyl D (2006) Relationship between herbaceous biomass and 1-km^2 Advanced Very High Resolution Radiometer (AVHRR) NDVI in Kruger National Park, South Africa. *International Journal of Remote Sensing* 27(5): 951–973. doi:10.1080/01431160500169098

Wessels KJ, Van Den Berg HM, Van Der Merwe JPA, Smith HJ, Van Zyl AJ and Twyman L (2001) Mapping and monitoring the conservation status of the natural resources of Mpumalanga Province by means of remote sensing and GIS technology. ISCW Report No. GW/A/2001/9. ARC-Institute for Soil, Climate and Water, Pretoria, South Africa

Whyte IJ (2001) *Conservation management of the Kruger National Park elephant population.* DPhil Thesis, University of Pretoria, South Africa

Wiens JA (2002) Central concepts and issues of landscape ecology. In: Gutzwiller KJ (ed.) *Applying landscape ecology in biological conservation*. Springer, New York. pp. 3–21. doi:10.1007/978-1-4613-0059-5_1

Williams C, Hanan N, Neff J, Scholes RJ, Berry J, Denning AS and Baker D (2007) Africa and the global carbon cycle. *Carbon Balance and Management* 2:3. doi:10.1186/1750-0680-2-3

Wilson AM and Jetz W (2016) Remotely sensed high-resolution global cloud dynamics for predicting ecosystem and biodiversity distributions. *PLoS Biol* 14(3): e1002415. doi:10.1371/journal.pbio.1002415

Wittemyer G, Northrupa JM, Blancd J, Douglas-Hamilton I, Omondif P and Burnham KP (2014) Illegal killing for ivory drives global decline in African elephants. *Proceedings of the National Academy of Sciences* 111: 13117–13121. doi:10.1073/pnas.1403984111

Wood SN (2006) *Generalized additive models: an introduction with R*. Chapman and Hall/CRC

Wright K (2016) corrgram: Plot a Correlogram. R package version 1.9. Available from https://CRAN.R-project.org/package=corrgram (accessed 01 December 2017)

Wulder M and Boots B (2000) Local Spatial Autocorrelation Characteristics of Landsat TM Imagery of a Managed Forest Area. *Canadian Journal of Remote Sensing* 27: 67–75. doi:10.1080/07038992.2001.10854921

Wulder MA, Hall RJ, Coops NC and Franklin SE (2004) High spatial resolution remotely sensed data for ecosystem characterization. *BioScience* 54(6): 511–521. doi:10.1641/0006-3568(2004)054[0511:HSRRSD]2.0.CO;2

Xie Y, Sha Z and Yu M (2008) Remote sensing imagery in vegetation mapping: a review. *Journal of Plant Ecology* 1(1): 9–23. doi:rg/10.1093/jpe/rtm005

Young KD, Ferreira SM and van Aarde RJ (2009) The influence of increasing population size and vegetation productivity on elephant distribution in the Kruger National Park. *Austral Ecology* 34: 329–342. doi:10.1111/j.1442-9993.2009.01934.x

Zambatis N (2003) *Determinants of grass production and composition in the Kruger National Park.* MSc. Thesis, University of Natal, Pietermaritzburg, South Africa

Zambatis N (2006) Average monthly and seasonal temperatures (°C) of the Kruger National Park. Unpublished report. SANParks, Skukuza. Available from http://www.sanparks .co.za/parks/kruger/conservation/scientific/weather/rainfall/2006/temps_rainfall_averag es.pdf (accessed December 2014)

Zambatis N (2010) Rainfall of the Kruger National Park. SANParks, Skukuza. Available from http://www.sanparks.co.za/parks/kruger/conservation/scientific/weather/rainfall/ 2006/temps_rainfall_averages.pdf. (accessed December 2014)

Zambatis N and Biggs HC (1995) Rainfall and temperatures during the 1991/92 drought in the Kruger National Park. *Koedoe* 38: 1–16. doi:10.4102/koedoe.v38i1.301

Zhao ZH, Hui C, Li ZH and Li BL (2015) Habitat heterogeneity stabilizes the spatial and temporal interactions between cereal aphids and parasitic wasps. *Basic and Applied Ecology* 16(6): 510–518. doi:10.1016/j.baae.2015.06.002

Zuur AF, Ieno EN, Walker NJ, Saveliev AA and Smith GM (2009) *Mixed effects models and extensions in ecology with R*. Springer-Verlag New York. doi:10.1007/978-0-387-87458-6

Zvoleff A (2016) glcm: Calculate Textures from Grey-Level Co-Occurrence Matrices (GLCMs). R package version 1.6.1. Available from https://CRAN.R-project.org/package=glcm (accessed 01 December 2017)

SUPPLEMENTAL MATERIAL

SUPPLEMENTAL CONTENTS AVAILABLE ONLINE AT

http://www.ub.vu.nl/nl/index.aspx

APPENDIX S2	Quantifying spatiotemporal drivers of environmental heterogeneity in Kruger National Park, South Africa
APPENDIX S3	Long-term rainfall regression surfaces for the Kruger National Park, South Africa: A spatiotemporal review of patterns from 1981-2015
APPENDIX S4	Space is not 'irrelephant': Spatiotemporal distribution dynamics of elephants in response to density, rainfall, rivers and fire in Kruger National Park, South Africa
APPENDIX S5	Landscape heterogeneity at the interface of herbivore, fire, climate and landform interactions
SUPPLEMENTAL REFERENCES	